From the Clinic of Neurology

of the University of Lübeck

Director: Prof. Dr. Thomas F. Münte

Neural networks underlying implicit motor sequence learning

Dissertation

for Fulfillment of

Requirements

for the Doctoral Degree

of the University of Lübeck

from the Department of Natural Sciences

Submitted by:

Elinor Tzvi-Minker

from Karmiel (Israel)

Lübeck 2015

First referee: Prof. Dr. rer. nat Ulrike M. Krämer

Second referee: Prof. Dr. rer. medic Lisa Marshall

Date of oral examination: 19.02.2016

Approved for printing. Lübeck, 2016

Acknowledgements

There are a few people that without whom this thesis would not have been possible. First and foremost I would like to thank Prof. Dr. Ulrike Krämer for introducing me to the field of cognitive neuroscience and for sharing her passion to research. For helping me discover my interests and follow them I would always be grateful. I would like to thank Prof. Dr. Rolf Verleger for sharing his data and collaborators with me. Without him a major part of this thesis would not have been possible. Thanks are also due to Prof. Dr. Thomas Münte for enabling me to perform this research work in the neurology department and for his very helpful comments and ideas on the studies in this thesis.

A big thank you goes as well to all my past and present colleagues. To Dr. Frederike Beyer for many valuable discussions and for her immense contribution to my understanding of cognitive aspects of human behavior. To Dr. Matthias Liebrand for always providing his help when it was needed. I also thank my collaborators of the second fMRI study as well, Dr. Anne Stoldt and Prof. Dr. Karsten Witt for sharing their data and ideas with me.

A special thank you goes to my parents and siblings for their constant support and enthusiasm. Ebenfalls möchte ich meiner Deutschen Familie Minker, für ihre Unterstützung in den Letzen Jahren bedanken. And finally, I would like to thank my partner, David, for his interest, involvement, and support and my lovely daughter Ella for allowing me the time to write this.

Contents

Acknowledgements iii

Zusammenfassung vii

Abstract ix

Chapter 1: Introduction 1

1.1. General outline of the thesis and research aims 1

1.2. Modelling of causal connectivity 2

1.2.1.Psychophysiological interactions 4

1.2.2.Granger Causality 5

1.2.3.Dynamic causal modelling 6

Generative models 7

Model evidence 8

Post-hoc Bayesian model selection 9

DCM limitations and critique 10

1.2.4.Summary 11

1.3. Learning and memory 11

1.3.1.Implicit learning and non-declarative memory 11

Procedural learning 12

Phases of motor skill learning 14

1.3.2.Neuroanatomical substrates of motor skill learning 15

Neural correlates of implicit vs. explicit MSL 15

Neural correlates of slow and "offline" MSL 16

The cortic-striato-cerebellar model of MSL 17

Connectivity in MSL networks 24

1.3.3.The role of neural oscillations in learning and memory 26

Cross-frequency coupling 27

1.4. Research aims 27

Chapter 2: Delineating the cortico-striatal-cerebellar network in implicit motor sequence learning 31

2.1. Introduction 31

2.1.1.Cortico-striatal-cerebellar networks during motor learning 32

2.1.2.Connectivity analyses of MSL and the present study 34

2.2. Materials and Methods 35

2.2.1 Subjects 35

2.2.2 The SRTT and implicit MSL 36

2.2.3 Experimental paradigm 36

2.2.4 Imaging 38

2.2.5 Behavioral analysis 39

2.2.6 Pre-processing and statistical analysis 39

2.2.7 Dynamic causal modeling 40
2.2.8 Time series extraction 41
2.2.9 DCM specification 42
2.3. Results 46
2.3.1 Behavioral results 46
2.3.2 DCM analysis 47
2.4. Discussion 50
2.4.1 Behavioral effects of motor learning 51
2.4.2 Effective connectivity 52
2.4.3 Role of cerebellum in MSL 53
2.4.4 Limitations 55
2.4.5 Conclusions 56
Chapter 3: Striatal-cerebellar networks mediate consolidation in a motor sequence learning task: an fMRI study using dynamic causal modelling 58
3.1. Introduction 58
3.1.1 Phases of motor learning 59
3.1.2 Neural correlates of motor learning and consolidation 60
3.1.3 Connectivity studies of motor learning 61
3.1.4 Current study 62
3.2. Materials and methods 64
3.2.1 Participants 64
3.2.2 Experimental paradigm 64
3.2.3 Procedure 65
3.2.4 Assessment of explicit awareness 66
3.2.5 Imaging 67
3.2.6 Behavioral analysis 68
3.2.7 Pre-processing and statistical analysis 68
3.2.8 Dynamic causal modelling 69
3.2.9 Post-hoc Bayesian model selection 70
3.2.10 Time series extraction 71
3.2.11 DCM specification 72
3.2.12 Parameter estimates 74
3.3. Results 75
3.3.1 Assessment of explicit awareness 75
3.3.2 Behavioral results 75
3.3.3 Dynamic causal modelling 77
3.4 Discussion 86
3.4.1 Changes in endogenous connections across sessions 87
3.4.2 Modulatory effects of learning in the early phase 89
3.4.3 Modulatory effects of learning in the late phase 91

3.4.4 Methodological considerations 92
3.4.5 Limitations 93
3.4.6 Conclusions 94
Chapter 4: Reduced α-γ_{low} phase amplitude coupling over right parietal cortex underlies implicit visuomotor sequence learning 95
4.1. Introduction 95
4.1.1 Implicit visuomotor sequence learning in the serial reaction time task 95
4.1.2 Learning, memory and neural oscillations 96
4.1.3 Phase amplitude coupling in learning and memory 97
4.2. Materials and Methods 99
4.2.1 Subjects 99
4.2.2 Experimental paradigm 100
4.2.3 Procedure 101
4.2.4 Behavioral analysis 102
4.2.5 Electrophysiological recordings 103
4.2.6 EEG data analysis 104
4.3. Results 108
4.3.1 Behavioral data 108
4.3.2 Learning related α-, θ- and γlow -power changes 109
4.3.3 Phase amplitude coupling 111
4.3.4 Analysis of transition blocks 113
4.4. Discussion 115
4.4.1 Behavioral effects of implicit visuomotor sequence learning 115
4.4.2 Alpha power changes as learning progresses 116
4.4.3 Theta and gamma-power effects during learning 117
4.4.4 Reduced alpha/low-gamma PAC in motor learning 118
4.4.5 Conclusions 121
Chapter 5: General discussion 122
5.1. Implicit learning in the serial reaction time task 122
5.2. Summary of the results: fMRI 124
5.3. Summary of the results: EEG 127
5.4. Implications for models of motor learning 128
5.5. Outlook 128
References 131
Curriculum Vitae 146

Zusammenfassung

Motorisches Lernen ist eine fundamentale Fertigkeit für unser tägliches Leben. Diese Art des Lernens kann unterschiedliche Formen annehmen, wie zum Beispiel das Lernen einer bestimmten Sequenz von Tastenantworten bis hin zu komplexen Bewegungen, die beispielweise beim Tennisspiel erforderlich sind. In dieser Dissertation untersuche ich die neuronalen Grundlagen von motorischem Sequenzlernen unter Verwendung von Daten aus funktioneller Magnetresonanztomographie (fMRT) und Elektroenzephalographie (EEG). Das erste Kapitel gibt eine allgemeine Einführung in die neuronalen Grundlagen des motorischen Lernens, die in elektrophysiologischen und Bildgebungsstudien gewonnen wurden. Diese Forschungsergebnisse resultierten in einem Modell für motorisches Lernen, welches ein Netzwerk verschiedener Gehirnregionen beschreibt, die für unterschiedliche Lernphasen zuständig sind. Nicht geklärt ist, wie diese einzelnen Regionen miteinander interagieren. Das Ziel dieser Arbeit ist es sich dieser Fragestellung mithilfe des seriellen Reaktionszeit-Tests (serial reaction time task; SRTT) zu nähern. Zwei Aspekte von Netzwerkinteraktionen wurden untersucht: der gegenseitige Einfluss von Hirnregionen während motorischen Lernens und die Natur dieser Interaktionen in Form von Oszillationen. Der erste Aspekt wurde untersucht, indem mathematische Modelle von Daten fMRT erstellt wurden (Kapitel 2 und Kapitel 3). Um den zweiten Aspekt zu ergründen, wurde oszillatorische Kopplung (oscillatory coupling) in EEG Daten als Maß für Kommunikation zwischen kortikalen Regionen verwendet (Kapitel 4).

In den fMRT Studien wurden kausale Interaktionen in dem kortiko-striato-cerebellaren Lernen Modell untersucht. Ergebnisse der ersten Studie (Kapitel 2) zeigten, dass die motorische Komponente von implizitem motorischem Sequenzlernen (MSL) durch kortiko-cerebelläre und nicht durch das kortiko-striatale Netzwerk moduliert wurde. Insbesondere wurde die Verbindung

zwischen dem primären motorischen Kortex (M1) und dem Cerebellum während des Lernens bilateral negativ moduliert, was möglicherweise in einer Deaktivierung des Cerebellums im Verlauf des Lernprozesses resultierte. In der zweiten Studie (Kapitel 3) wurden diese Ergebnisse repliziert und im Weiteren konnten eine spezifische Verbindung vom Cerebellum zum Putamen gefunden werden, die während der langsamen Lernphase negativ moduliert wurde. Diese Resultate betonen die Bedeutung der Verbindung des Cerebellums mit einerseits kortikalen und andererseits subkortikalen Strukturen während impliziten MSL. Die dritten Studie (Kapitel 4) zeigte, das Oszillationen im Theta, Alpha und Gamma Frequenzband in implizitem visuomotorischen Sequenzlernen involviert sind. Alpha Oszillationen waren über parietalen Arealen während der frühen Phase des Lernen erhöht und nahmen später ab. Die Kppplung zwischen der Alpha-Phase und der Amplitude von Gamma (alpha/gamma *phase amplitude coupling*, PAC) zeigte während des Lernens eine Reduktion über parietalen und prämotorischen Arealen. Dies legt nahe, dass die alpha-gamma PAC für visuo-motorische Integration entscheidend ist und diese im Verlauf des Lernens der visuo-motorischen Sequenz abnimmt. Schließlich werden in Kapitel 5 die Resultate dieser Studien in Bezug auf Modelle und kommende Entwicklungen in der Erforschung von Netzwerkinteraktionen während motorischen Lernens diskutiert.

Abstract

Motor learning is profoundly important for our daily life. This type of learning ranges from tapping fingers in a sequence to learning complex series of movements needed for example to precisely hit a tennis ball. In this thesis, I investigated the neural underpinnings of motor sequence learning using fMRI and EEG studies. The first chapter gives an overview on the neural correlates of motor learning which have been thoroughly investigated using animals, patients, imaging and electrophysiological studies. These efforts resulted in a motor learning model which describes a specific network of brain regions which are involved in the different learning stages. However, questions regarding the nature of the interactions in this network remain unanswered. The aim of this thesis is to address these questions by tapping into the neural correlates of implicit motor sequence learning (MSL) using the serial reaction time task (SRTT). Two aspects of network interactions were addressed: influence of brain regions involved in motor learning on each other and the nature of these interactions as expressed by oscillatory measures. The first aspect was addressed using mathematical modelling of functional magnetic resonance imaging (fMRI) data (Chapter 2 and Chapter 3). The second aspect was addressed by assessing oscillatory coupling measures from Electroencephalography (EEG) data as a measure of long-range communication between cortical regions (Chapter 4).

In the fMRI studies, causal interactions within a cortico-striato-cerebellar model were investigated. Results from the first study (Chapter 2) showed that the motor component of implicit MSL modulated the cortico-cerebellar and not the cortico-striatal loop. Specifically, learning negatively modulated the connection from M1 to cerebellum bilaterally, probably resulting in cerebellar deactivation as learning progresses. In the second study (Chapter 3), these results were replicated and a specific connection from cerebellum to putamen was found to be

negatively modulated by learning during the slow phase. Together, these results demonstrate the importance of cerebellum connection to cortical and subcortical structures to implicit MSL. The third study (Chapter 4) showed that oscillations in the theta (4-8Hz), alpha (8-12Hz) and gamma (30-49Hz) frequency bands are involved in implicit visuomotor sequence learning. Alpha oscillations over parietal areas were increased during the early learning phase and decreased later on. Alpha phase to low-gamma amplitude coupling (alpha/gamma PAC) was shown to decrease during learning over both parietal and motor areas suggesting that alpha/gamma PAC is important for visuo-motor integration. Finally, in Chapter 5 the results of these studies are discussed together with implications on models of motor learning and future perspectives of research on network interactions during motor learning.

Chapter 1

Introduction

1.1. General outline of the thesis and research aims

The extent to which motor learning plays a role in our life can be appreciated when viewing a small child develop. From the first goal-directed movements through crawling, sitting, standing and walking, each of the steps follow numerous trials and errors. Eventually children develop enough motor skills to function in dependently of their parents but motor learning never stops.

For this reason and others, neural correlates of motor learning have attracted much attention in the cognitive neuroscientific community (Dayan and Cohen, 2011). First highlighted in patients with movement disorders such as Parkinson's disease, Spino-cerebellar ataxia and Huntington's disease, clinical studies provided first clues to the loci of motor learning in the brain (Doyon et al., 1997; Jackson et al., 1995; Knopman and Nissen, 1991; Pascual-Leone et al., 1993). Followed up by transcranial magnetic stimulation (TMS) studies (Muellbacher et al., 2002) and animal models (Matsuzaka et al., 2007; Miyachi et al., 1997), plastic and dynamic changes over primary motor cortex and striatum were associated with the different phases of motor learning. Later on, numerous imaging studies (Hardwick et al., 2013) aimed to clarify which regions of the brain participate and contribute to motor learning. This line of evidence has pushed forward theoretical models of motor learning implicating several cortical and subcortical brain regions which together contribute to learning processes as well as motor memory encoding and consolidation (Doyon et al., 2003; Hikosaka et al., 2002). However, questions regarding the nature of the interactions between those brain regions remained largely unanswered.

In the experiments of this thesis, I sought to answer some of these questions with a very well established paradigm used to investigate implicit motor sequence learning: the serial reaction time task (Nissen and Bullemer, 1987). Using the excellent spatial resolution of fMRI I tried to understand the causal interactions (Friston et al., 2003) in a specific motor cortical-basal ganglia-cerebellar network during the acquisition (Study 1 and 2) and consolidation (Study 2) of motor memory. Next, I attempted to tap into specific oscillatory mechanisms, namely phase amplitude coupling (Canolty and Knight, 2010), as means of integrating local computation across large-scale networks while participants implicitly learned a visuomotor sequence (Study 3).

The following introduction is comprised of two parts: the first is a methodological evaluation of connectivity in brain networks which serves as the basis for my choice of "Dynamic causal modelling" (Friston et al., 2003) as a method for investigating causal interactions in studies 1 and 2. The second part is an overview of concepts and current knowledge on the neural correlates of learning and memory with special focus on implicit motor sequence learning.

1.2. Modelling of causal connectivity

Traditionally, cognitive neuroimaging studies adopted the modular view of brain function, in which each brain region plays a specific functional role for cognitive processes such as perception, cognition and action. Recently, there has been a shift to a functional integration view stressing that complex cognitive processes may involve spatially segregated, yet interacting brain regions. This has led researchers to explore connectivity between brain regions which were shown by means of functional neuroimaging to be implicated in different cognitive processes. The term connectivity may refer to different aspects of brain network organization.

The following distinctions have been made:

1. Structural connectivity refers to measures of white matter architecture or axonal connections between neurons and neural populations. Non-invasive techniques for tracing fibers of axonal connections make use of diffusion weighted imaging methods to identify tracts between brain regions.
2. Functional connectivity refers to statistical, non-mechanistic dependencies between signals from different brain regions. Usually inferred based on measures of correlations, this type of connectivity does not rely on any model of statistical dependencies among brain regions.
3. Effective connectivity refers to causal, directed connections between signals from different brain regions which explicitly depend on a certain statistical model. This implies that inferences in effective connectivity rely on model comparison and optimization.

In this section, I will discuss typical methods for assessing connectivity: psychophysiological interactions, granger causality and dynamic causal modeling. These methods are commonly used in EEG and fMRI studies to explore connectivity in the context of specific experimental manipulations.

Psychophysiological interactions (PPI) tests whether correlations in activity between two given brain regions differ based on certain experimental manipulations – hence in a psychological context.

Granger Causality (GCA) tests whether a signal extracted from a certain region X "granger causes" a signal from another region Y. This is true only if X contains information that will help predict the future of Y better than only the information stored in Y itself.

Dynamic causal modeling (DCM) is a relatively new framework, which attempts to fit a mathematical model of differential equations to the underlying dynamic connections between neural populations. Thereafter Bayesian methods are used to compare models and assess probability of connectivity parameters.

1.2.1. Psychophysiological interactions

Psychophysiological interactions (PPI) (Friston et al., 1997), describe the relationship between activity in two (or more) brain regions under a specific experimental context in fMRI studies. It relies on a linear regression model between a signal from a seed region and other voxels in the brain during a particular context of a behavioral task. The following statistical model is therefore used:

$$\mathbf{x}_i = \mathbf{x}_k \times \mathbf{g}_p \cdot \beta_i + \left[\mathbf{x}_k \mathbf{g}_p \boldsymbol{G}\right] \cdot \beta_G + \boldsymbol{e}_j \qquad (1)$$

Where x represents the activity in a specific region, g the experimental context, and β is the parameter estimate. Multiplying these elements results in the interaction between physiological activity in region k and an experimental parameter g. G is a matrix whose columns contain effect of no interest and e is an additive error-term.

An interaction means that the contribution of the seed region to other brain regions expressed as the slope of the regression model is specifically dependent on a certain experimental context and changes when this context is no longer present in the task. Notably, this type of interaction does not predict the directionality of influence of one brain region to another (as opposed to other measures of effective connectivity such as DCM and GCA). In addition, a major caveat in PPI analysis is that it describes the interactions using the BOLD signal measured with a lag of ~6 (sec) while the experimental manipulation is measured in real-time. A proper

psychophysiological interaction should occur on the neuronal level and thus require the hemodynamic activity to be deconvolved in order to achieve the underlying neural signal (Gitelman et al., 2003). This step, which is critical for PPI analysis (as well as standard GLM analyses) might be tricky as the HRF shape is not exactly known and might cause spurious deconvolution results (O'Reilly et al., 2012).

1.2.2. Granger Causality

Granger causality (GCA) was first introduced in the field of economics (Granger, 1969) and thereafter been widely applied to neuroimaging and neurophysiological data as it provides a relatively simple framework in which causality measures could be estimated given stationary (i.e. mean and variance which do not change in time) stochastic time series. The idea behind GCA is straight forward: given two time series X and Y, if we are able to predict the future of X more successfully by incorporating the information from the past of Y compared to incorporating only the information of the past of X then we can conclude that Y "granger causes" X. Commonly implemented as linear vector autoregressive models, GCA can be formulated as follows:

$$\mathbf{x}_t = \sum_{j=1}^{p} \mathbf{A}_j \mathbf{x}_{t-j} + \boldsymbol{\varepsilon}_t \tag{2}$$

$$\mathbf{x}_t = \sum_{j=1}^{p} \mathbf{A}'_j \mathbf{x}_{t-j} + \sum_{j=1}^{p} \mathbf{A}'_j \mathbf{y}_{t-j} + \boldsymbol{\varepsilon}'_t \tag{3}$$

$$\mathcal{F}_{Y \to X} = \ln \frac{\mathrm{var}(\varepsilon_t)}{\mathrm{var}(\varepsilon'_t)} \tag{4}$$

Where p represents the order of the autoregressive model, equation (2) is the restricted model (depending only on the past of x), equation (3) is the unrestricted model (depending also on the

past of y) and equation (4) is the definition of granger causality based on the variance of the residuals ε (also referred to as "prediction errors"). This means that if the residual of the unrestricted model is smaller than the residual of the restricted model then the model improved its prediction by including Y. Importantly, GCA methodology assumes that the time series are wide-sense-stationary which is almost never the case with neurophysiological data. Differencing the data or analyzing GCA in short time-windows (Ding et al., 2000) could provide a solution to this problem. GCA has been mostly applied to electrophysiological data recorded using EEG/MEG either at the sensor level or at the source level following appropriate source reconstruction techniques. However, attempts to apply GCA to fMRI time series data have been widely criticized given the slow dynamics of the BOLD signal and regional variations in hemodynamic latency (David et al., 2008). Some recent work however showed that GCA could be robust to hemodynamic variations but not when performing down sampling and in the presence of measurement noise (Deshpande et al., 2010; Seth et al., 2013).

1.2.3. Dynamic causal modelling

Dynamic causal modelling (DCM; Friston et al., 2003) is an input-state-output framework which uses differential equations and Bayesian inference to describe the dynamics of interacting brain sources using neurophysiological signals. Importantly, unlike PPI and GCA described above, DCM is regarded as a hypothesis-driven approach which allows testing specific competing models in terms of statistical evidence and connectivity parameters. An interacting network modeled using DCM requires an input which will in turn elicit a state change that will produce the observed output. Here, the input is the experimental manipulation; the output is the measured signal: electrophysiological in case of LFP/EEG measurements or a hemodynamic response in case of fMRI; and the state is the regional specific neuronal activity which changes in time.

In this thesis I used DCM for fMRI data measured in Study (1) and Study (2). The following section will therefore focus on mathematical models underlying DCM for fMRI (but see (David et al., 2006) for the theory and foundations of DCM for EEG/MEG).

Generative models

Neurodynamics are described by a deterministic bilinear differential so-called "evolution" equation:

$$\frac{d\boldsymbol{z}}{d\boldsymbol{t}} = \left(\boldsymbol{A} + \sum_{i=1}^{m} \boldsymbol{u}_i \boldsymbol{B}^{(i)}\right)\boldsymbol{z} + \boldsymbol{C}\boldsymbol{u} \qquad (5)$$

Where Z is the time dependent regional specific neural activity, A represents the endogenous connections in the absence of input, B represents the modulatory effects (i.e. the influence of the input on the connection), and C the extrinsic (non-state-dependent) additive effects on regional neuronal activity. A, B and C are specified based on the assumptions (hypotheses) on the model structure.

The hidden state Z is then mapped to the experimental measure, here the BOLD signal. The neurodynamics described above give rise to changes in BOLD fMRI activity. These changes have been described previously by the balloon model (Buxton et al., 1998). In short, regional neuronal activity causes increase in vasodilatory signal which is subject to auto-regulatory feedback. Inflow responds to this feedback and in turn causes changes in blood volume and deoxyhemoglobin content. The predicted BOLD signal is a nonlinear function of volume and deoxyhemoglobin (Stephan et al., 2007). This procedure results in a modelled BOLD response which is estimated using a Bayesian scheme.

Model evidence

The Bayesian scheme estimates two very important quantities: the model evidence $p(y|m)$ which is the probability of obtaining observed data y given model m and the posterior estimates of the model parameters $p(\theta|m)$ given model m, where $\theta = \{A, B, C\}$. According to the Bayes Theorem one could describe the model evidence as follows:

$$p(y|m) = \int p(y|\theta, m)p(\theta|m)d\theta \tag{6}$$

As equation (6) is not straight forward to compute, it is approximated using variational free energy (Friston et al., 2007). This is done by iteratively updating the posterior moments of the parameters through a gradient ascent on a free-energy bound F on the log evidence:

$$\log p(y|m) = F(m) + KL(q(\theta|y, m)||p((\theta|y, m)) \tag{7}$$

$$F(m) = \log p(y|m) - KL(q(\theta|y, m)||p((\theta|y, m)) \tag{8}$$

Where KL is the Kullback-Leibler divergence between the approximated posterior density q and the true posterior p. This quantity is always positive or zero when the densities are identical. Importantly, F contains two opposing requirements of a good model: First, if the log likelihood is high, the data fits well to the model. Second, the second term in equation (8) ensures that complexity of the model (more parameters used) is penalizing the evidence such that simpler models would be advantageous.

The model evidence is then used for comparing different competing hypotheses using Bayesian model selection (BMS; Rigoux et al., 2014; Stephan et al., 2009). In neuroimaging data this procedure entails comparison between models across a group of subjects. If one assumes fixed

effects (for a random effects treatment please refer to Stephan et al. (2009)) across subjects (all subjects use the same model) then the Bayes factor could be used to compare between two models:

$$BF_{ij} = \frac{p(Y|m = i)}{p(Y|m = j)} \quad (9)$$

Post-hoc Bayesian model selection

The DCM framework as described above requires that each hypothesized model is estimated and fitted for the purpose of model comparison using BMS. This approach is challenging when dealing with large-scale networks or when a-priori knowledge about the network connectivity patterns is limited. Such circumstances will require more free parameters to be added to the model space which will increase the computational time exponentially. A possible solution to this challenge was suggested by Friston and Penny (Friston and Penny, 2011). This paper describes a framework in which only one "full" model is fitted and estimated. Subsequently, model evidence for all reduced nested models could be post-hoc approximated from the full model. A full model in this case could be a fully connected network and the nested models would be models with a sparser connectivity pattern. Importantly, connectivity parameters for all reduced models could be estimated from the posterior density over the parameters of the full model.

The post-hoc approach allows searching over very large model spaces using a greedy search scheme as follows: a subset of parameters with the least evidence is identified and a search is

conducted across all reduced models within that subset. Redundant parameters are removed and the search continues until all parameters in the full model have been searched through.

While the original "post-hoc" BMS publication referred to a specific stochastic DCM implementation (Li et al., 2011), a more recent study (Rosa et al., 2012) showed that the "post-hoc" approach could also be applied to bilinear deterministic DCMs. In addition the authors compared the results achieved with this approach to results of the traditional DCM approach in which each model is estimated separately, and found that both in synthetic and real fMRI data similar results could be achieved both for model evidence and parameter estimates.

DCM limitations and critique

Since the publication of the seminal DCM paper (Friston et al., 2003) DCM framework has been used quite extensively for analyzing effective connectivity mostly in fMRI studies (as for 1.2015 the seminal DCM paper was cited 1970 time). Recently, some methodological concerns have been raised (Daunizeau et al., 2011; Friston et al., 2013; Lohmann et al., 2012) which are crucial for the correct interpretation and generalization of DCM results.

(1) DCM network. While measures of functional connectivity allow whole brain investigations, DCM is limited to a pre-specified number of regions which might be only a small part of a more complex network. Therefore interactions within the network described by DCM might only underlie complex interactions with other brain regions as well.

(2) Statistical inference. It is not possible to falsify models using DCM. The Bayesian framework allows testing a large set of relatively equally probable models. The winning model then represents the most plausible model out of this specific set of models but can be actually false by itself.

(3) Model space combinatorial explosion. The number of possible models for a DCM analysis has been first raised by Lohmann and colleagues (Lohmann et al., 2012) and subsequently debated in later work (Friston et al., 2013; Lohmann et al., 2013). In short, in search for a "true" model, the number of possible arrangements of the user-defined parameter space (i.e. A, B, and C matrices) can be extremely large up to a combinatorial explosion. For example a 3-node network with 3 experimental conditions will require 272 million potential models. The argument against this critique is that DCM framework is motivated for scientific questions in which competing hypotheses are compared against each other. This means two things: there is no "true" model but a model which can explain the results observed better, and second, a-priori knowledge on network connectivity is explicitly implied while constructing the model space.

1.2.4. Summary

This section reviewed three commonly used methods for assessing connectivity in fMRI data. While each method comes with advantages and disadvantages, it is quite clear that for hypothesis driven questions DCM allows to most directly investigate underlying effective connectivity patterns compared to GCA and PPI. Importantly, this kind of scientific questions should be motivated by literature (including animal models) and should thus provide a clear specification of model space.

1.3. Learning and memory

1.3.1. Implicit learning and non-declarative memory

Memory is often classified along the time dimension into short-term memory and long-term memory. Short-term memory transiently maintains current information and has limited capacity.

A concept which was developed in order to extend on short-term memory in terms of the mental processes involved is working memory. A classical model subdivides working memory into three systems: verbal, visuo-spatial, and executive control which is the system that coordinates the former two by monitoring, manipulating and updating stored information (Baddeley, 1992). The storage of information for long periods of time (days, months or years) is referred to as long-term memory which is commonly divided into declarative and non-declarative memories. Declarative memory is defined as a memory for events (episodic) and facts (semantic) whereas non-declarative memory is directly linked to the process in which it was acquired, i.e. implicit learning, a learning process without conscious awareness. There are several different types of implicit learning mechanisms such as priming, classical conditioning, non-associative learning (habituation, sensitization) and procedural learning. Procedural learning is characterized by incremental improvement in accuracy and speed of motor behavior which is achieved through repetition.

Procedural learning

Procedural learning involves learning of cognitive and motor skills, for example, learning to ride a bike or to tie a shoe. We are not really able to describe how exactly we learned these skills but most of us are able to do them. Interestingly, this type of learning is not affected by anterograde amnesia such as the one of the famous H.M, whose bilateral hippocampi were resected in an attempt to control his severe epileptic seizures. H.M was able to perform a difficult motor learning task, namely, mirror tracing and showed normal learning curve over days, despite not remembering having done that task the previous days.

Several experimental paradigms are used for testing procedural learning. For example, in an artificial grammar task (Reber, 1967), the subject is requested to memorize a set of letter strings.

Once this is done, the subject is informed that the strings follow a certain rule and are asked to classify new strings as grammatical (i.e. following the rule) or not. Evidently, participants are more accurate than chance in this task even though they are not able to verbalize a specific rule. A very popular paradigm to study the nature of procedural memory is sequence-learning. The sequence may be a series of light flashes or tones which correspond to a specific button press. One example of sequence-learning is the number reduction task (Rose et al., 2002). Here, participants learn to respond to a series of numbers based on explicit rules. In addition, an abstract hidden structure is implemented such that irrespective of the stimulus-response associations in a given trial, the response pattern follows a specific pattern.

The serial reaction time task (Nissen and Bullemer, 1987) is a standard experimental paradigm to test implicit motor sequence learning (MSL). Here, participants are asked to respond to a series of visual stimuli on the screen by pressing the spatially corresponding buttons on a button-pad. Unbeknownst to the participants, the stimuli on the screen follow a specific sequence which correspondingly requires a sequence of button presses. With time participants become faster in performing the sequence compared to completely random button presses which indicates that they have indeed learned the sequence pattern. However, when asked about it, participants do not seem to recollect any kind of pattern in the stimuli presented to them. Importantly, although viewed as a motor learning task, the SRTT may not only involve the motor domain (Robertson, 2007). Participants may adopt different strategies as either the sequence of the visual cues could be learned (perceptual component) or the sequence of the button presses (motor component) or a combination of both. If the sequence is practiced enough times though, studies show that participants may gain explicit knowledge (Doyon et al., 1996).

Other forms of motor learning exist as well, for example, visuomotor adaptation (Galea et al., 2011). Here, participants learn a certain movement trajectory by moving a cursor to a target on the screen. Next, a transformation is imposed unexpectedly forcing the participants to adapt to a new target location. This type of motor learning as well as learning of sequential finger tapping, whether implicit or explicit (Karni et al., 1995), is sometimes referred to in the literature as skilled behavior (Dayan and Cohen, 2011).

Phases of motor skill learning

Motor skills are initially acquired very fast but learning later slows down, nearing asymptotic performance. Following a series of behavioral and fMRI studies of sequential finger tapping, Karni and colleagues (Karni et al., 1998) suggested that motor skill acquisition could be subdivided into several stages: fast stage, slow stage and an intermediate offline stage. In the early, fast stage which is highly dependent on the task at hand may take minutes (for the SRTT) or even months (for piano playing), rapid improvement in performance can be observed on a relatively short period of time. In the late, slow stage small behavioral increments are still observed but over a much longer time window. During the offline stage, although no further practicing of the motor skill is taken place, participants may still show improvements in performance. This process is called memory consolidation (Robertson et al., 2004a) and might be sleep-dependent in explicit MSL (Debas et al., 2010; Fischer et al., 2002; Wagner et al., 2004; Walker et al., 2002). For procedural learning and implicit MSL however, consolidation might not be specifically related to sleep (Meier and Cock, 2014; Nemeth et al., 2010; Robertson et al., 2004b; Song et al., 2007).

1.3.2. Neuroanatomical substrates of motor skill learning

The neural substrates of motor skill learning have been studied in both healthy humans and patients using imaging techniques (PET, fMRI) and electrophysiological recordings (EEG, MEG) as well as in rodents and non-human primates using invasive recordings of local field potentials. Findings in humans show involvement of basal ganglia structures including striatum and thalamus as well as motor cortical areas, parietal cortex, dorsolateral prefrontal cortex and cerebellum (for meta-analysis see Hardwick et al., 2013). Differences in regional activity and involvement of those regions greatly depend on the learning stage, whether the task was learned implicitly or explicitly and the type of skill to be learned. Recently, studies using diffusion imaging methods showed white matter changes related to the acquisition of motor skill (Scholz et al., 2009; Schulz et al., 2014; Sisti et al., 2012; Steele et al., 2012) which suggests that motor learning influences white matter architecture in humans.

Neural correlates of implicit vs. explicit MSL

Based on studies of amnesic patients such as H.M, medial temporal lobe (MTL) structures which include the hippocampus were mainly implicated with explicit learning processes resulting in declarative memory (Squire and Zola-Morgan, 1991). Early research on MSL has therefore distinguished neuroanatomical substrates of implicit and explicit learning mechanisms with findings being largely inconsistent (Doyon et al., 1996; Grafton et al., 1995; Hazeltine et al., 1997; Honda et al., 1998; Rauch et al., 1995). In the SRTT, explicit awareness is usually measured by simply asking the participants whether they were aware of an underlying sequence or by performing different sequence generation tasks. In later studies researchers used more sophisticated approaches in order to appropriately disentangle implicit and explicit learning mechanisms (e.g. in Fletcher et al., 2005). A consistent finding was striatal involvement in

implicit sequence learning in the SRTT (Albouy et al., 2008; Badgaiyan et al., 2007; Destrebecqz et al., 2005; Karabanov et al., 2010; Rose et al., 2011; Schendan et al., 2003). A recent Meta-analysis study corroborated these findings and showed that when comparing 17 explicit vs. 15 implicit versions of the SRTT, caudate nucleus activity was more consistent with implicit SRTT with no other brain regions showing this effect (Hardwick et al., 2013).

Neural correlates of slow and "offline" MSL

In the SRTT, improvement in performance mainly occurs in short time scales (minutes to hours) however additional smaller "offline" improvement may occur in longer time scales of days to weeks (Press et al., 2005). Early imaging (Karni et al., 1995; Karni et al., 1998) and TMS (Muellbacher et al., 2002; Pascual-Leone et al., 1995; Robertson et al., 2005) studies on the neural effects of "offline" explicit MSL showed involvement of M1 in consolidation of motor memories. Investigating whole-brain changes following consolidation, reduced activity over striatum and cerebellum were found after one month practice of a sequential finger tapping task (Lehericy et al., 2005). Early recruitment of striatum and hippocampus in an implicit MSL task predicted "offline" improvement in performance (Albouy et al., 2008). A recent meta-analysis study of motor skill acquisition across different time scales revealed consistent decreases for MSL over days or weeks, over dorsolateral prefrontal cortex (DLPFC), PMC and preSMA along with superior and inferior parietal lobule whereas increases for those studies were observed over M1, putamen and globus pallidus pars interna (Lohse et al., 2014).

A central question regarding "offline" consolidation processes is whether sleep modulates the ability to consolidate motor memories (Stickgold et al., 2001). Walker and colleagues showed differences between sleep- or awake-consolidation in an explicit MSL task with increased activity after sleep in M1, hippocampus, medial frontal lobe and cerebellum (Walker et al.,

2005). On the other side, Fischer and colleagues found reduced activity over M1, PMC and prefrontal areas following a night's sleep compared to sleep-deprivation (Fischer et al., 2005). Importantly, studies show that consolidation of implicit motor sequence memories are not necessarily sleep-dependent and could also occur without sleep (Robertson et al., 2004b; Song et al., 2007).

The cortic-striato-cerebellar model of MSL

Theoretical models suggest that distinct cortico-striatal and cortico-cerebellar loops (Doyon and Benali, 2005; Doyon et al., 2003; Hikosaka et al., 2002) mediate the different phases of motor skill learning. The model by Doyon and colleagues (2005) suggests that striatum, cerebellum, parietal cortex and motor cortical regions are mediating the fast learning stage. During slow learning and retention however, the model differentiates motor sequence learning and motor adaptation in terms of the brain structures involved. Specifically, the authors suggest that striatum is involved in MSL and cerebellum in motor adaptation. Hikosaka and colleagues (2002) on the other hand, suggest a model in which learning of spatial sequence and learning of motor sequence are differentiated. During the fast learning stage, the movements to be executed are represented by a cortical loop of prefrontal, parietal and motor cortex. When learning is established, the motor sequence is represented by motor territories of basal ganglia and cerebellum together with the motor cortex. Penhune & Steele (2012) recently suggested that M1, basal ganglia and the cerebellum may engage in parallel interacting processes which underlie MSL. In this section I will therefore focus on these main components and provide the evidence for their involvement in MSL.

Primary motor cortex

The primary motor cortex (M1; BA4), located at the anterior wall of the central sulcus and extending to the precentral gyrus, is known to be important for movement initiation. As revealed by early studies, M1 is organized as a motor map containing somatotopic representations: specific sites over M1 correspond to movement of specific body parts (Kandel et al., 2013). M1 has somatotopically organized reciprocal connections with supplementary motor area (SMA), dorsal premotor cortex (PMC) and ventral PMC. Sensory information input to M1 is received from the primary somatosensory cortex and parietal cortex and serves to guide motor acts. The output of M1 is sent through the pyramidal tract to motor neurons controlling muscles on the contralateral side (Porter, 1985).

Studies in monkeys showed that neuronal populations in M1 code for specific movement direction (Georgopoulos et al., 1983; Moran and Schwartz, 1999) and movement kinetics (Evarts, 1968; Kalaska et al., 1989). M1 also plays a major role in online movement control, as many neurons over M1 receive sensory input about the body's current state which is used to adjust the output signal of specific movement related neuronal populations in M1 (Hoffman and Strick, 1995; Nudo and Milliken, 1996). Studies in animals showed that when M1 or paths connecting M1 to sensorimotor areas were lesioned, the animals were either paralyzed or experienced severe loss of motor function of the corresponding limb (Pavlides et al., 1993; Sakamoto et al., 1989). This was evident as well in patients with lesions to M1 after stroke which lost the ability to move the contralateral side of the body.

Single-neuron recordings from M1 in monkeys provide evidence for the importance of M1 to motor skill learning. In a force field task, recordings from single neurons over M1 showed specific learning-related plasticity (Kirov et al., 2015) and in a MSL task, differential activation

over M1 was observed for sequence compared to random blocks (Matsuzaka et al., 2007). In humans, M1 modulation due to motor skill learning was first described using TMS. Dynamic changes in motor cortical output were observed using TMS over the course of 5-days practice of a motor sequence (Pascual-Leone et al., 1995). Repetitive TMS over M1 was shown to disrupt the retention of behavioral improvement (Muellbacher et al., 2002) and was specific to the "offline" learning phase over the day but not overnight (Robertson et al., 2005). The same effect was observed using theta burst stimulation over M1 in a probabilistic SRTT (Wilkinson et al., 2010). On the other hand, studies using anodal transcranial direct current stimulation (tDCS) on M1 show a positive effect on skill acquisition in the "offline" phase (Galea et al., 2011; Reis et al., 2009; Schambra et al., 2011; Sehm et al., 2013) and specifically on consolidation in an implicit MSL task (Kang and Paik, 2011). Using Magnetic resonance spectroscopy, Kim and colleagues (2014) showed that these effects are mediated by significant reduction in GABA concentration over M1 which were correlated with behavioral parameters of motor learning and memory in a force adaptation task.

Imaging studies using PET and fMRI in healthy participants performing sequential finger tapping tasks showed increased activity over M1 in the fast and slow learning stages further establishing its role in the learning process (Jenkins et al., 1994; Karni et al., 1995; Seitz et al., 1990). In a SRTT, Honda and colleagues showed specific increase in activity over M1 during implicit MSL which was not evident when subjects gained explicit knowledge of the sequence (Honda et al., 1998). Later fMRI studies employing variants of the SRTT (Aznarez-Sanado et al., 2013; Bapi et al., 2006; Rose et al., 2011) corroborated these results establishing the fundamental role that M1 plays in implicit MSL.

Researchers have suggested that M1 is the site of storage of skilled sequential knowledge (Penhune and Steele, 2012) and internal representations of movements (Karni et al., 1995; Matsuzaka et al., 2007) as well as long-term consolidation (Robertson et al., 2005).

Basal ganglia

The basal ganglia are a set of subcortical structures: striatum, globus pallidus, substantia nigra, and subthalamic nucleus. The striatum, separated into putamen and caudate nucleus, receives projections from cerebral cortex, brain stem and thalamus and as such serves as the main input structure to the basal ganglia. Electrophysiological studies in animals showed that the basal ganglia serve as an important link within the cortico-basal ganglia-thalamo-cortical circuit which guides a wide range of motor behaviors (Alexander et al., 1990; Alexander et al., 1986). Originating from pre- and post-central sensorimotor cortical areas, neurons project onto putamen in somatotopical manner. Basal ganglia output is then conveyed to several thalamic nuclei and then, closing the loop, to motor cortex, SMA and PMC (Alexander et al., 1986). Within the basal ganglia, the processing can take place in two paths: the direct monosynaptic path through the internal segment of the globus pallidus and pars reticularis of the substantia nigra, or the indirect polysynamptic path through the external part of the globus pallidus, subthalamic nucleus and internal part of the globus pallidus. The direct pathway results in removal of inhibition from thalamo-cortical neurons which excite the motor cortical areas whereas the result of the indirect pathway is increased inhibition of thalamo-cortical neurons which inhibits the motor cortical areas.

While M1 lesions impose direct effects on motor control and response selection, lesions in the basal ganglia could cause indirect interference with coordinated movements. For example, in Huntington's disease (HD) striatal changes occur in inhibitory neurons forming the indirect

pathway. These changes will cause reduced output from the basal ganglia and thus greater excitation of thalamic neurons which will in turn excite the motor cortex. In Parkinson's disease (PD), dopaminergic neurons atrophy in the substantia nigra pars compacta and thus cause the output along the direct pathway to decrease which will increase the inhibitory effect on the thalamus. Along with other effects on the indirect pathway the net result would be reduced excitation of the motor cortex due to excessive thalamic inhibition.

The importance of basal ganglia, and more specifically the striatum, for motor sequence learning was first uncovered using a series of studies in patients with movement disorders as described above. Performance of PD (Doyon et al., 1997; Jackson et al., 1995; Pascual-Leone et al., 1993) and HD (Knopman and Nissen, 1991) patients in the SRTT was tested against healthy aged matched controls. Mild to severe impairments in learning were found in the patients group which led researchers to hypothesize that striatal structures are crucial for the learning process. These studies have paved the way to lesions studies in primates which showed that striatum was essential for learning behavior (Matsumoto et al., 1999; Miyachi et al., 1997). Electrophysiological recordings in primates and in behaving rats showed that patterns of neuronal activity in the striatum are specific to the stage of learning and may differ between associative and sensorimotor areas of the striatum (Miyachi et al., 2002; Thorn et al., 2010; Thorn and Graybiel, 2014; Yin et al., 2009). In healthy humans, fMRI and PET studies supported the significant involvement of putamen (Doyon et al., 2002; Jenkins et al., 1994; Rauch et al., 1997; Seitz et al., 1990; Toni et al., 1998) and caudate nucleus (Rauch et al., 1997; Toni et al., 1998) in both the early and the late phase of MSL. SRTT studies in PD patients showed learning-related deficits providing further evidence for the importance of striatum to MSL (Doyon et al., 1997; Jackson et al., 1995; Pascual-Leone et al., 1993). However, these findings were not always

consistent (Seidler et al., 2007; Smith et al., 2001), probably due to strong variability in the disease progression (Muslimovic et al., 2007; Stephan et al., 2011) and type of medication taken (Kwak et al., 2010, 2012) as well as variability in task demands.

The evidence above has led researchers to hypothesize that the role of striatum in motor sequence learning is to create probabilistic associations between subgroups of movements within a sequence through reward-based mechanisms (Graybiel, 1998, 2008). Penhune and Steele (2012) suggested that these associations develop with practice and the extent to which striatum is involved depends on the degree to which reward-based mechanisms are required.

Cerebellum

The cerebellum, positioned atop of the spinal cord, is around one-ninth of the neocortex volume but contains more than half of the neurons in the central nervous system. It has been long presumed that the cerebellum contributes primarily to planning and execution of movement (Stein and Glickstein, 1992) but recent evidence from neuroanatomical, imaging and behavioral studies has shown that cerebellar functions extend beyond the sensorimotor domain (Buckner, 2013; Ramnani, 2006). Efferent connections from cerebellum to contralateral cerebral cortex relay through a polysynaptic channel that projects to deep cerebellar nuclei through the thalamus. In turn, afferent connections to the cerebellum come from cortical areas through the brain stem (specifically, the pontine nuclei). Connections between the cerebellum and non-motor areas of the cerebrum, such as the prefrontal cortex, were first discovered in monkeys using an advanced transneuronal tracing technique which makes use of viruses to map such polysynaptic circuits (Bostan et al., 2013; Middleton and Strick, 1994). This evidence revealed an anatomical substrate for cerebellar contribution to cognition. Behavioral studies in patients with localized cerebellar lesions due to stroke or with specific cerebellar atrophy, further established the

contribution of cerebellum to cognitive functions. In a study by Schmahmann and Sherman (1998) cerebellar patients performed neuropsychological tests which revealed impairments in executive functions, visuospatial cognition, language, and social behavior. Evidence from a resting state fMRI study using functional connectivity measures showed that distinct regions of the cerebellum were communicating with cerebral premotor, association and limbic networks, supporting the contribution of cerebellum to functionality of these regions (Buckner et al., 2011). A topographic organization of higher order functions in the cerebellum was created using a meta-analysis study of 526 neuroimaging studies reporting cerebellar activations (Bernard and Seidler, 2013). The authors found that sensorimotor tasks activated the anterior lobe (lobule V) and lobule VI whereas language and verbal working memory were activating lobule VI and crus I, and executive functions activated lobule VI, crus I and lobule VIIB.

Theoretical models suggested (separately) by Marr (1969) and Albus (1971) predicted that the cerebellum is involved in motor skill learning due to the special regular organization of cerebellar microcircuit architecture. The model focused on long-term depression of the synapses from parallel fibers to Purkinje cells which contribute to eye-limb coordination and error-correction. With movement succession the parallel fiber input is increasingly suppressed which results in the climbing-fiber error signal to disappear. On the system level, error-based learning studies (Floyer-Lea and Matthews, 2005; Lehericy et al., 2005) and MSL studies (Grafton et al., 2002; Jenkins et al., 1994; Toni et al., 1998) showed that cerebellar activation decayed as learning progresses which may relate to the physiological model of the cerebellum as suggested above. It has been suggested that cerebellum's role in motor learning is to continuously adjust internal models in order to create a rapid and accurate representation of the complex movement (Ito, 2008; Ramnani, 2006).

To sum, evidence from electrophysiological studies in animal as well as imaging studies in humans show the specific involvement of M1 (together with PMC and SMA), striatum and cerebellum in motor learning. This line of evidence has led researchers to hypothesize a cortical-striatal-cerebellar network which is modulated as motor skill learning progresses with time (Doyon and Benali, 2005; Hikosaka et al., 2002; Penhune and Steele, 2012). Questions still remain though as to the nature of specific interactions between these brain regions which could shed light on the role each play within the network for the purpose of motor learning. In the following chapter I will review connectivity studies in motor skill learning.

Connectivity in MSL networks

As discussed in greater detail in section 1 of this chapter, exploring connectivity between different brain regions has become a standard practice in cognitive neuroimaging as the focus has shifted from a modular view on brain function to a functional integration perspective. Importantly, three different types of connectivity should be differentiated: structural, functional and effective connectivity. Structural connectivity refers to white matter architecture, functional connectivity to simple correlated activity between brain regions and effective connectivity to causal, directed interactions between brain regions.

Although implicated in numerous studies and suggested by several theoretical models, only recently, attempts have been made to characterize interactions between brain regions involved in MSL. In an elegant study using twin-coil TMS, a conditioning pulse applied to the cerebellum resulted in facilitation of contralateral M1 during learning in the SRTT (Torriero et al., 2011). A PPI analysis of SRTT revealed differential fronto-thalamic interactions associated with explicit vs. implicit MSL (Fletcher et al., 2005). Findings from explicit MSL tasks provided evidence for dynamic connectivity changes between motor and premotor regions which in turn affect

subcortical brain regions. For example, using coherence maps, increased connectivity was observed between a seed over left M1/S1 and premotor areas as well as parietal cortex, when comparing early to late learning stages of a novel sequence (Sun et al., 2007). A network of M1, PMC, parietal cortex and cerebellum was activated in an explicit MSL task which employed tensor independent component analysis approach for investigating whole-brain connectivity (Tamas Kincses et al., 2008). When motor performance becomes automatic, connectivity between M1 and cerebellum increases (Steele and Penhune, 2010) as well as between cerebellum, preSMA, putamen and cingulate motor area (Wu et al., 2008). On the other hand, Coynel and colleagues (2010) observed reduced functional integration as performance became automatic in a network comprising premotor areas, parietal cortex, basal ganglia and cerebellum. Effects of "offline" consolidation after sleep show increased functional integration in a network of premotor, putamen, parietal cortex and basal ganglia (Debas et al., 2014) in addition to specific striatal-hippocampal connections which were modulated by performance (Albouy et al., 2013). Finally, changes in resting-state functional connectivity were observed between dentate cerebellum, thalamus and basal ganglia shortly after implicit learning in the SRTT whereas following consolidation, enhanced connectivity was found between medial temporal lobe structures (Sami et al., 2014).

Recent studies show that learning of sequential motor tasks may also affect white matter integrity between motor cortical areas and subcortical regions such as basal ganglia and cerebellum. Using diffusion tensor imaging, structural integrity in the dentate-thalamo-cortical tract was correlated with early consolidation of the sequence, specifically with DLPFC (Schulz et al., 2014). Similarly, Bennet and colleagues showed sequence-specific learning effects on fractional

anisotropy values in a tract connecting a seed over DLPFC with caudate nucleus and in a later learning phase with hippocampus (Bennett et al., 2011).

To summarize, there is ample evidence for the involvement of motor cortical networks as well as basal ganglia and cerebellum in both early and late stages of MSL. However, specific influences of learning on causal interactions within these networks remain unclear. This is important because when attempting to specify a role for each of the brain regions in motor learning, one should explore the influence of learning on the directed interactions within this network.

1.3.3. The role of neural oscillations in learning and memory

One of the key markers of brain activity are coherent rhythmic fluctuations of activity within neuronal populations. In humans, neural oscillations are usually measured at the scalp using electroencephalography (EEG) but other methods to measure neural oscillations in patient populations exist (such as: electrocorticography or using deep brain stimulation electrodes). These oscillations which occur at different rhythms serve as a signature for the neural network properties and relate to different cognitive processes (Ward, 2003). Early studies have shown that increased oscillatory power at the theta (4-8 Hz) frequency band underlies long-term memory and memory encoding (Klimesch, 1999). Theta oscillations measured in hippocampus and surrounding structures in rodents were shown to be tightly related to spatial as well as episodic memory (Buzsaki, 2005). In humans, theta oscillations were shown to be modulated by working memory (Roux and Uhlhaas, 2014) over hippocampus (Tesche and Karhu, 2000) and other cortical sites (Moran et al., 2010; Raghavachari et al., 2001). Oscillations in alpha and in beta (13-30Hz) frequency range on the other hand, reduce in power during long-term memory processes (Hanslmayr et al., 2012) with the underlying function still under debate. Finally, gamma (>30Hz) frequency oscillations were shown as well to be related to successful memory

formation in humans (Osipova et al., 2006; Sederberg et al., 2007). It is therefore clear that one cannot simply pinpoint one specific frequency band which underlies memory processes in humans but probably interactions between oscillations in different frequency bands such as those discussed in section 0 serve a role in formation and maintenance of memory.

Much less is known about the relevance of oscillatory activity for visuomotor sequence learning. In a study which addressed this question, participants learned a visual sequence while high-density EEG was recorded (Moisello et al., 2013). Significant changes in alpha and theta power were observed during sequence performance over frontal and posterior regions. In a work from the same group, subjects learned to adapt to a visuomotor rotation (Perfetti et al., 2011). Increased gamma power was evident over right parietal region during initial learning while theta power increased in the same region during late learning stages. In another study, increased gamma band coherence was observed over caudal SMA around stimulus onset when rhesus monkeys produced visually guided series of movements (Lee, 2003). Thus it seems that oscillations in theta, alpha and gamma range may increase during visuomotor sequence learning, probably depending on the learning stage.

Cross-frequency coupling

Flexible and effective communication between neuronal populations is essential for cognitive behavior. Recently, theoretical models and empirical evidence have suggested that this communication is supported through cross-frequency coupling and particularly phase-based coupling mechanisms. Phase means the momentary deflection of an oscillation. These mechanisms entail: cross-electrodes phase coupling (Fries, 2005), cross-frequency phase coupling (Varela et al., 2001) and phase-amplitude coupling (Canolty and Knight, 2010).

Phase coherence takes place when the instantaneous phase of an oscillation from brain area A correlates to the instantaneous phase of an oscillation from brain area B (Lachaux et al., 1999). Phase coherence is based on the idea that the phase of an oscillation relates to time windows of increased excitability and thereby facilitated communication (Fries, 2005). Theta phase coupling has been shown to relate to working memory (Sarnthein et al., 1998; Sauseng et al., 2004; Serrien et al., 2004) as well as long-term memory processes (Sato and Yamaguchi, 2007; Summerfield and Mangels, 2005; Weiss and Rappelsberger, 2000). However, evidence also exist for alpha (Crespo-Garcia et al., 2013; Palva et al., 2010) and gamma (Gruber et al., 2001; Palva et al., 2010) phase coupling involvement in relation to working memory and long-term memory. The phase of an oscillation may also be coupled to the phase of an oscillation of a different frequency band in a process termed cross-frequency phase coupling. This type of synchronization, specifically between theta and gamma oscillations, has been also observed in the context of working memory (Sauseng et al., 2009; Schack et al., 2005). For phases to be coupled between different frequencies, highly coordinated activity should exist between neuronal populations such that a few cycles of the high frequency oscillation would match with one cycle of the slow oscillation. Therefore, cross-frequency phase coupling may serve as a mechanism for precise and specific communication between brain regions (Fell and Axmacher, 2011).

Phase-amplitude coupling (PAC) is the process in which the phase of a slow oscillation modulates the amplitude of a high-frequency oscillation. PAC has been hypothesized to serve as a mechanism in which local computation (in the form of gamma oscillations) communicate information over large-scale, global networks using slow oscillations such as theta and alpha (Canolty and Knight, 2010). Both in animal and human models, PAC was shown to underlie complex cognitive processes associated with decision making (Cohen et al., 2009; Tort et al.,

2008; van Wingerden et al., 2014), reward (Lee and Jeong, 2013), and cognitive control (Dürschmid et al., 2014) as well as motor dysfunction in patients with PD (de Hemptinne et al., 2013; de Hemptinne et al., 2015; Shimamoto et al., 2013). Recently, PAC has also been shown to mediate between different brain regions such as the thalamo-cortical connection (Malekmohammadi et al., 2015; Roux et al., 2013). Methods to assess PAC largely vary across studies (Penny et al., 2008; Tort et al., 2010) and thus may confound the results reported (Aru et al., 2015). Despite this caveat, PAC is considered to be a key mechanism for the coordination of neural dynamics.

Regarding learning and memory processes, most evidence exists for theta phase to gamma amplitude coupling. In rats, increased theta/gamma PAC was observed over the hippocampus and was correlated with performance accuracy in an associative learning task (Tort et al., 2009). In monkeys, theta/gamma PAC in the PFC (prefrontal cortex) was evident when items were stored in short-term memory (Siegel et al., 2009). In a task requiring working memory, theta/gamma PAC was also evident over medial PFC in a rodent study (Li et al., 2012). In humans, theta/gamma PAC was evident during working memory operations over different cortical regions (Canolty et al., 2006) as well as medial temporal lobe (Mormann et al., 2005) and hippocampus (Axmacher et al., 2010). Friese and colleagues (2012) showed that successful encoding of items into long-term memory was associated with increase in theta/gamma PAC over fronto-parietal network. Recent evidence from intracranial recordings in 56 patients revealed theta/gamma PAC associated with formation of new episodic memories in the hippocampus (Lega et al., 2014). Similar results were obtained in a MEG study of context-dependent memory: changes in theta/gamma PAC were evident during successful encoding and were sensitive to the encoding-retrieval overlap (Staudigl and Hanslmayr, 2013).

To sum, oscillations in various frequency bands were shown to be involved in memory processes (Hanslmayr and Staudigl, 2014). Evidence for oscillatory markers in visuomotor learning point to involvement of theta, alpha and gamma oscillations (Lee, 2003; Moisello et al., 2013; Perfetti et al., 2011) however, much less is known regarding implicit sequence learning. Cross frequency coupling mechanisms such as phase coherence, cross-frequency phase coupling and phase amplitude coupling, are suggested to facilitate long-range communication in the brain. Previous studies showed that phase amplitude coupling underlies various cognitive processes including learning and memory. It is therefore plausible that PAC provides a mechanism of communication between brain regions involved in motor sequence learning.

1.4. Research aims

In the series of experiments described in this thesis I aimed to address questions regarding the communication between different brain regions during motor sequence learning using the SRTT. For both fMRI studies (Chapter 2 and Chapter 3) I used dynamic causal modelling to delineate the causal interactions within the cortico-striato-cerebellar network. In Study 1 (Chapter 2) different dynamic causal models of M1-putamen-cerebellum network were compared and analyzed. Study 2 (Chapter 3) aimed at answering how these causal interactions change between early learning and after the sequence was consolidated after a night's sleep. Here a broader network of M1-PMC-SMA-putamen-cerebellum was investigated in order to answer questions regarding the role of premotor area in motor learning and consolidation. Finally, the EEG study (Chapter 4) enabled tapping into neural mechanisms that allow long-range communication, namely phase amplitude coupling of neural oscillations.

Chapter 2

Delineating the cortico-striatal-cerebellar network in implicit motor sequence learning [1]

2.1. Introduction

In our daily life we constantly acquire and retain motor skills that are crucial for basic as well as more complex motor behaviors. Motor sequence learning (MSL) is especially important for tasks such as typing or playing a musical instrument and is defined as the gradual increase in performance through repetition of a serial pattern (Willingham, 1998). Motor sequences can be learned explicitly, while subjects are aware of a sequence in the task, or implicitly, i.e. without a conscious recollection of a sequence. A well-established method for studying implicit MSL is the serial reaction time task (SRTT) in which subjects learn a sequential pattern of finger presses. Abundant evidence from animal and human work identified wide-spread neural circuits which are involved in the early stage of MSL in which rapid improvement in performance is observed. These include cortical (dorsolateral prefrontal cortex (dLPFC), motor and pre-motor regions, parietal cortex) and subcortical regions such as striatum and cerebellum (see recent review (Dayan and Cohen, 2011)). Theoretical models (Doyon et al., 2003; Hikosaka et al., 2002) and experimental evidence (Doyon et al., 2002; Jenkins et al., 1994; Jueptner et al., 1997; Seitz et al., 1990) stress the relevance of cortico-striatal and cortico-cerebellar circuits which work in parallel in order to mediate MSL. Previous studies have shown that different brain networks are involved in implicit and explicit MSL with striatal involvement being more pronounced in implicit MSL (Destrebecqz et al., 2005; Karabanov et al., 2010). Here, we aimed to study the dynamical

[1] This chapter corresponds largely to: Tzvi, Elinor, Thomas F. Münte, and Ulrike M. Krämer. "Delineating the cortico-striatal-cerebellar network in implicit motor sequence learning." *NeuroImage* 94 (2014): 222-230.

interactions within cortico-striatal and cortico-cerebellar circuits and their specific contributions to implicit acquisition of a motor sequence using dynamic causal modeling (DCM) on fMRI data of the SRTT.

2.1.1. Cortico-striatal-cerebellar networks during motor learning

MSL can be divided into two phases: an early learning stage characterized by rapid improvement in performance and a late phase in which further gains in performance occur over several practice sessions (Karni et al., 1998). The early stage of MSL in a SRTT usually lasts minutes (Karni et al., 1995) and modulates activity in a distributed brain network. Several studies showed that activity in cortical areas such as motor and parietal cortex as well as the cerebellum decreases as learning progresses, whereas the striatum was shown to be more active in the late learning stage (Lehericy et al., 2005; Seidler et al., 2005; Steele and Penhune, 2010). Based on human and animal studies, an influential model (Doyon et al., 2003; Hikosaka et al., 2002) suggests that a cortico-cerebellar network is recruited during the early phase of MSL while adjustments of movement kinematics to the sensory inputs are required. Once motor learning is established in the late learning phase, the activity is shifted to a cortico-striatal circuit when performance is more automatic. In a recent review, Penhune and Steele (2012) propose that the role of the striatum is to learn predictive associations between the individual movements in the sequence. The role of the cerebellum is suggested to create an optimal internal model, whereas the function of M1 is retention of the motor memory. Other regions as supplementary motor areas (SMA) and premotor cortex are also implicated in MSL (see e.g. (Hardwick et al., 2013)), but based on the outlined theoretical models, we focused on connectivity between M1, cerebellum and striatum in the present study. In the following we detail the experimental evidence pointing to the importance of each of these regions for MSL.

The role of the cerebellum in motor learning has recently been reviewed in an ALE meta-analysis by Bernard and Seidler (2013). Importantly, activation of the anterior cerebellum was found early in the task when the motor memory of the sequence is established. This activity decreased as learning progressed (Grafton et al., 2002; Jenkins et al., 1994; Toni et al., 1998). Although one study reported cerebellum activity to be related to performance improvement rather than sequence learning per se (Seidler et al., 2002), others showed that cerebellum is involved in the early stage of motor sequence learning and that this involvement depends on stimulus-response (S-R) mapping demands (Bo et al., 2011; Spencer and Ivry, 2009). Some studies hypothesized that the role of the cerebellum in motor learning is to form internal models of action (for review see (Wolpert et al., 1998)), whereas others attributed cerebellar activity to the generation of prediction errors (Ohyama et al., 2003).

The striatum is thought to play a critical role in encoding motor programs and has consistently been shown to be involved in motor learning (for reviews see (Doyon et al., 2009; Penhune and Steele, 2012)). In contrast to the cerebellum, the striatum increases in activity as learning progresses, suggesting that it is involved in storage and retention of the learned sequence. However, this increase might be more specific to sensorimotor regions of the putamen while more associative regions are actually decreasing in activity as learning progresses (Lehericy et al., 2005). Supporting the significant role of striatum in MSL, patients with striatal dysfunction (e.g., Parkinson's disease) showed deficiency in acquiring new motor sequences (Doyon et al., 1997; Jackson et al., 1995; Laforce and Doyon, 2001). Evidence from animal work points to both striatonigral (known as the direct pathway) and striatopallidal circuits (indirect pathway) which were specifically activated while mice were learning a new sequence of movements (Jin and Costa, 2010; Jin et al., 2014). Specifically, distinct subsets of neurons encoded the initiation or

termination of sequences whereas other neurons were active or suppressed during the whole period of sequence execution. These findings indicate that basal ganglia circuits are responsible not only for movement sequence initiation or termination but also for concatenation of individual movements into action chunks.

The final key brain structure involved in MSL is M1, the main motor cortical output. Apart from many imaging studies showing involvement of M1 in MSL (e.g: (Karni et al., 1995; Muellbacher et al., 2002)), it has been shown that stimulation of M1 using TMS (Muellbacher et al., 2002) or inhibitory TBS (Wilkinson et al., 2010) disrupted the early stage of motor consolidation, whereas tDCS (transcranial direct-current stimulation) of M1 facilitated motor skill learning (Nitsche et al., 2003; Schambra et al., 2011) and enhanced consolidation and long-term retention (Galea et al., 2011; Reis et al., 2009). On the other hand, tDCS of lateral or medial prefrontal as well as premotor cortex did not cause changes in performance (Nitsche et al., 2003). Moreover, single-neuron recordings in monkeys provided evidence for differential activation of M1 neurons in random and sequence blocks after extensive motor training, pointing to M1 as storage site for motor memory (Matsuzaka et al., 2007).

2.1.2. Connectivity analyses of MSL and the present study

With the current study, we set out to characterize the dynamic interactions between M1, cerebellum and striatum during implicit MSL. A few studies have examined the dynamic interactions between these brain regions using connectivity analyses. For example, a study employing structural equation modeling (SEM) showed that connection from cerebellum to M1 was weakened with time whereas connection from striatum to M1 was strengthened (Ma et al., 2010). In a study using tensor independent component analysis (tICA) (Tamas Kincses et al.,

2008), an M1-premotor-parietal-cerebellar network showed significantly higher mean activity during explicit sequence learning in comparison to random material.

Here, we used DCM to study cortico-striatal and cortico-cerebellar connectivity. In contrast to methods of functional connectivity analysis, DCM allows to infer on the directionality of connections and thus determine whether learning influences forward, backward or reciprocal connectivity. Moreover, using DCM we could compare models in which learning modulates cortico-cerebellar and/or cortico-striatal connections. DCM has been proven useful to characterize specific connectivity changes within cortical motor networks related to uni- vs bimanual motor actions (Grefkes et al., 2008a), to detect altered cortical connectivity after subcortical strokes correlating with motor deficits (Grefkes et al., 2008b) and to delineate performance-related changes in effective connectivity within cortico-striato-cerebellar motor networks (Pool et al., 2013).

We predicted negative modulatory effects in M1-cerebellar connectivity as cerebellum becomes less activated during learning and decreased functional connectivity was observed in a wider network including M1 and cerebellum (Tamas Kincses et al., 2008). In addition, we predicted positive modulatory effects of learning on connectivity between M1 and putamen as suggested by the model of Doyon and colleagues (Doyon et al., 2003).

2.2 Materials and Methods

2.2.1 Subjects

25 healthy subjects (15 women, age: 20-32) participated in the study after giving informed consent. Participants were right handed and had normal or corrected to normal vision with no reported color vision deficiency. All 25 subjects were included in the behavioral analysis. In two subjects we found brain tissue abnormalities (as assessed by a neuroradiologist) which prevented

us from further using their functional imaging data. For the purpose of group analysis using statistical parametric mapping (SPM) and the general linear model (GLM), we had to exclude an additional subject due to failed normalization to the template brain image. 22 subjects were therefore included in this analysis. In five additional subjects, we could not extract time-series for the effective connectivity analysis (see below for further explanation), therefore 17 subjects (10 women, age: 20-32) were finally analyzed using DCM. The study was approved by the Ethics Committee of the University of Lübeck.

2.2.2 The SRTT and implicit MSL

The SRTT is a commonly used method to study implicit motor sequence learning (Nissen and Bullemer, 1987). In this task, subjects are asked to respond with a key press to a visual cue that changes in each trial. Embedded within the task and usually unknown to the subject is a pattern of visual cues which will produce sequential key presses. Subjects who implicitly learn the sequence become faster in the sequential trials in comparison to trials with random visual cues.

It is debated (Robertson, 2007) whether the motor and perceptual domains can be distinguished in the classical SRTT, i.e., whether RT changes are due to participants' learning of the sequence of button presses (motor learning) or rather due to their acquisition of the visual sequence (perceptual learning). Here, we implemented a SRTT with a trial-by-trial remapping of the visuo-motor response (Rose et al., 2011). By de-correlating the motor from the perceptual domain, observed learning effects can be attributed to the motor domain only.

2.2.3 Experimental paradigm

Subjects performed the SRTT in the magnetic resonance imaging (MRI) scanner. In each trial, six randomly ordered colored squares (red, yellow, black, blue, magenta, and green) were

presented around the center of a white colored screen through MR-compatible goggles. An additional target square in one of these six colors was presented in the middle of the screen (see Fig. 2.1A). Subjects were instructed to respond to the target square by pressing on the corresponding key on MR-compatible keypads, one for each hand. Each of the four sessions in the experiment contained six blocks: three blocks of sequence material (SEQ) and three blocks of random material (RND) in an alternating order (See Fig. 2.1B). Fifteen seconds breaks were introduced in between the blocks during which participants were instructed to fixate on a black cross in the center of the screen. In each block there were 36 targets to which the participants had to respond. There were three repetitions of a hidden 12-element sequence (5-4-1-4-2-6-3-6-1-3-5-2) in SEQ blocks or 36 randomly assigned targets in RND blocks. The random material was generated using MATLAB (Natick, MA) such that elements were not repeated. Visual stimuli were presented until the onset of button press or the onset of the next trial. Inter-stimulus interval was kept at 1.5s in order to avoid explicit awareness of the underlying sequence (Destrebecqz and Cleeremans, 2001). We used Presentation® software (Version 16.3, www.neurobs.com) to present stimuli and to synchronize the stimulus presentation and the MR functional sequences.

Immediately after performing the SRTT in the scanner, subjects were asked (outside of the scanner) whether they had noticed any regularity in the task they just performed. Subjects were then informed about the hidden sequence and performed in a completion task in order to assess possible explicit awareness. In this task, the exact same stimulus of the main task was presented (see above). The 12-element sequence was repeated 15 times. In each repetition two regular trials were substituted by completion trials. In a completion trial, the target square was replaced by a question mark and subjects had to press a button corresponding to one of the six colored squares which they believed should be the current target square color. Each position in the sequence

except the beginning and the end of the sequence was therefore tested three times producing 30 completion trials. After guessing, subjects were asked whether they were sure of their choice and gave YES/NO answer. We thus differentiated between a correct response and a correct assured response.

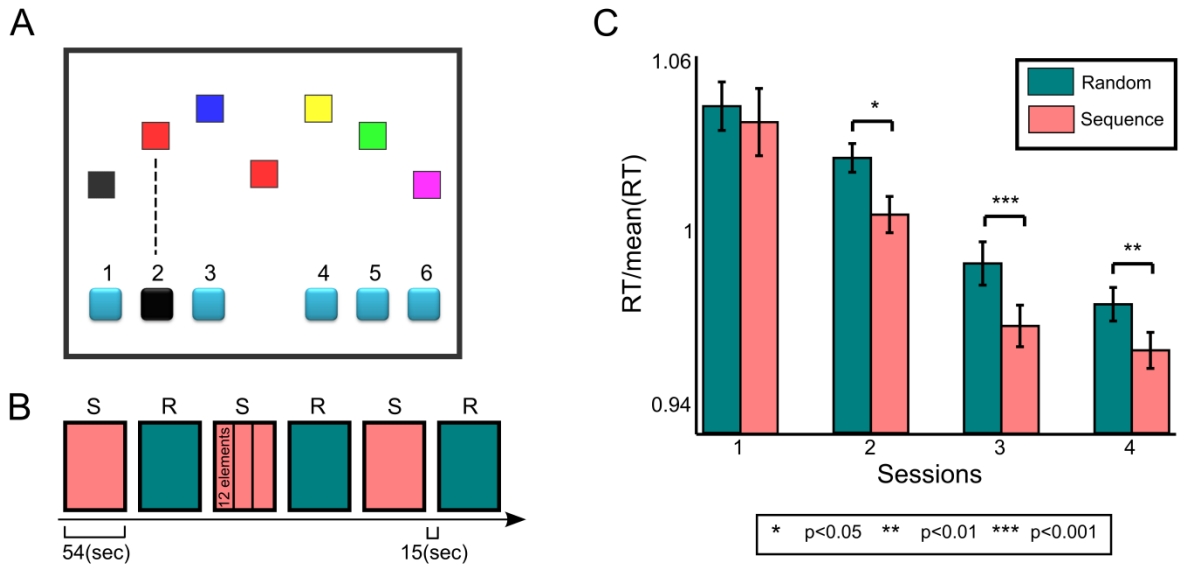

Figure 2.1. A Serial reaction time task (adapted from Rose et al., 2011). In each trial, 6 squares arranged around the center were assigned a random color. A target square in the middle of the screen was assigned a color corresponding to one of the 6 colors. During sequence blocks the color of the target square always corresponded to a specific button press as part of the 12-element sequence. During random blocks the color of the target square was chosen randomly. **B** Experimental design for a single session contained three blocks of sequence elements and three blocks of random elements. In each block there were 36 targets to which the participant had to respond: three repetitions of a hidden 12-element sequence (5-4-1-4-2-6-3-6-1-3-5-2) in Sequence blocks (marked with 'S') or 36 randomly assigned targets in Random blocks (marked with 'R'). **C** Behavioral performance in the SRTT. Normalized reaction times (by mean reaction time of each subject across task conditions) are presented for each condition. Error bars are standard errors of the normalized reaction times. Significant differences between conditions are marked with an asterisk.

2.2.4 Imaging

MR protocol was carried out with a 3T Philips Achieva head-scanner in the Department of Neuroradiology, University of Lübeck. Functional MRI data (T_2*) was collected using blood oxygen level dependent (BOLD) contrast in 4 sessions each with 284 volumes. Gradient-echo EPI sequence was used with the following specifications: repetition time TR = 1466ms, echo

time TE = 28ms, flip angle = 90°, matrix size 64x64mm, FOV = 192x192mm with a whole brain coverage, 31 axial ascending slices of 3mm thickness and 1mm gap; In-plane resolution of 3x3mm; SENSE factor of R = 2. Subsequently, a high resolution T_1-weighted structural image was acquired with FOV = 240x240mm; matrix size 240x240mm; 180 sagittal slices of 1mm thickness.

2.2.5 Behavioral analysis

For the SRTT, we computed reaction times (RTs) for both the SEQ and RND conditions with the difference being our measure of implicit sequence learning. To assess statistical significance, we used a repeated measure ANOVA with factors condition (SEQ, RND) and session (sessions 1-4) and subsequent t-tests to determine whether there were significant differences between the conditions for each session. We also compared the median error rate between both task conditions for each session using the Wilcoxon signed-rank test. Both wrong button presses and missing responses were regarded as errors.

For the completion task, we evaluated the median number of correct responses and correct assured responses.

2.2.6 Pre-processing and statistical analysis

Preprocessing of fMRI data was done using SPM8 software package (http://www.fil.ion.ucl.ac.uk/spm/) and comprised slice timing correction, realignment to correct for head motion artifacts, co-registration to T_1 structural image, segmentation, normalization to Montreal Neurological Institute (MNI) template brain image, smoothing with a Gaussian kernel of 8mm full width half maximum and resampling of functional images to 3x3x3 mm. In one subject, normalization of functional images to standard space failed. As normalization is a crucial step for specifying regions of interest for our DCM analysis, this subject was excluded

from further analysis. Imaging data from 22 subjects was subsequently modeled using the general linear model (GLM) in a block design manner. Linear regressors were obtained for each of the experimental conditions (SEQ and RND) and each session in each subject. Statistical parametric maps (SPMs) were generated by convolving a box function with duration of one block with a hemodynamic response function. Movement related parameters from the realignment process were included in the GLM as regressors of no-interest to account for variance caused by head motion.

2.2.7 Dynamic causal modeling

Dynamic causal modeling (DCM) (Friston et al., 2003) allows inferring on the "hidden" neural states from measured brain data using predefined models. This method estimates the posterior moments of connectivity parameters as well as selecting, using Bayesian model selection (BMS), a "winning" model out of a candidate set of equally plausible models. In DCM for fMRI (as implemented in SPM8 version DCM12), a bilinear forward model is used to describe the neuronal dynamics of a system of distributed brain regions, each represented by a single state variable. Regional- and time-dependent changes in activity $\frac{d\vec{x}}{dt}$ could be then constructed as a system of differential equations:

$$(1) \quad \frac{d\vec{x}}{dt} = \left(A + \sum_{j=1}^{m} u_j B^{(j)} \right) \vec{x} + C\vec{u}$$

Here, $\vec{x}$ is the state vector and $\vec{u}$ is the input vector to the system. A matrix represents the endogenous (context independent) connections, B represents the modulatory (context dependent) connections, and C is the influence of direct inputs to the system. Together with a biophysically motivated hemodynamic model, an estimated BOLD signal is modeled using Bayesian methods and subsequently compared to the acquired data. Bayesian model estimation

procedure results in two quantities: model evidence, which is the probability of the data given the model, and a posterior distribution over model parameters. Approximation of the model evidence is done using a variational Bayes (VB) approach in which the posterior estimates of the parameters are updated iteratively through a gradient ascent on the free-energy bound. Subsequently, model comparison using BMS is achieved using this free-energy approximation which is a tight lower-bound on the log-model evidence (Friston et al., 2007).

2.2.8 Time series extraction

We aimed at investigating the causal interactions between primary motor cortex (M1), putamen (Pu) and cerebellum (CB) as suggested by theoretical models of motor learning (Doyon et al., 2009; Hikosaka et al., 2002). We therefore used six regions of interest (ROIs; three in each hemisphere) to extract time series from significant voxels (see Table 2.1) in task>baseline contrast (both SEQ and RND conditions) in order to account for both learning and non-learning related changes in the BOLD signal. Based on results of a recent motor learning meta-analysis (Hardwick et al., 2013) we selected the coordinates of the sphere center for each ROI (see Table 2.1). For each individual subject, the sphere center of each ROI was moved to the closest suprathreshold voxel which was always kept within 10mm of the original sphere center. Using the xjview toolbox (http://www.alivelearn.net/xjview) and AAL brain atlas we verified that sphere centers for all subjects were within the regions of interest. For left and right M1, sphere centers were kept within BA4. Significant voxels were chosen based on a strict p-level threshold ($p<0.001$ for M1 and Pu and $p=0.05$ FWE corrected for CB) in order to specifically capture the effects driven by the motor task (for a similar approach see (Grefkes et al., 2008a; Pool et al., 2013)) and to prevent noise from entering the model as this would affect model estimation. Using a singular value decomposition procedure implemented in SPM8, we computed the first

eigenvariate across all suprathreshold voxels within 4mm (Pu) or 6mm (M1 and CB) radius from the sphere center for each subject in each session. Time series were then adjusted for the effects of interest and sharp improbable temporal artifacts were smoothed by an iterative procedure implementing a 6-point cubic-spline interpolation. Temporal artifact smoothing was done in order to achieve a more robust measure for model fitting in the subsequent DCM analysis. Time series in bilateral Pu in 5 subjects could not be obtained because of no suprathreshold voxels in those ROIs, so these subjects were excluded from further analyses.

Table 2.1: Regions of interest for the DCM analysis

Region	MNI-coordinates	p-level	Sphere Radius (mm)
lM1	-38,-24,58	0.001	6
rM1	40,-20,54	0.001	6
lPu	-24,4,4	0.001	4
rPu	26,0,2	0.001	4
lCB	-20,-52,-22	0.05 FWE	6
rCB	10,-58,-20	0.05 FWE	6

2.2.9 DCM specification

FMRI data from 17 subjects was used for the DCM analysis. Input vector $\vec{u}$ was constructed as a stick function of the single events of stimulus presentation. In the first step, we determined the optimal intrinsic connections in our data set by constructing 8 models with reciprocal (bidirectional) connections within all ROIs in each hemisphere, and task inputs either to CB (4 models) or Pu (4 models) (see Fig. 2.2). M1 was not tested to be an input region as it is known to

be the main cortical output. We assumed that during a bi-manual motor task, connectivity patterns are symmetric for both hemispheres and therefore examined the connections between hemispheres by systematically reducing them in the models (see Fig. 2.2). We chose to test models with bilateral connections between brain regions for intrinsic connectivity based on results from a DCM study of bi-manual motor task (Grefkes et al., 2008a). For this analysis we did not include any modulatory parameters (B=0). After inverting and estimating the models, we used fixed-effects (FFX) BMS to find the optimal model for intrinsic connections. Following guidelines for DCM analyses (Stephan et al., 2010), we chose FFX analysis since we assume that the optimal model of intrinsic connections driven by a visuo-motor task is consistent across subjects.

In the second step, we used the optimal model of intrinsic connections and tested 22 models which varied across three main factors that represented our main research questions:

2. Which modulatory input can best explain the data: task performance or motor sequence learning?

   This model comparison procedure addresses whether the connectivity between M1, CB and Pu can be explained by motor performance in the task (taking both the RND and SEQ conditions) or specifically by learning during the SEQ condition only.

3. Which circuitry is modulated,

   the cortico-striatal, cortico-cerebellar or both?

4. Which directional connections are modulated,

   backward (cortical to subcortical), forward (subcortical to cortical) or reciprocal (backward and forward) connections?

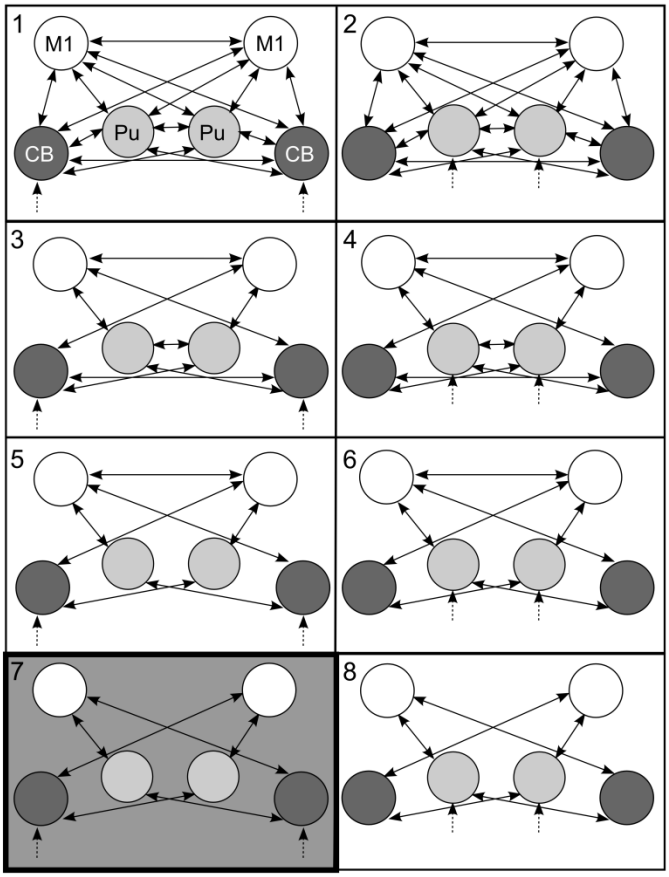

Figure 2.2. Eight models of intrinsic connections during a motor task were compared using Bayesian Model selection. Models were kept symmetric between hemispheres. Along the rows, connections across regions of interest (ROIs) are gradually removed. Along the columns, CB and Pu are tested for the motor task input. Dotted arrows are task inputs. The winning model is marked with a green frame.

Model comparison

We then performed RFX BMS to compare the 22 models. RFX analysis computes the likelihood of a specific model to generate the data of a randomly chosen subject and therefore outliers have little impact on the result (Stephan et al., 2009). This analysis was chosen here since it is plausible that networks for implementing MSL are not consistent across subjects. RFX BMS was implemented using Gibbs sampling (in our study we used a total of 2e6 samples) which randomly draws model probabilities based on the posterior distribution (Penny et al., 2010).

In some cases, RFX BMS might give spurious results as it depends on the model space. This means that adding or subtracting even one model can reverse the ranking of the best models (Penny et al., 2010). In order to address this issue we performed RFX family level inference as implemented in SPM8 ('spm_compare_families.m' version 5007). Bayesian model averaging within each family produces a more stable result (Penny et al., 2010). Based on the factors which were varied across models (detailed above), we obtained three families for comparisons:

- Family 1 contains two types of models: models in which the motor task modulates connectivity and models in which learning modulates the connectivity.
- Family 2 contains three types of models: models in which putamen-M1 (pu-M1) connection is modulated, models in which Cerebellar-M1 (CB-M1) connection is modulated and models in which putamen-M1 and CB-M1 connections are modulated.
- Family 3 contains three types of models: models in which the forward architecture (from subcortical to cortical) is modulated, models in which the backward architecture (from cortical to subcortical) is modulated and models in which reciprocal connections are modulated.

Parameter estimates in the winning model

After selecting the "winning model" out of the candidate set of 22 models with modulatory connections, we evaluated the significance of intrinsic connections as well as the significance of the modulatory effects across subjects. Using a Wilcoxon signed rank test ($p<0.05$, Bonferroni corrected for multiple comparisons), we tested across subjects how likely the effect of interest is different than zero. This analysis provided a statistical estimate for the consistency of our findings across subjects. For the intrinsic connections this procedure was done across sessions, whereas the significance of modulatory connections was evaluated in each session separately in

order to examine session-dependent changes. We report the strength of the connections in Hz across subjects (mean±SE) and the corresponding p-value.

In addition we performed correlation analysis of parameter estimates of each subject in each session with normalized RTs.

2.3 Results

2.3.1 Behavioral results

Response times and errors

Behavioral results are based on data of all 25 subjects. RTs differed significantly between task conditions and across sessions. An ANOVA with the factors condition and session showed a decrease in RTs with sessions ($F_{3,72}$ = 15.9, p<0.0001) and faster responses in sequence relative to random blocks ($F_{1,24}$ = 24.89, p<0.0001). When comparing RTs for the different sessions separately, we did not observe significant differences in the first session (t_{24} = .47, p = .64), but in sessions 2 – 4 (all p < .05). However, the interaction session x condition was not significant ($F_{3,72}$ = 2.78, p = .28). Data analyses were done on non-normalized data. Presented in Figure 2.1C are normalized RTs, which were calculated for each subject by dividing the RTs in each condition and each session by the mean RT of the subject across all trials.

The error rate was very low (1.66%±0.25%) and no differences between task conditions were found (p = .97). This result is comparable to previous findings with this paradigm (Rose et al., 2011). When comparing session 1 with sessions 2 (p = .032) or with session 4 (p = .032), we found that subjects committed less errors indicating that subjects improved in task performance with time.

Assessment of implicit learning

When asked whether they noticed anything in the task, subjects did not report any awareness of a regular structure. One subject reported that the task involved learning but could not specify whether it was the order of the colors or the locations that needed to be learned.

In the completion task, we found that the median rate of correct responses was 16.7% (range: 10%-36.7%, chance level: 20%). Median rate of correct assured responses was 3.3% (range: 0%-13.3%). These results show that participants did not gain explicit knowledge of the sequence.

2.3.2 DCM analysis

Bayesian model selection

When testing for the optimal model of intrinsic connections (with no modulatory effects on connections) we found that model 7 (Fig. 2.2) in which task inputs were to the CB bilaterally and reciprocal connections existed within hemisphere but not across hemispheres, was the most probable. Based on this model, we tested modulatory effects of both the learning condition (SEQ blocks) and task condition (both SEQ and RND blocks). Using RFX BMS on all sessions, we found that in the winning model (see Fig. 2.3B) with the largest exceedance probability (p_ex = 0.33), learning modulated backward connections from M1 to CB bilaterally. In the next most probable model (p_ex = 0.18), learning modulated the forward connection from Pu to M1 bilaterally (see Fig. 2.3A). When comparing this model to the winning model using the fixed effects BMS procedure, a relative log-evidence of 16.6 corresponding to a Bayes factor (BF) of $e^{16.6} = 1.6 \cdot 10^7$ was obtained, which is considered to be a very strong difference for one model over another (Kass and Raftery, 1995).

Using RFX family level inference, we could then corroborate the results of the BMS procedure on each individual model. We observed that models, in which learning modulated the different connections, had a higher exceedance probability (p_ex = 0.91) in comparison to models, in which the motor task was modulating the connections (p_ex = 0.09) (see Fig. 2.3C). This result demonstrates that dynamic network interactions between the regions of interest are modulated specifically by learning and not by motor performance in the task. Family level inference on the directionality of the connections showed that models with backward connections were superior to models with forward or reciprocal connections. Finally, models that included CB-M1 connections were superior in comparison to Pu-M1 connections or to both CB-M1 and Pu-M1 connections (see Fig. 2.3C).

Model parameters

Endogenous connectivity parameters (fixed connections strengths) in the winning model across sessions were positive and significant across subjects for the connections from CB to M1 and from CB to Pu bilaterally (see Table 2.2). An additional relatively weak positive connection from rM1 to rPu was as well significant across subjects.

For each session separately, we then investigated how learning modulated the connectivity from M1 to CB as suggested by the winning model. We observed that during the first and fourth session there were no significant modulatory effects. During the second session, bilateral connections from M1 to CB were significantly negatively modulated by learning (rM1 to lCB: p = 0.0036; lM1 to rCB: p = 0.0026). During the third session, only the modulatory effect on the connection between lM1 and rCB was significant (p = 0.0006 and see Figure 2.3D). Note that the intrinsic connections from M1 to CB were very close to zero across sessions in most subjects (see Table 2.2).

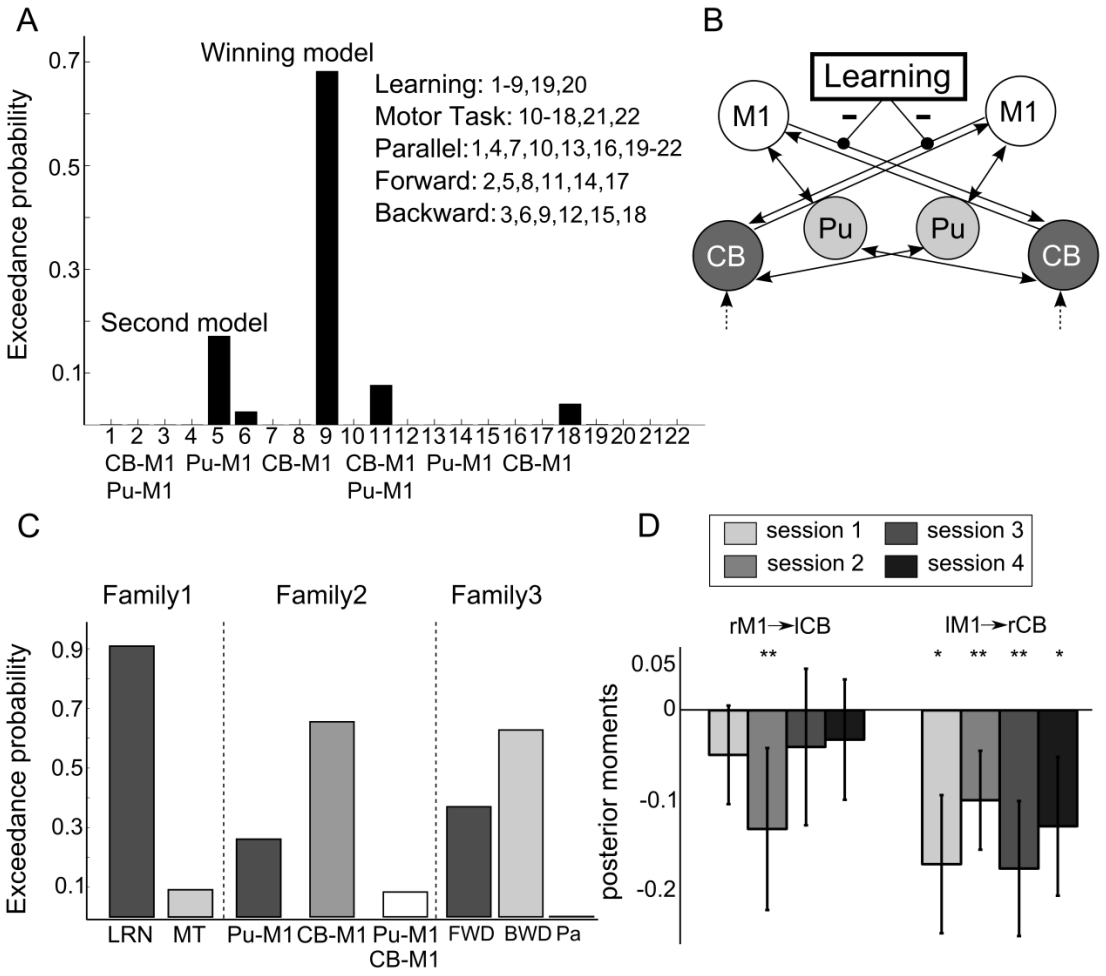

Figure 2.3. Bayesian model selection results. **A** Exceedance probability in 22 models compared using RFX BMS. **B** The winning model architecture. Learning is modulating the connections from M1 to CB bilaterally. **C** RFX family-wise inference. Family 1 compares models in which the motor task (MT) modulates connectivity to models in which the learning condition modulates the connectivity (LRN). Family 2 contains three types of models: models in which the putamen-M1 (pu-M1) connection is modulated, models in which the cerebellum-M1 (CB-M1) connection is modulated and models in which both the putamen-M1 connection and the CB-M1 connection are modulated. Family 3 contains three types of models: models with forward architecture (FWD - from subcortical to cortical), models with backward architecture (BWD-from cortical to subcortical) and parallel (Pa) or bi-directional connectivity. **D** Posterior moments of connectivity parameters (mean±SE). Significant parameters are indicated with asterisks (* $p<0.05$, ** $p<0.05$, Bonferroni corrected).

We were not able to analyze differences in connectivity parameters between "good learners" (defined as performing above chance level in the completion task) and "bad learners" due to low

sample size (only five "good-learners" were analyzed using DCM). In addition, we found no significant correlations between behavioral performance in the task and the parameter estimates.

Table 2.2: Posterior estimates of intrinsic connections in the winning model (mean±SE)

Connections	Strength (Hz)	p-value
rPu -> rM1	-0.157±0.061	0.0312*
rPu -> lCB	-0.115±0.066	0.4631
lPu -> lM1	-0.217±0.097	0.0217*
lPu -> rCB	-0.207±0.127	0.7583
rM1 -> rPu	0.050±0.015	0.0007**
rM1 -> lCB	-0.004±0.024	0.9434
lM1 -> lPu	0.013±0.011	0.2097
lM1 -> rCB	-0.004±0.032	0.4925
rCB ->lPu	0.246±0.045	0.0006**
rCB ->lM1	0.357±0.088	0.0003**
lCB -> rPu	0.209±0.037	0.0006**
lCB -> rM1	0.381±0.061	0.0003**

Starred values are significant (*p<0.05, **p<0.05, Bonferroni corrected)

2.4. Discussion

We used DCM (Friston et al., 2003) to study dynamic network interactions within the cortico-striatal-cerebellar loop during implicit motor sequence learning. Behavioral effects indicated that subjects were able to learn the 12-element sequence without explicit awareness of the sequence. Using BMS across a set of hypothesized models, we found that in the most probable model, causal connections from M1 to cerebellum bilaterally were negatively modulated by learning.

This might be the cause of the decreased activity in cerebellum as learning progresses. Importantly, using family level inference we could show that models in which connections between M1 and putamen were modulated by learning were inferior to models in which connections between M1 and cerebellum were modulated by learning. This finding suggests that the cortico-cerebellar loop, as proposed by theoretical models of motor sequence learning (Doyon et al., 2003; Hikosaka et al., 2002) plays a distinctive role in implicit MSL.

2.4.1. Behavioral effects of motor learning

In order to assess the specific effects of the motor component in motor sequence learning, we employed an experimental design in which random presentation of colored stimuli prevent perceptual sequence learning (Rose et al., 2011). Learning related effects were addressed by comparing RTs during the 12-element sequence blocks to the random stimuli blocks. Performance differed significantly between task conditions from the second session onwards. In addition, RTs in both conditions significantly decreased during the experiment pointing to a general improvement in task performance. While improved performance in the sequence material was expected based on a previous study employing this paradigm (Rose et al., 2011), we found no interaction effect between session and condition. The behavioral results indicate that subjects did not reach the learning asymptote and thus might have remained in the early stage of implicit motor sequence learning. It might be that the quick succession between sequence and random blocks prevented early-on consolidation of the sequence. However, our design was similar to the work by Rose et al. (2011) in this regard, which did show an interaction between condition and session. The lack of explicit awareness of an underlying sequence was successfully achieved in all subjects by taking a short inter-trial interval (Destrebecqz and Cleeremans, 2001) and randomizing the colors in each trial.

2.4.2 Effective connectivity

We constructed dynamic causal models (DCMs) to test whether and how interactions within the cortico-striatal-cerebellar loop are modulated by motor sequence learning based on the hypothesized main role of this loop in theoretical models of motor learning (Doyon et al., 2003; Hikosaka et al., 2002). To our knowledge, effective connectivity changes within this network related specifically to learning and not motor performance per se have not been investigated previously. Using BMS procedures, we were able to show that changes in causal connections within this network could be best explained by models which included modulation through learning. In order to ensure the stability of our results we conducted the analysis in two steps: comparing all inverted models using RFX BMS procedure and subsequently using RFX family level inference (Penny et al., 2010) to corroborate the results of the first step. We showed with high confidence (very strong BF in comparison to the next most probable model) that learning-related modulation of bilateral M1 to cerebellum connections is more probable than modulation of putamen-M1 connectivity. We suggest that since subjects did not reach the learning asymptote and thus did not enter the late learning stage, the cortico-cerebellar network might dominate over the cortico-striatal loop.

Intrinsic connections within the cortico-striatal-cerebellar network, representing the underlying connectivity patterns without task-related modulation (context independent connection strength) were significantly positive for causal connections from cerebellum to both putamen and M1. These might represent the positive feed-forward connections related to the task input to the network. We found that modulatory effects on the connections from M1 to cerebellum bilaterally were significantly negative across subjects in session 2, when reaction times started to differ between sequence and random material. Compared to a close to zero intrinsic connection

strength from M1 to cerebellum, this result represents a strong inhibitory effect. In session 3 this inhibitory effect, causing a decrease in activity in cerebellum as learning progresses, was even strengthened but only for the left M1-right cerebellar connection.

2.4.3 Role of cerebellum in MSL

The cerebellum ROI in the present study was located in the area of lobules V/VI in the anterior part of the cerebellum. The anterior cerebellum is known to be polysynaptically connected to cortical motor areas via deep cerebellar nuclei and the thalamus, whereas the posterior cerebellum is connected primarily to prefrontal and association cortex (Bernard and Seidler, 2013; Buckner et al., 2011; Schmahmann and Pandya, 1997). Moreover, the anterior cerebellum shows topographically organized somatomotor representations with the current cerebellum ROI corresponding to the hand area which is strongly connected to the hand area in M1 (Buckner et al., 2011). Importantly, a few studies have recently investigated the relationship between the structural quality of the cerebello-thalamo-cortical pathway and behavioral performance in motor sequence learning tasks (Carbon et al., 2011; Schulz et al., 2014). In a study by Schulz and colleagues (2014), the relationship between learning gains in a rhythmic MSL task and white matter (WM) structural quality of the dentato-thalamo-cortical tract was assessed by means of diffusion tensor imaging and probabilistic tractography. The authors report significant correlation between behavioral improvement during early consolidation of the temporal sequence and WM structural quality of a tract connecting the dentate nucleus of the cerebellum and the right DLPFC. This finding stresses the significant contribution of cerebellar-cortical connectivity particularly to movement timing. Notably, the authors investigated also tracts connecting the dentate nucleus of the cerebellum to either left or right M1 or PMC, however no significant correlations between these tracts and any of the behavioral parameters in the MSL task were

found. How the effective connectivity between these regions relates to anatomical connections remains to be studied therefore.

A decrease of cerebellar activity with motor learning has been observed in several studies (Grafton et al., 2002; Jenkins et al., 1994; Toni et al., 1998) and was hypothesized to be related to the computation of prediction errors which takes place during the early stage of learning but less when the motor sequence is already established (Doyon et al., 2009). A decreased BOLD signal after learning might reflect long-term depression of synaptic connections within cerebellar circuits which has been hypothesized previously as learning mechanism in the cerebellum (Albus, 1971; Ito, 1982; Marr, 1969). Our results suggest that the cause for this decrease in cerebellar activity is M1. In the MSL model, cerebellum receives motor task input which is then communicated to M1 and reciprocally communicates back to cerebellum. In the winning model, this backward communication is modulated by implicit acquisition of a motor sequence. Based on this network model, we would predict that impairing M1 or cerebellum will disrupt this reciprocal connection and will cause behavioral deficits in MSL. This is exactly what is observed in studies impairing M1 using stimulation techniques (Muellbacher et al., 2002; Wilkinson et al., 2010) and in a procedural learning study stimulating cerebellum using TMS (Torriero et al., 2004).

Supporting our hypothesis of the cerebellum's role in MSL, cerebellar lesion patients showed consistently impaired or absent learning when tested with the SRTT (Doyon et al., 1997; Gomez-Beldarrain et al., 1998; Molinari et al., 1997; Pascual-Leone et al., 1993; Shin and Ivry, 2003). However, a study of patients with cerebellar degeneration attributed performance deficits to impaired working memory and representation of S-R mappings rather than to motor sequence learning per se (Spencer and Ivry, 2009). Interestingly, Bo and colleagues (Bo et al., 2011) have

investigated this assumption with a group of healthy subjects using a learning paradigm with both symbolic and spatial representation of a sequence. The authors showed that the left cerebellum was recruited specifically in the symbolic condition and that activity of this region was correlated with the learning magnitude. They concluded that cerebellar contribution to motor learning is to maintain relevant S-R mappings. Data from patients with chronic cerebellar lesions after stroke (Dirnberger et al., 2013) pointed to stronger impairment in perceptual than motor sequence learning. In the current task, working memory demands were rather low but performance was still depended on the transformation of the representation in stimulus space to response space. Cerebellar degeneration as in the ataxic patients in Spencer et al. (2009) affects the cerebellum globally which makes it difficult to relate performance deficits to specific cerebellar substructures. Measuring task-related effective connectivity in ataxic patients might be promising to specifically relate behavioral impairments to altered cortico-cerebellar networks.

2.4.4 Limitations

Some limitations of this study should be mentioned. Researchers have argued that when disentangling task performance and motor learning per se, cerebellar contribution might be limited to improvement in performance rather than learning (Seidler et al., 2002). Together with evidence pointing to specific cerebellar contribution to maintaining S-R mappings, one could question whether the modulation of connectivity from M1 to cerebellum is in fact specific to motor learning. Similarly to other studies that use the SRTT to study motor sequence learning, we were not able to disentangle these processes with our paradigm, which remains to be addressed in future studies. In addition, motivated by specific theoretical models of motor learning as well as many imaging studies employing SRTT to study motor sequence learning, we examined a very specific set of models comprising a limited number of brain regions. The

"winning" model we found is the best out of this candidate set of models and might not be the best when investigating effective connectivity in a data-driven approach in which thousands of models are specified or more brain regions are included. The approach we took in this study however allows us to answer specific questions about causal interactions between key nodes in the motor learning network as suggested by previous theoretical and empirical work. Moreover, we qualitatively showed that improved performance in sequence material during the second session was related to significant negative modulatory effects on the connection from M1 to cerebellum. However, quantitatively we did not find any correlation between performance in the task and the parameters obtained from the modeling procedure. In addition, due to the low sample size we were not able to compare differences in connectivity parameters between "good leaners" and "bad learners". Future studies could address this question by analyzing a larger sample of subjects or by incorporating behavioral parameters directly into the models and thus address the relationship between connectivity parameters and behavioral effects.

2.4.5 Conclusions

Using DCM, we demonstrated that implicit motor sequence learning modulates the effective connectivity between M1 and cerebellum bilaterally such that M1 exhibits an inhibitory effect on cerebellum, causing it to decrease in activity as learning progresses. We hypothesize that this is related to reduced prediction error processing in the cerebellum when subjects have successfully learned a new motor sequence. Interpretation of these results on the molecular level should be considered speculative, however, as inhibition mechanisms expressed by the BOLD signal are less clear. Future electrophysiological studies could specifically address this hypothesis using recordings from M1 and cerebellum in animals or in humans (for example in ECoG studies). In addition, studies of effective connectivity of the cortico-cerebellar network during early motor

learning after cerebellar damage or temporary lesions (induced through e.g. TMS or tDCS) as well as studies in populations showing motor learning deficiencies (such as older adults) would greatly benefit our understanding of cerebellar contribution to implicit motor sequence learning.

Chapter 3

Striatal-cerebellar networks mediate consolidation in a motor sequence learning task: an fMRI study using dynamic causal modelling [2]

3.1. Introduction

Acquiring and retaining novel motor skills plays a fundamental role in human behavior. During the process of motor learning, a labile motor memory is formed, probably already after a few practice trials, and then stabilizes into a robust representation through consolidation (McGaugh, 2000). Consolidation, which can be dependent on sleep, is reflected in performance improvement without any further practice (Diekelmann and Born, 2010). Studies investigating the neural correlates of motor memory consolidation have revealed inconclusive findings and to date little is known about changes in network interactions mediating motor memory consolidation. It is hypothesized that consolidation requires the synaptic reorganization of the neural networks involved in encoding of motor memories (Dudai, 2004). A theoretical model by Doyon and colleagues (Doyon et al., 2003) suggests that encoding, consolidation and retention phases in motor learning are based on distinct cortico-striatal-cerebellar networks. In previous work (Tzvi et al., 2014), we showed that the encoding stage of implicit motor sequence learning (MSL) is mediated by a specific M1-cerebellum loop which was negatively modulated by learning. Here we extend this finding by investigating how this cortico-striatal-cerebellar network is altered after consolidation in the slow learning phase. To this end, we used dynamic causal modelling (DCM) of fMRI data from specific brain regions within this network (primary motor cortex (M1), premotor cortex (PMC), supplementary motor area (SMA), putamen and cerebellum) to

[2] This chapter corresponds largely to: Tzvi, Elinor, et al. "Striatal–cerebellar networks mediate consolidation in a motor sequence learning task: An fMRI study using dynamic causal modelling."*NeuroImage* 122 (2015): 52-64. The author contributed to the analysis of the data and writing of the manuscript.

investigate changes in causal connectivity patterns between these regions while participants performed the serial reaction time task (Nissen and Bullemer, 1987) before and after sleep.

3.1.1. Phases of motor learning

Motor learning has been suggested to pass through three distinct phases: an early phase in which significant gains in performance are observed in a short time window, a late phase when further smaller gains can be observed over an extended time frame and an intermediate "offline" phase in which consolidation of the initial motor memory occurs (Doyon et al., 2009; Robertson et al., 2004a). Consolidation is reflected by improved performance after this "offline" phase despite no further practice of the sequence.

Changes in memory representations during sleep have been suggested to significantly contribute to learning and memory consolidation (for review see (Diekelmann and Born, 2010)). In the motor learning domain, abundant evidence points to sleep-specific enhancement in performance in an explicit MSL task (Fischer et al., 2002; Korman et al., 2007; Walker et al., 2002; Walker et al., 2003). In case of implicit sequence learning however, sleep might not be the main factor influencing consolidation. A study by Robertson and colleagues, for instance showed that participants who were unaware of a regularity in the task showed similar improvement in performance after time had passed regardless of whether they had slept during that time or not (Robertson et al., 2004b). In the present study, we investigated the neural network effects of offline consolidation of implicit motor sequence memories after a sleep period. As all participants slept between recording sessions, the results remain silent as to whether the effects are specific to sleep.

3.1.2 Neural correlates of motor learning and consolidation

Previous studies have shown that multiple cortical and subcortical brain regions are activated during MSL (for review see (Dayan and Cohen, 2011)). A meta-analysis (Hardwick et al., 2013) of 70 motor learning tasks identified a wide-spread network of brain regions including M1, primary somatosensory cortex (S1), SMA, dorsal PMC, superior parietal lobule, thalamus, putamen and cerebellum. Theoretical models (Doyon et al., 2003; Hikosaka et al., 2002) suggest that a distinct cortico-cerebellar-striatal network is mediating the different phases in MSL. The neural signature of motor memory consolidation is however less clear and results are inconsistent. Whereas in one study involving an explicitly known sequence of motor movements (Fischer et al., 2005), activity in right PMC and M1 was decreased when comparing post-sleep to pre-sleep sessions, another study with a similar design (Walker et al., 2005) reported increased activity after sleep in right M1 but also in left cerebellum, medial prefrontal cortex, hippocampus and striatum. Increased activity in the striatum after sleep was reported by another explicit MSL study (Debas et al., 2010) suggesting that the striatum plays a crucial role in consolidation of the motor memory during sleep. Supporting this notion, an implicit oculomotor sequence learning study found striatal and hippocampal activity during training to be predictive of performance gain after sleep (Albouy et al., 2008). Steele and colleagues (Steele and Penhune, 2010) investigated offline consolidation effects on explicit motor sequence learning and found that increased activity in left M1 correlated with improved performance after the offline phase. Altogether these results show that M1 and PMC as well as striatum and cerebellum might have crucial roles in the consolidation of motor memory, no previous study has thus far investigated causal interactions between these structures with respect to consolidation.

3.1.3 Connectivity studies of motor learning

Functional connectivity studies of motor learning in humans have mainly focused either on the early fast stage of MSL (Sun et al., 2007; Tamas Kincses et al., 2008) or the prolonged effects of slow-learning over days or weeks of practice (Coynel et al., 2010; Ma et al., 2010; Steele and Penhune, 2010). These studies showed evidence for increased connectivity within the cortico-striato-cerebellar network (Ma et al., 2010; Steele and Penhune, 2010), however decreased connectivity has also been reported (Coynel et al., 2010). Two recent studies investigated connectivity during encoding and after consolidation of an explicit motor sequence (Albouy et al., 2013; Debas et al., 2014). Albouy and colleagues (2013) used a seed in caudate nucleus to investigate whole brain functional connectivity with the striatum. In addition to connectivity with the hippocampus, the authors also found that connectivity with several cortical areas and the cerebellum was correlated with gain in performance after consolidation during sleep. Debas and colleagues (2014) investigated the offline consolidation effects during sleep compared to an equivalent wake period using a measure of functional integration. The authors found evidence for a significant increase in functional integration in the cortico-striatal network following sleep compared to the wake condition and a similar tendency, however not significant, in the motor network suggesting a stronger sleep-specific involvement of these networks in the slow learning stage.

Other studies investigated network reorganization during motor memory consolidation in the offline phase using resting-state (RS) functional connectivity (Albert et al., 2009; Sami and Miall, 2013; Sami et al., 2014; Vahdat et al., 2011). In one such study (Sami et al., 2014), BOLD fMRI at RS was measured at three time points after learning a SRTT under implicit or explicit conditions. Enhanced connectivity between dentate cerebellum, thalamus and basal ganglia was

observed shortly after implicit learning (30 min) whereas 6 hours later, presumably after consolidation, enhanced connectivity was found between medial temporal lobe structures. When contrasting implicit vs. explicit learning after consolidation, a network containing bilateral premotor cortex as well as bilateral superior and inferior parietal lobule was found to be more engaged in implicit learning.

In addition to functional connectivity studies, analyses of effectivity connectivity can provide further insight in the interactions within the cortico-striatal-cerebellar network during the different phases of motor learning. Dynamic causal modelling (DCM) as one method for effective connectivity analyses was used in several studies to delineate causal connections within this network during motor actions in healthy participants (Grefkes et al., 2008a; Pool et al., 2013) and in the cortico-cortical network in patients after stroke (Grefkes et al., 2008b; Grefkes et al., 2010; Rehme et al., 2011). In previous work (Tzvi et al., 2014), we used DCM to investigate the specific effects of encoding during the early stage of implicit MSL on the cortico-striatal-cerebellar network. We found that the cortico-cerebellar loop was more dominant compared to the cortico-striatal loop and that learning negatively modulated the connection from M1 to cerebellum. Of note, these results are in-line with previous findings of a PET study (Penhune and Doyon, 2005) in which inter-regional correlation analysis during early learning showed that increase in blood-flow over cerebellum correlated with a decrease of blood flow in M1.

3.1.4 Current study

Here, we extended this work and investigated how causal interactions within this specific cortico-striato-cerebellar network change after motor memory consolidation during sleep. In contrast to our previous study, here we used a paradigm in which learning can occur in both the motor and the perceptual domain. Therefore, we expected a more extensive network to be

modulated by learning reflecting both learning components. An additional difference to our previous study is that here participants performed the SRTT with their non-dominant left hand. Previous studies have shown that motor learning with the non-dominant left hand can give rise to activity in both the "performing" right hemisphere but also the dominant left hemisphere (Fischer et al., 2005; Grafton et al., 2002; Lehericy et al., 2005; Orban et al., 2010). Hence, we expected that modulation of connections by learning would be evident in either hemisphere. Moreover, compared to our previous work, we sought to include additional cortical regions, namely bilateral PMC and SMA, in addition to M1, striatum and cerebellum, as those regions were shown to be involved in motor learning as well (Hardwick et al., 2013). This allowed us to investigate also potential cortico-cortical connectivity changes due to motor learning. These changes posed the methodological challenge of specifying and estimating hundreds of models. Due to recent advancements in DCM methodology, i.e., post-hoc Bayesian model selection (Friston and Penny, 2011; Rosa et al., 2012) we were able to approach this problem.

We hypothesized that causal connectivity patterns in the cortico-striatal-cerebellar network, which play a crucial role in the encoding phase of MSL, are altered when comparing pre- to post-sleep MSL sessions as a consequence of motor memory consolidation. Based on our previous results, we expected the connectivity from M1 to cerebellum to be negatively modulated in the early pre-sleep learning session. In the post-sleep session we expected to find a modulation of connectivity between cortical areas and the striatum as suggested by evidence of the studies detailed above.

3.2 Materials and methods

3.2.1 Participants

Thirty-one healthy participants (17 men; mean age: 24.9 standard-deviation: 1.8 years) took part in this study. All participants were right-handed (assessed using a handedness questionnaire (Oldfield, 1971)), were not taking any medication, were neurologically and mentally healthy (self-report) and had no history of sleep disorders. Musicians and professional-typists were not included in this study. Participants were not allowed to ingest alcohol or caffeine throughout the experiment. Participants were recruited from the University community and gave written informed consent to take part in the study. The study was approved by the Ethics committee of the University of Kiel and performed according to the Declaration of Helsinki.

Four participants gained explicit knowledge of the sequence already in the pre-sleep session and were therefore excluded from any further analysis. In the post-sleep session, despite awareness of potential regularity in the stimuli, only six additional participants were explicitly aware of the specific sequence. We therefore excluded those participants from the behavioral analysis, resulting in 21 participants who remained implicit of the specific sequence throughout the experiment. For the fMRI analysis of the pre-sleep session, we included the six participants who gained explicit knowledge only in the post-sleep session. However, coregistration failed due to suboptimal image quality in four participants in the pre-sleep session, resulting in 23 participants for this fMRI analysis. In the post-sleep session, two participants had to be excluded due to coregistration problems resulting in 19 participants for this fMRI analysis.

3.2.2 Experimental paradigm

Participants completed a modified version of the serial reaction time task (Nissen and Bullemer, 1987) in the evening and again in the morning after sleep. Throughout the task, four grey stimuli

were presented in a horizontal array on a screen, with each stimulus associated to one of the four fingers of the left hand. Whenever one of the four stimuli turned blue, participants were instructed to press the corresponding button on an MRI-compatible keypad as precise and as quickly as possible. Button presses were recorded using E-Prime 2.0 (Psychology Software Tools, Inc., 2002). Unbeknownst to the participants, stimuli were presented in either a random order or as a 12-items-sequence ("2-4-1-2-3-1-4-2-1-3-4-3"). Random stimuli were created such that items were not repeated. The task consisted of 6 blocks with 96 trials each. Each block contained 4 repetitions of the 12-element sequence (i.e. 48 trials) as well as 24 randomly presented stimuli before the sequence material and right after (see Figure 3.1). The inter-stimulus interval was 800 ms. A 28 s break was introduced between the blocks. Prior to the first SRTT session (in the evening), participants performed a test run with 96 randomly presented stimuli to familiarize with the task.

3.2.3 Procedure

Participants performed the SRTT in the evening at 7:00 p.m. while fMRI was recorded (Figure 3.1). Immediately afterwards, participants were asked to recall the hidden sequence using the "free recall task" (FRT). Subsequently participants were sent to sleep at home. In the next morning at 7:00 a.m. participants completed the FRT again before performing the SRTT re-test in the fMRI. Thereafter explicit sequence knowledge was measured for a third time using the FRT. Before the adaptation night and before the two SRTT sessions in the evening and in the morning, participants completed standardized questionnaires acquiring wakefulness (Stanford Sleepiness Scale, SSS; Hoddes et al., 1972) and subjective activation, concentration and mood using a standard adjective check list (Janke and Debus, 1978).

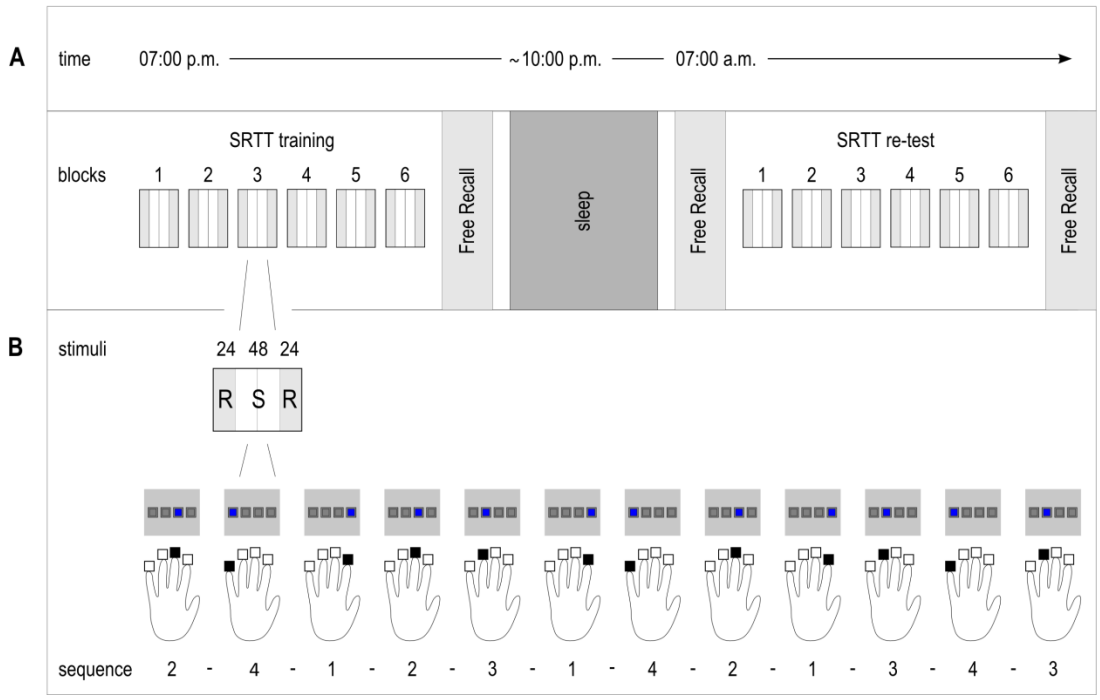

Figure 3.1. Experimental design. **A** Participants completed the initial SRTT training in the evening (7 p.m.) and approximately 12 hours later the SRTT re-test (7 a.m.), both consisting of 6 blocks with 96 trails each. „„Free recall“ was measured after initial training of the SRTT as well as before and after the SRTT re-test **B** Each block of the SRTT training and re-test consisted of 24 random trails, followed by 48 sequential trials (i.e. 4 x the 12-items-sequence) and 24 random trials.

3.2.4 Assessment of explicit awareness

Explicit knowledge of the hidden sequence was assessed using the FRT. In the FRT, participants were required to recall the hidden 12-element sequence as precisely as possible. The sequence recalled by the participants was then compared to the actual hidden sequence. The number of correctly recalled consecutive items of the hidden sequence was then used as a measure of explicit awareness.

The FRT performance was measured at three time points: (1) in the evening directly after the first SRTT session (all participants who acquired explicit knowledge after this initial training were excluded from further analysis), (2) in the morning before the second SRTT session to

investigate implicit-explicit conversion during sleep without further practice of the SRTT and (3) in the morning after the second SRTT session. It should be mentioned here that the FRT informs the participants about the hidden sequence such that they are explicitly aware of a rule in the second SRTT session.

We used Monte Carlo simulations and an in-house "R" script (version 2.130; R Foundation for Statistical Computing, 2011, Vienna, Austria, http://www.R-project.org) in order to define a threshold in which the number of correctly recalled consecutive items would suggest that the subject gained explicit knowledge of the sequence (and not by mere chance). Chance level was assessed as follows: 10,000 sequences of 12 items each were randomly generated using the program Visual Studio Version 6.0 (Microsoft, Redmond, WA, USA). The sequences contained the numbers 1 to 4 without repetitions. All 10,000 randomly generated sequences were then compared to the hidden sequence. In 94% of the 10,000 randomly generated sequences, 5 and less than 5 consecutive correct items of the sequence were found. Therefore any randomly generated 12-items sequence has a chance of less than 6% to attain 6 or more consecutive correct hits. Consequently, six and more consecutive correct items of the sequence were considered as "above chance level" and as "explicit awareness". Participants who gained explicit knowledge according to this criterion already after the pre-sleep SRTT session or in the post-sleep session were excluded from further analyses.

3.2.5 Imaging

MR protocol was carried out with a 3T Philips Achieva whole-body scanner (Philips Achieva, Philips, Best, Netherlands) and a standard 8-channel SENSE head coil in the department of neurology of the university Kiel. Functional MRI data (T2*) was collected using blood oxygen level dependent (BOLD) contrast in two sessions (pre- and post-sleep) each with 250 volumes.

Gradient-echo EPI sequence was used with the following specifications: repetition time TR=2400ms, echo time TE=36.8ms, flip angle = 90°, matrix size 64 x 64mm, FOV = 216 x 118.5 x 216mm, 36 transversal ascending slices of 3mm thickness and 10% gap and in-plane resolution of 3.375 x 3.375mm. Subsequently, a high resolution T1-weighted structural image was acquired with TR=8.12ms, TE=3.73ms, flip angle=8°, FOV = 240 x 240 x 160mm; matrix size 240x240mm; 160 sagittal slices of 1mm thickness.

3.2.6 Behavioral analysis

In the SRTT, we computed reaction times for both the SEQ and RND conditions with the difference being our measure of implicit sequence learning. To assess statistical significance, we used a repeated measure ANOVA with three factors: condition (SEQ, RND), blocks (1-6), and session (pre- and post-sleep). We also compared the median error rate between both task conditions for each session using the Wilcoxon signed-rank test. Wrong button presses and missing responses were regarded as errors.

3.2.7 Pre-processing and statistical analysis

Preprocessing of fMRI data in both pre-sleep and post-sleep sessions was done using SPM8 software package (http://www.fil.ion.ucl.ac.uk/spm/) and consisted of: slice timing correction, realignment to correct for head motion artifacts, co-registration to T1 structural image, segmentation, normalization to Montreal Neurological Institute (MNI) template brain image, smoothing with a Gaussian kernel of 8mm full width half maximum and resampling of functional images to 3x3x3 mm. Coregistration failed in four participants in the pre-sleep session and in two participants in the post-sleep session. These participants were excluded from further analyses in the respective sessions.

Imaging data was subsequently modeled using the general linear model (GLM) in a block design manner. We used separate GLM analyses for each session. Imaging data of 23 participants was used for the pre-sleep analysis and of 19 participants for the post-sleep analysis. For the analysis of sleep-related motor memory consolidation (changes from pre- to post-session) we included 17 participants. Linear regressors were obtained for each of the experimental conditions (SEQ and RND) and each block in each subject. Statistical parametric maps (SPMs) were generated by convolving a box function with duration of either 24 random trials for RND condition or 48 sequence trials for SEQ condition, with a hemodynamic response function. Movement related parameters from the realignment process were included in the GLM as regressors of no-interest to account for variance caused by head motion.

3.2.8 Dynamic causal modelling

Dynamic causal modelling (DCM) (Friston et al., 2003) is a well-established method for estimating and comparing models of brain connectivity. DCM allows inferring on the causal coupling parameters between brain regions influenced by experimental conditions. We employed a deterministic bilinear model in which a system of differential equations is used to describe the neuronal dynamics of the motor learning network:

$$\frac{d\vec{x}}{dt} = \left(A + \sum_{j=1}^{m} u_j B^{(j)} \right) \vec{x} + C\vec{u}$$

Here, $\vec{x}$ is the state vector and $\vec{u}$ is the input vector to the system. A matrix represents the endogenous (context independent) connections, B represents the modulatory (context dependent) connections, and C is the influence of direct inputs to the system. Together with the Balloon model for the hemodynamic response function, the above system of equations is inverted and compared to the observed data using Bayesian methods. The model evidence, which is the

probability of the data given the model, is approximated using variational Bayes (VB) approach in which the posterior estimates of the parameters are updated iteratively through a gradient ascent on the free-energy bound (Friston et al., 2007).

3.2.9 Post-hoc Bayesian model selection

In the conventional DCM analysis procedure, a small set of hypothesized models is defined and compared using Bayesian model selection (BMS) procedures to issue an optimal model. This procedure requires individual fitting and estimation of each of the models using the procedures described above. If the model space is quite large (>16 free-parameters) this estimation procedure will require significant amount of computational time. Recently, a novel method for estimation and selection of an optimal dynamic causal model was introduced by Friston and colleagues (Friston and Penny, 2011; Rosa et al., 2012). Here, only one full model is estimated and fitted to the data. This full model contains all connectivity parameters which are a-priori hypothesized to be modulated by a specific task input. Using the posterior density of the full model, this "post-hoc" BMS procedure systematically "removes" model parameters by using a greedy-search scheme resulting in an optimal model and its posterior estimates. This procedure allows to explore a very large number of models as only one full model is estimated.

A recently published study which made use of this "post-hoc" BMS procedure (Hillebrandt et al., 2013) specified the endogenous connections (matrix A) and the inputs (matrix C) of the full model which will be used for the "post-hoc" BMS procedure based on specific a-priori knowledge. Here we performed an initial BMS analysis in order to identify both the optimal structure and the best driving node (see similar approach in (Seghier et al., 2010)). We therefore performed the DCM analysis as a three-step procedure. First, the structure and the input node/s were determined by systematically comparing models with task input and without modulatory

connections (similar approach as in (Tzvi et al., 2014)). Using family level inference the optimal model for endogenous connections was determined. In the second step we used this model to specify and estimate a full model with modulatory effects on connections which could be possibly modulated by learning. Third, using "post-hoc" BMS the full estimated model was optimized and a winning model was chosen with its optimal connectivity patterns (see Figure 3.3 for a visualization of the analysis scheme).

3.2.10 Time series extraction

We aimed at investigating the causal interactions between primary motor cortex (M1), supplementary motor area (SMA), premotor cortex (PMC), putamen (Pu) and cerebellum (CB). We therefore used ten regions of interest (ROIs) to extract time series from significant voxels (see Table 3.1) in task>baseline contrast in order to account for both learning and non-learning related changes in the BOLD signal.

Table 3.1: Regions of interest for the DCM analysis

Region	MNI-coordinates	p-level	Sphere Radius (mm)
lM1	-38,-24,58	0.001	6
rM1	40,-20,54	0.001	6
lSMA	0, -2,56	0.001	4
rSMA	2,8,52	0.001	4
lPu	-24,4,4	0.05	4
rPu	26,0,2	0.05	4
lCB	-20,-52,-22	0.001	6
rCB	10,-58,-20	0.001	6

Coordinates of the sphere center for M1, SMA, CB, and Pu ROIs (see Table 3.1) were selected based on meta-analysis of motor learning (Hardwick et al., 2013). For each individual subject, the sphere center of each ROI was moved to the closest supra-threshold voxel within the boundaries of the functional ROI as assessed by xjview toolbox (http://www.alivelearn.net/xjview) and AAL brain atlas. The PMC sphere center was always kept over BA6 and middle frontal gyrus and sufficiently apart (>10 voxels in each direction) from the M1 sphere center. This procedure verified that sphere centers in all ROIs were kept approximately consistent across participants. The coordinates of PMC were selected to be the individual local maxima of each subject in the contrast task>baseline. Significant voxels were chosen based on a p-level threshold of $p<0.001$ for M1, SMA, PMC and CB and $p<0.05$ for Pu (activity in putamen was less pronounced on the single subject level). Using a singular value decomposition procedure implemented in SPM8, we computed the first eigenvariate across all suprathreshold voxels within 4mm (Pu, SMA) or 6mm (M1, PMC and CB) radius from the sphere center for each subject in each session. Time series were then adjusted to effects of interest contrast (mean-corrected) and sharp improbable temporal artifacts were smoothed by an iterative procedure implementing a 6-point cubic-spline interpolation (see previous use of this method in (Tzvi et al., 2014). Using these criteria, we could not obtain time series in four participants for the pre-sleep session and in one subject for the post-sleep session so these participants were excluded from further analyses in the respective sessions. This resulted in 19 participants for the pre-sleep session and 18 for the post-sleep session.

3.2.11 DCM specification

DCMs were specified for each of the experimental sessions (pre- and post-sleep) separately using DCM12 routines as implemented in SPM8. Input vector $\vec{u}$ was constructed as a stick

function of the single events of stimulus presentation. An overview of the modelling process is described in Figure 3.3. In the first step, we determined the optimal endogenous connections in our data-set by constructing 22 models with reciprocal (bidirectional) connections within all ROIs in each hemisphere. For simplicity, we assumed symmetric connectivity patterns within each hemisphere and therefore examined models with different between-hemispheres connections by systematically reducing them in the models (see Figure 3.4). Based on previous studies, we used RFX BMS to test whether task inputs were to CB (Tzvi et al., 2014) or to premotor and supplementary motor areas (Pool et al., 2013) and whether this input was unilateral or bilateral. Accordingly, models were specified whether task input was to bilateral CB (6 models), bilateral premotor and supplementary motor areas (PMC and SMA; 6 models), left CB (5 models) or right PMC and SMA (5 models). Only five models were defined for the aforementioned unilateral input since model 6 (see Figure 3.4) does not allow interhemispheric connections which means that no signals could be predicted for the left hemisphere if unilateral input is specified. For this analysis we did not include any modulatory parameters (B=0). In order to account for spurious results of RFX BMS, we performed family level inference using SPM8 ('spm_compare_families.m' version 5007) using Gibbs sampling with a total of 2e6 samples (Penny et al., 2010). The following families were compared:

- Input Family: contains 4 types of models based on the different inputs
- Structure family: contains 6 types of models based on connectivity patterns across hemispheres (see Figure 3.4)

In the second step, we used the optimal model of endogenous connections to specify and estimate a reliable full model which was used for the subsequent "post-hoc" BMS procedure. For the full model we assumed that all within hemisphere connections could be modulated by motor

learning. Modulations of self-connections within each ROI were not allowed for simplicity (see similar approach in Hillebrandt et al., 2013). In the third step, we performed the "post-hoc" BMS procedure (as implemented in SPM8 version 4307) and obtained the winning model for modulatory effects for each subject in each session.

In order to test whether this optimal model is specifically describing connectivity patterns evoked by motor learning and not by task performance, we created and estimated two test models based on the modulatory connections in the winning model of the "post-hoc" BMS procedure (see Figure 3.3). In Model 1 the connections were modulated by motor task performance (SEQ and RND conditions) and in model 2 (as in the winning model) the connections were modulated by learning (SEQ condition). We then used RFX BMS to compare which of the two models is best describing the data.

3.2.12 Parameter estimates

In each session we evaluated the connectivity parameters of each subject using an RFX non-Bayesian statistical approach. We evaluated the endogenous connectivity parameters from the "winning" models obtained in the first analysis step, and the modulatory connectivity parameters from the optimal model obtained in the second analysis step. Using a Wilcoxon signed rank test ($p<0.05$, Bonferroni corrected for multiple comparisons), we tested across participants how likely the effect of interest is different than zero. We report the strength of the connections in Hz across participants (mean±SE) and the corresponding p-value. Importantly, pre- and post-sleep sessions resulted in different intrinsic models (see Results section). It was therefore not possible to quantitatively compare connectivity parameters before and after sleep, but only qualitatively.

Finally, we performed correlation analysis of parameter estimates of each subject in each session with normalized RTs in order to relate behavioral learning effects and neural connectivity parameters.

3.3. Results

3.3.1 Assessment of explicit awareness

Explicit knowledge of the hidden sequence was assessed using the FRT. Using a Monte-carlo simulation we established that six and more consecutive correct items of the sequence were considered as "above chance level" and as "explicit awareness". Four participants gained explicit knowledge of the sequence according to this criterion already in the pre-sleep session and were therefore excluded from any further analysis. In the post-sleep session, six additional participants were explicitly aware of the specific sequence. We therefore excluded those participants from the behavioral analysis, resulting in 21 participants who remained implicit of the specific sequence throughout the experiment.

3.3.2 Behavioral results

We first tested whether participants learned the sequence in the pre-sleep session. For this purpose, we performed repeated measures ANOVA with factors condition and block on data from the 21 participants who remained implicit throughout the experiment according to our assessment of awareness (see section 3.2.4 - assessment of explicit awareness). We found a main effect of condition: ($F_{1,20} = 19.22$, $p < 0.001$) which indicates that participants were faster when performing the sequence compared to random performance. A significant condition x block interaction ($F_{5,100} = 2.33$, $p = 0.048$) reflected improved learning of the sequence with time in the

pre-sleep session. No main effect of block was observed ($F_{5,100}$ = 2.01, p = 0.08) suggesting that unspecific task improvements were not found during the pre-sleep session.

Next, we tested whether further learning improvements were evident in the post-sleep session using a similar ANOVA with factors condition and block. Here as well we found a main effect of condition ($F_{1,20}$ = 55.97, p < 0.001) indicating that participants performed faster during sequence blocks compared to random blocks, as well as a significant interaction ($F_{5,100}$ = 3.27, p = 0.009) which mainly reflected the slowing down during random blocks performance rather than speeding up during sequence blocks (see Figure 3.2A). A main effect of block ($F_{5,100}$ = 3.77, p = 0.004) was also evident which might be driven by the slower reaction times during random blocks.

In order to specifically test whether participants consolidated the sequence during the off-line phase, we tested the differences between the block preceding sleep (pre-sleep: block 6) and the block performed just after sleep (post-sleep: block 1) using a repeated measures ANOVA with factors condition and sleep (pre-sleep: block 6, post-sleep: block 1). We found main effects of condition ($F_{1,20}$ = 20.06, p < 0.001) and of sleep ($F_{1,20}$ = 6.52, p = 0.02). Although the sleep effect for the sequence condition (t_{20}=3.88, p<0.001) was nominally larger than for the random condition (t_{20}=3.15, p=0.005), the interaction was not significant ($F_{1,20}$ = 1.10, p = 0.31).

Error rates were generally very low (1.95%±0.77), but significantly higher during random blocks (2.78%) compared to sequence blocks (1.77%) in the post-sleep session (p<0.001) but not in the pre-sleep session (random: 3.1%, sequence: 2.55%; p=0.15) (see Figure 3.2B). This reflects that the motor sequence was consolidated and implemented in the post-sleep session such that fewer errors were made during sequence material.

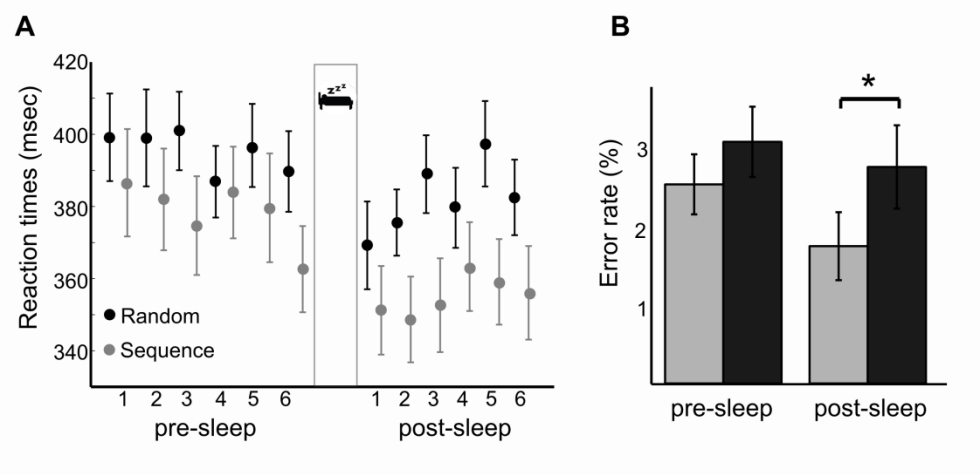

Figure 3.2. Behavioral performance in the serial reaction time task. Error bars represent standard errors of the mean (SEM). **A** Reaction times are plotted for the sequence condition (in grey) and for the random condition (in black) across blocks, before and after sleep. **B** Error rates are plotted across each session for each of the conditions (Sequence: gray, Random: black). A significant difference between sequence and random is observed in the post-sleep session.

3.3.3 Dynamic causal modelling

Bayesian model selection

As explained in the methods section, we followed the same analysis procedure for both pre- and post-sleep sessions (see Figure 3.3 for an overview):

1. We compared 22 models in order to identify the optimal model for endogenous connections driven by a motor task input using standard RFX BMS and RFX family wise inference.
2. Based on the winning model, we defined and estimated the full model for the "post-hoc" BMS procedure.
3. The modulatory effects found in the winning model were then re-evaluated by creating and estimating two test models according to the modulatory connections in the winning model of the "post-hoc" BMS procedure.

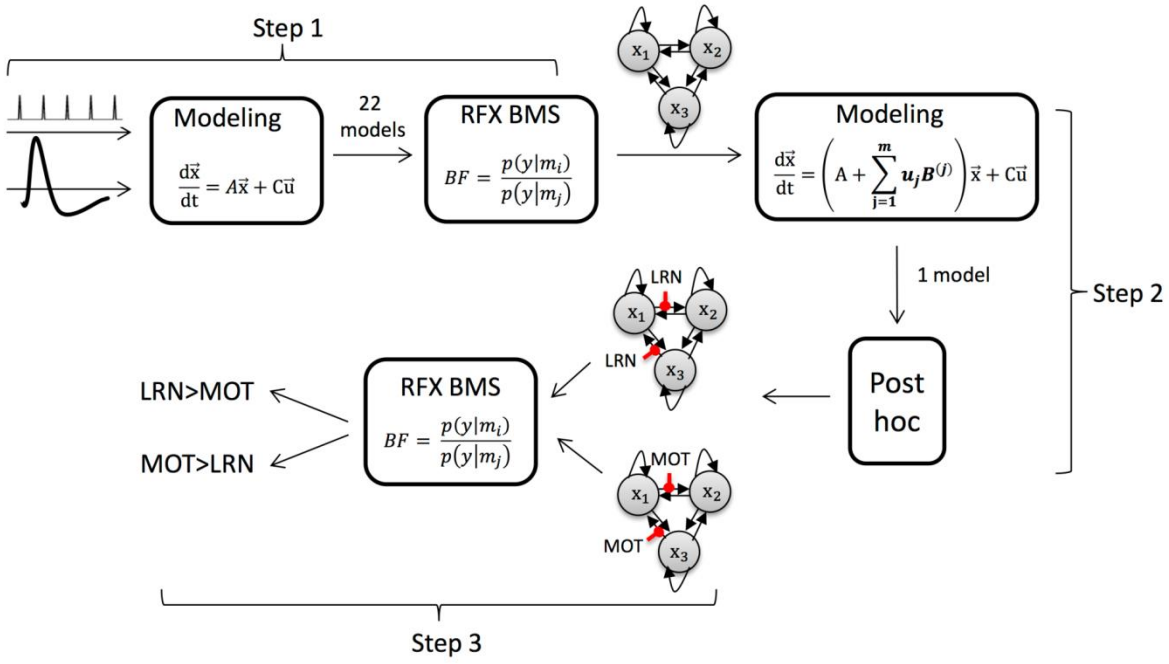

Figure 3.3. Analysis scheme. In the first step, the endogenous connections driven by the motor task are identified using random effects Bayesian models selection employing 22 models. In the second step, using the optimal model from the first step a learning model is estimated and hundreds of models are compared using the post-hoc BMS procedure. Finally, the optimal model of the previous step is compared to an identical model with task modulation to test the specificity of learning-related connectivity modulations.

Pre-sleep

We found that model 9 which is based on structure-model 3 with inputs to right premotor areas had the largest exceedance probability (p_ex = 0.145) compared to the next best model (p_ex = 0.096) which was as well based on structure-model 3 however with input to left cerebellum. Family level inference results showed that left CB input-family had a slightly higher exceedance probability than right premotor input-family (p_ex = 0.498 and p_ex = 0.482 respectively). When comparing structure families, structure-family 3 had the highest exceedance probability (p_ex = 0.698) with structure-family 4 being the next most probable structure family (p_ex = 0.232). Family level inference has been shown to produce more robust and reliable results

(Penny et al., 2010), so we proceeded with defining and estimating the full model based on structure-family 3 with input to left CB. We compared 256 models using the "post-hoc" BMS procedure. The winning model (see Figure 3.4C) had an exceedance probability of p_ex = 0.068 (see Figure 3.5E).

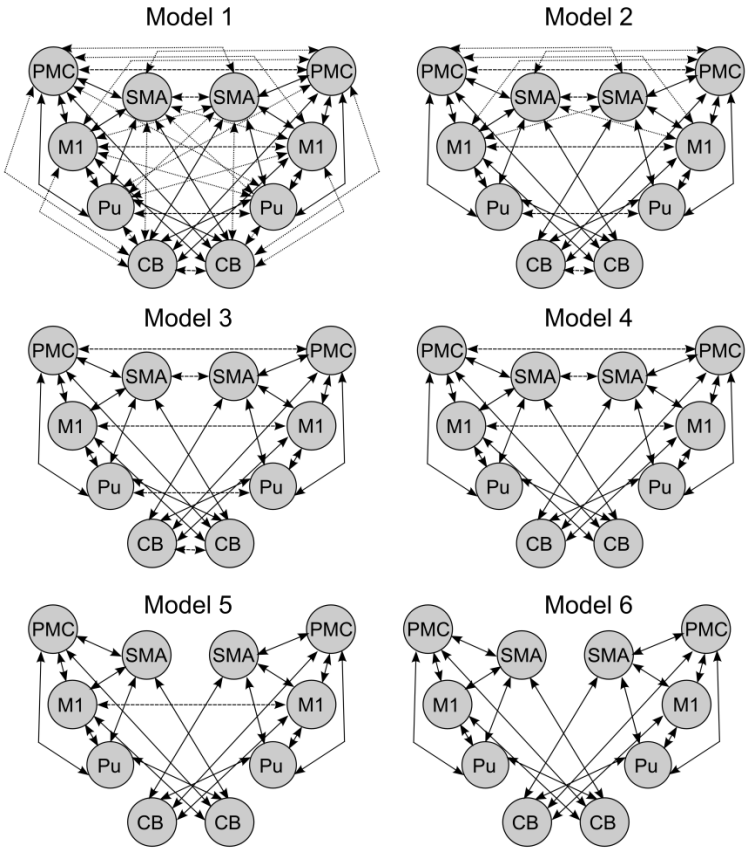

Figure 3.4. Six models for task-driven intrinsic connections. Dotted lines stand for inter-hemispheric connections, dashed lines stand for homolog brain regions connections, and full lines stand for within hemisphere connections. In all models – all within hemisphere connections between all nodes were kept for all the models. Connections are systematically removed from Model 1 to Model 6. Model 1: all 10 nodes are connected to each other. Model 2: only cortical between hemisphere connections are kept. Model 3: only homolog connections are kept. Model 4: only cortical homolog connections are kept. Model 5: only M1 homolog connections are kept. Model 6: no connections between hemispheres.

In order to assess whether modulations in the winning model were specific to learning, we compared two test models (test model 1: task modulation; test model 2: learning modulation)

using RFX BMS (See analysis scheme in Figure 3.3). Test model 2 had higher exceedance probability (p_ex = 0.76) in comparison to test model 1 (p_ex = 0.24). This result indicates that connectivity patterns observed in the winning model were indeed reflecting learning-related causal effects.

Post-sleep

We found that model 10 which is based on structure-model 4 with inputs to right premotor areas had the largest exceedance probability (p_ex = 0.41 and see Figure 3.5B). Model 21 which is also based on the structure-model 4, but with inputs to left CB, had a slightly lower exceedance probability (p_ex = 0.39). Family level inference showed that right premotor family had higher exceedance probability (p_ex = 0.71) than left CB input-family (p_ex = 0.27). When comparing structure families, we observed that indeed there was a shift in the post-sleep session to structure-family 4 (p_ex = 0.83). The next most probable family was structure-family 5 (p_ex = 0.10).

We proceeded with defining and estimating the full model based on structure-family 4 with input to right premotor areas. We compared 256 models using the "post-hoc" BMS procedure. The winning model (see Figure 3.5D) had an exceedance probability of p_ex = 0.31 (See Figure 3.5F).

We compared the two test models using RFX BMS and found that test model 1 in which connections were modulated by the motor task had a higher exceedance probability (p_ex = 0.94) in comparison to test model 2 (p_ex = 0.06) in which the connections were modulated by learning. This comparison shows that in the post-sleep session, activity in the motor network was no longer driven by learning but was more dominated by task performance.

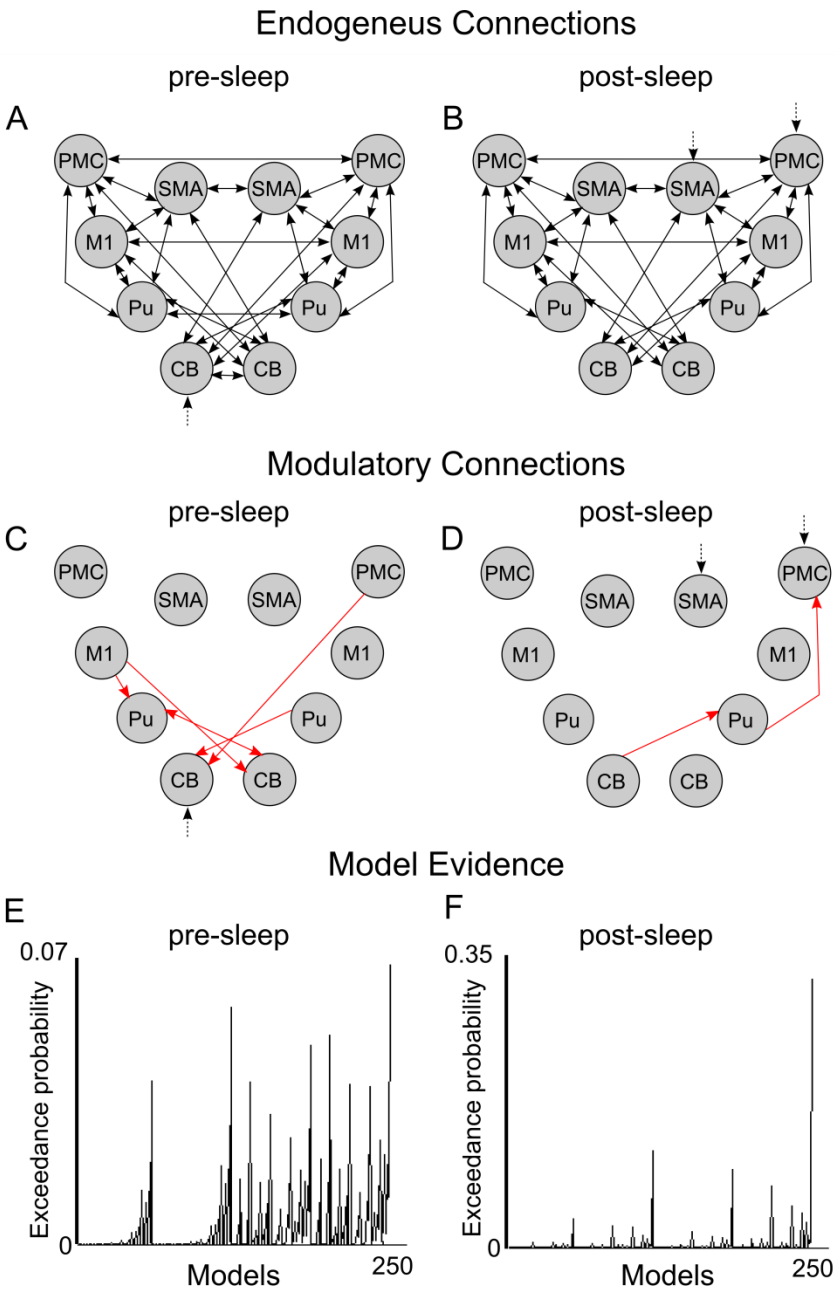

Figure 3.5. Results of Bayesian model selection in pre- and post-sleep sessions. **A-D** Optimal models. Input to the models are marked with a dotted arrow. PMC- premotor cortex; SMA- supplementary motor area; M1- primary motor cortex; Pu- putamen; CB- cerebellum. **A** Pre-sleep optimal model for endogenous connections. Note that all homolog brain regions are connected and the input is to left cerebellum. **B** Post-sleep model for endogenous connections. Note that only cortical homologs are connected (right and left cerebellum and putamen are not connected) and input is to right premotor and SMA. **C-D** optimal model for learning-related modulatory effects. **E-F** Exceedance probability measures for the compared models in the post-hoc Bayesian model selection procedure.

To summarize our initial BMS analysis, we found different models for the input node/s and the endogenous connections in pre- and post-sleep sessions. Before sleep, input to left cerebellum and connections between all homolog brain areas were found to be optimal, whereas after sleep a model with an input to both right SMA and PMC and connections between only cortical homolog brain areas was optimal. We proceeded with our analysis procedure using these models.

Connectivity parameters in the winning models

Endogenous connections

In general we found that most of the endogenous connections which showed consistency across participants were positive indicating active information transfer from the respective input nodes (pre-sleep: lCB; post-sleep: rSMA, rPMC) to the network during task performance. Connections in the post-sleep session were markedly sparser compared to the pre-sleep session (see Table 3.2).

In addition, during pre-sleep, both left and right cerebellar nodes had positive forward connections to other nodes in the network, whereas in the post-sleep session, lCB had positive forward connections to rPu and rM1 and rCB had no forward connections at all. For both pre- and post-sleep sessions, we found a negative connection from lM1 to rM1 (Session: mean±SEM; pre-sleep: -0.239±0.064; post-sleep: -0.201±0.046) indicating interhemispheric inhibition from the dominant left M1 onto the "performing" right M1. During the pre-sleep session, we found an additional negative connection from lPMC to rPMC (-0.163±0.048) which was no longer significantly consistent across participants in the post-sleep session (-0.071±0.034). Other bilateral connections between the same regions from the dominant left hemisphere on the "performing" right hemisphere were not consistent across participants in either session (see Table 3.2). Additionally, we found consistent positive bilateral connections between homolog

brain regions from right to left hemisphere in the pre-sleep session (see Table 3.2) suggesting that information transfer from right to left is important for the early stage of motor learning with the non-dominant hand. In the post-sleep session, only positive connections from rPMC to lPMC and from rSMA to lSMA (see Table 3.2) were found to be consistent across participants. This might indicate that during the slow learning phase, the involvement of the dominant hemisphere was reduced.

Table 3.2: Posterior estimates of significant endogenous connections (A parameters) in the winning models in either pre- or post-sleep (mean±SE).

Connection	**Pre-Sleep**		**Post-Sleep**	
	Strength (Hz)	p-Value	Strength (Hz)	p-Value
rPu -> lPu	0.134±0.049	0.007*		
lPu -> lPMC	-0.070±0.060	0.968	-0.169±0.045	0.002*
rM1 -> rPu	0.046±0.016	0.002*	0.004±0.019	0.327
rM1 -> lM1	0.079±0.020	0.0006**	0.051±0.028	0.058
rM1 -> rPMC	0.086±0.041	0.008*	0.017±0.028	0.048
rM1 -> rSMA	0.119±0.050	0.005*	-0.015±0.051	0.214
lM1 -> rM1	-0.239±0.064	0.005*	-0.201±0.046	0.001*
rCB -> lPu	0.118±0.049	0.006*	0.065±0.029	0.025
rCB -> lM1	0.102±0.039	0.006*	-0.016±0.017	0.446
rCB -> lPMC	0.316±0.065	0.0001**	-0.080±0.026	0.014
rCB -> lSMA	0.266±0.063	0.0004**	-0.108±0.052	0.031
lCB -> rPu	0.194±0.049	0.006*	0.084±0.023	0.002*
lCB -> rM1	0.446±0.089	0.0001**	0.054±0.019	0.004*
lCB -> rCB	0.396±0.070	0.0003**		
lCB -> rPMC	0.430±0.068	0.0001**	0.026±0.018	0.048
lCB -> rSMA	0.356±0.072	0.0005**	0.046±0.023	0.048
rPMC -> rM1	0.051±0.024	0.053	0.308±0.047	0.0002**
rPMC -> lCB	0.031±0.020	0.049	0.131±0.077	0.003*
rPMC -> lPMC	0.256±0.053	0.0001**	0.524±0.080	0.0002**
rPMC -> rSMA	0.137±0.040	0.0005**	0.190±0.035	0.0003**

lPMC -> lPu	0.035±0.013	0.006*	0.037±0.029	0.133
lPMC -> lM1	0.051±0.023	0.011	0.098±0.016	0.0002**
lPMC -> rCB	-0.008±0.024	0.445	0.131±0.039	0.003*
lPMC -> rPMC	-0.163±0.048	0.001*	-0.071±0.034	0.039
lPMC -> lSMA	0.065±0.028	0.010	0.206±0.047	0.0003**
rSMA -> rPu	-0.029±0.023	0.970	0.089±0.017	0.0002**
rSMA -> rM1	-0.004±0.025	0.629	0.219±0.028	0.0002**
rSMA -> lCB	-0.030±0.034	0.421	0.258±0.071	0.0002**
rSMA -> rPMC	-0.004±0.017	0.398	0.146±0.021	0.0002**
rSMA -> lSMA	0.211±0.039	0.0001**	0.365±0.045	0.0002**

* p<0.01; **p<0.05, Bonferonni corrected

Modulatory connections

Pre-sleep

The modulated connections in the optimal model are detailed in Table 3.3 and depicted in Figure 3.5C. Similarly to our previous study, we observed a negative modulatory effect by motor learning on the connection from lM1 to rCB. This effect however, was not consistent across participants ($p = 0.18$). Additional negatively modulated connections were found from rPMC to lCB, lM1 to lPu, rPu to lCB and bidirectional connection between lPu and rCB. Consistent negative modulatory effects across participants were observed only on the connections between bilateral Pu to CB (see Table 3.3). We found no correlation between performance measures and modulation parameters.

Table 3.3: Posterior estimates of modulatory connections (B parameters) in the winning models (mean±SE)

Connection	pre-sleep		post-sleep	
	Strength (Hz)	p-Value	Strength (Hz)	p-Value
rPu -> lCB	-0.08±0.03	0.016*		
rPu->rPMC			-0.01±0.10	0.50
lPu -> rCB	-0.14±0.08	0.007**		
lM1 -> lPu	-0.02±0.10	0.40		
lM1 -> rCB	-0.09±0.09	0.18		
rCB-> lPu	-0.04±0.11	0.15		
lCB->rPu			-0.30±0.07	0.0006**
rPMC-> lCB	-0.05±0.09	0.20		

*p<0.05; **p<0.05 Bonferroni corrected

Post-sleep

In this session we found that modulation by motor task performance had higher exceedance probability than modulation by motor learning. The winning model (see Figure 3.5D) had negative modulatory effects of both SEQ and RND conditions on connections from rPu to rPMC and from lCB to rPu.

When testing for consistent effects across participants, we found that only during SEQ condition, the connection from lCB to rPu was consistently negatively modulated across participants (-

0.15±0.05; p = 0.008. RND: -0.06±0.05; p=0.35). The connection from rPu to rPMC was neither for the RND nor for SEQ condition consistently modulated across participants (p=0.058 and p=0.711 respectively). We found no correlation between performance measures and modulation parameters.

3.4 Discussion

We investigated the effects of implicit motor memory consolidation on effective connectivity in a specific cortico-striatal-cerebellar network. Dynamic causal modelling allowed us to investigate dynamic changes in causal patterns of connectivity in this network due to motor learning and consolidation. Participants performed the motor sequence significantly faster in the post-sleep session compared to the pre-sleep session and made less errors during post-sleep sequence relative to random blocks, indicating that they had consolidated the motor memory during sleep. In addition, reactions times of the post-sleep session suggested that no additional learning took place in this session.

DCM analysis revealed both general changes of the network as well as learning-specific changes. First, in terms of endogenous connections, we found differences in inter-hemispheric connections between pre- and post-sleep sessions as well as differences in the input node(s). Second, learning-related effects were assessed using post-hoc BMS analysis comparing hundreds of models. We found that pre-sleep learning modulated connectivity in several cortical-subcortical connections, whereas during the post-sleep session, modulatory effects were restricted and could not be attributed specifically to learning. The “loss” of a learning-related network in the post-sleep session might be directly related to the absence of behavioral effects of

learning in this session. During the pre-sleep session, implicit learners showed learning-related negative modulation of connections from bilateral putamen to cerebellum and, less consistently, from left M1 to cerebellum. Although the winning model was not specific to learning during the post-sleep session, we found that the connection from left cerebellum to right putamen was only consistently negatively modulated by the sequence condition in all participants. In contrast to our previous study in which we investigated changes due to ”pure” motor learning, the network changes observed here might reflect effects of additional perceptual learning. We conclude that together with other cortico-subcortical connections, putamen to cerebellar connectivity might be important for the encoding phase of a sequence whereas cerebellar to putamen connectivity could underlie the slow learning phase.

3.4.1 Changes in endogenous connections across sessions

We used random-effects Bayesian model selection combined with family level inference (Penny et al., 2010) to identify the optimal intrinsic network driven by the motor task and the input nodes to this network. This process uses the model evidence to reduce the susceptibility of the post-hoc Bayesian model selection procedure to falsely identify connections which are initially less probable (Stephan et al., 2010). There are two noteworthy differences between the two sessions in terms of endogenous connections, one being the different input node(s) and the other being different connectivity patterns of homolog brain areas. The input node(s) to the model play an important role as changes in activity due to general task performance propagate to the other nodes in the network through the input. Thus, it serves as a “gate” for the task-related signal changes. The pre-sleep session was characterized by driving input to cerebellum whereas in the post-sleep session, inputs were to premotor and supplementary motor regions. This suggests that the cerebellum serves as an input node when correct stimulus-response associations are to be

learned compared to when these are already automatized (Wolpert et al., 1998). In addition, during the pre-sleep session, both left and right cerebellar nodes had positive forward connections to putamen as well as motor cortical regions, whereas the post-sleep session had markedly sparser connections with no positive forward connections from right cerebellum to any other region. This connectivity pattern further strengthens the argument that the cerebellum is more important during the early learning phase (Bernard and Seidler, 2013). The cerebellum was identified as an input node in our previous study as well, in which we investigated the early learning phase (Tzvi et al., 2014). Input to the SMA and premotor areas in the post-sleep session might indicate that the task performance has been automatized such that continuous updating of the internal model by the cerebellum is no longer needed.

The second noteworthy difference was in connectivity patterns between homolog brain regions. In the pre-sleep session we found consistent positive connections between all cortical and subcortical homolog brain regions, whereas in the post-sleep session, connections were only found between homolog cortical areas. Pool and colleagues showed, similarly to our results, motor-related changes in connections between all homolog brain regions (premotor cortex, SMA, putamen and cerebellum), except for M1 (Pool et al., 2013). Moreover, we found significant positive connections from right ("performing") SMA and PMC to the left dominant SMA and PMC in both sessions, but between other brain regions (M1, cerebellum and putamen) only before sleep. This finding might indicate that interhemispheric transfer between M1, cerebellum and putamen is important for establishing the correct stimulus-response associations when the task demands are initially encoded whereas interhemispheric transfer between SMA and PMC are probably important for maintaining the stimulus-response representation for accurate performance. In a previous DCM study investigating causal connectivity patterns

between bilateral M1, PMC and SMA during whole hand closing movements, similar results were evident for PMC but not for M1 and SMA (Grefkes et al., 2008a). A positive connection from rPMC to lPMC was also observed in a stimulus response compatibility task (Cieslik et al., 2011), and during a simple left hand fist closure task (Pool et al., 2013), further strengthening the importance of this causal connection over PMC to general motor task demands. When participants performed a finger tapping task with the left hand, a positive connection was observed from rSMA to lSMA similarly to our results (Gao et al., 2014). We also found significant negative connections from lM1 to rM1 in both sessions (Grefkes et al., 2008a; Pool et al., 2013), however the observed negative connection from lPMC to rPMC in the pre-sleep session was not evident in previous DCM studies of the motor network (Cieslik et al., 2011; Grefkes et al., 2008a; Pool et al., 2013), suggesting that this connection might be specific for motor sequence learning demands. Future studies investigating dynamical interactions between cortical and subcortical regions during tasks with different stimulus-response mappings could shed more light on these important interhemispheric connections.

3.4.2 Modulatory effects of learning in the early phase

We developed a procedure based on recent advancements in DCM methodology in order to investigate causal information flow in brain networks involved in acquisition, consolidation and late learning phases of MSL. This "post-hoc" BMS procedure (Friston and Penny, 2011; Rosa et al., 2012), allowed us to approach the effective connectivity analysis with fewer a-priori assumptions (e.g. existence of certain connections or specific connections to be modulated) and a more distributed network (10 nodes). Using this protocol we identified several connections which were specifically modulated by learning in the pre-sleep session including connections

between bilateral putamen to cerebellum as well as connections from left M1 to right cerebellum and from right premotor cortex to left cerebellum.

The finding of left M1 to cerebellum connectivity replicates results of our previous study (Tzvi et al., 2014) using a bimanual SRTT. There, we found negative modulatory effects of learning on the connections from bilateral M1 to CB which corresponded to the effects found in the PET study by Penhune and Doyon (2005). Specifically, the connection from left M1 to right cerebellum was consistent across participants in all sessions. In the present study however, this connection was not consistently negative across participants. This inconsistent finding might be related to different learning strategies employed across participants in the SRTT paradigm we used here. If the connection from M1 to cerebellum represents the motor component of learning as suggested by our previous work, it will be less relevant in participants who performed in the current task by means of perceptual learning.

We also found that connections from bilateral putamen to cerebellum were negatively modulated by early learning, which we had not observed previously. However, we previously only compared models with learning-related modulations of the cortico-cerebellar network and modulations of the cortico-striatal network, which was based on theoretical considerations (Doyon et al., 2003). Hence, striatal-cerebellar connectivity was not directly investigated in the last study.

It might also be that the observed modulation of the connection from putamen to cerebellum reflects the perceptual learning in the task. This hypothesis is in accordance with the suggested role of putamen within the cortico-striatal-cerebellar network (Penhune and Steele, 2012) to (implicitly) form predictive associations between the stimuli and responses or between chunks of the sequence. Supporting evidence for this hypothesis is found in a study which directly

compared the perceptual and motor component in a MSL task and found that activity in putamen was increased in the perceptual component compared to the motor component during early learning (Bapi et al., 2006). In another study investigating the dissociation between the two components in the SRTT (Rose et al., 2011), bilateral putamen was found to be involved in both the perceptual and the motor components, the authors however did not directly compare putamen activity for the two representations. It is important to mention that in the work presented here, we did not attempt to study the effects of motor and perceptual learning separately, therefore the interpretations above remain speculative. Further investigations focusing specifically on the perceptual learning component of the SRTT are needed in order to address the changes in connectivity patterns between cerebellum and putamen in the course of MSL.

3.4.3 Modulatory effects of learning in the late phase

In the post-sleep session, modulatory effects identified by the "post-hoc" BMS procedure were unspecific to learning. This means that the connections in the model are modulated by general demands of the visuo-motor task rather than by sequence learning per se. Perhaps during the slow learning phase, as the motor memory is already consolidated, the computational efforts required to implement the learned motor sequence are reduced compared to the efforts needed for performing the task. In accordance with this finding, our participants did not show any further decrease in RTs in the post-sleep session. In addition, compared to the extended network of connections modulated by learning in the pre-sleep session, after sleep we found only two connections which were modulated by task performance. This result suggests that a general pruning of the network is taking place in the slow learning phase. Interestingly, when investigating condition-specific effects in the winning model, we found a negative modulation of the connection from the left cerebellum to the right putamen which was consistent across

participants only for the sequence condition. Thus, it seems that during the slow learning phase, the connection from cerebellum to putamen is weakened by additional practice, and this effect is more robust for sequence material.

This observation as well as the general pruning of the network after sleep is in accordance with a study showing decrease in the overall connectivity of the cortico-striatal-cerebellar network with extended practice over 4 weeks (Coynel et al., 2010). It also agrees with a resting-state network analysis which showed recruitment of the cortico-basal ganglia-thalamic-cerebellar network directly after motor learning but not in resting-state measured after 6 hours (Sami et al., 2014).

How might these changes in cerebellar-striatal connectivity come about? Direct anatomical connections between cerebellar and striatal circuits were previously thought to relay mainly through the cerebral cortex (Bostan et al., 2013). Only recently, studies using retrograde tracing demonstrated dense anatomical inter-connections between the striatum and the cerebellum (Bostan et al., 2010; Hoshi et al., 2005). Importantly, cerebellar projections were also found to non-motor (associative) regions of the putamen and the caudate nucleus (Hoshi et al., 2005). These findings led researchers to hypothesize that reciprocal connections between striatum and cerebellum may have a functional role in non-motor functions and specifically in learning (Bostan et al., 2013). Here, we took the first steps in showing that bilateral connections from putamen to cerebellum are relevant for the acquisition phase of a sequence whereas left cerebellum to right putamen connectivity is mediating the slow learning phase of the motor sequence.

3.4.4 Methodological considerations

We found that pre- and post-sleep sessions indeed differed in their optimal endogenous connectivity patterns and input nodes, preventing us from quantitatively comparing the

connectivity parameters across sessions. This is an interesting methodological finding since some DCM studies model several different sessions or several different groups assuming the same intrinsic network pattern and/or input node/s (see for example: (Cardenas-Morales et al., 2013; Eickhoff et al., 2008; Grefkes et al., 2010)). Although this is necessary for a quantitative comparison of groups or sessions, the present results show that caution should be taken when making such assumptions.

3.4.5 Limitations

There are a few limitations to be mentioned. First, as motor memory consolidation has been shown to involve hippocampal-striatal networks (Albouy et al., 2013) it would have been interesting to include hippocampal ROIs in the DCM analysis. We were however not able to obtain signals from more than half of the participants from the hippocampus based on the criteria set above (see Methods section) and therefore could not include the hippocampus in this analysis. This might be related to acquisition parameters which were not optimized for such small subcortical structures. Future fMRI studies might be able to specifically target the basal ganglia and hippocampus in order to investigate these connections. Second, the comparisons between pre- and post-sleep session with regard to network analysis are mainly qualitative comparisons. We were not able to quantitatively compare the different sessions as the optimal intrinsic models differed between pre- and post-sleep sessions. Third, we performed an assessment of awareness of the sequence material after both the pre- and post-sleep session. This was done to identify those participants who had already gained explicit knowledge of the sequence after the first session or after sleeping. Although this is a critical issue when investigating the effects of implicit motor sequence learning, it might be that due to this assessment participants became aware of a potential regularity and thus might have changed their

learning strategy. Importantly, only six participants indeed gained explicit knowledge of the sequence after the post-sleep session and those participants were therefore excluded from our analysis.

3.4.6 Conclusions

Motor sequence learning has been repeatedly shown to involve several cortical and subcortical structures in both the early and the late phase in which consolidation of motor memory takes place. Using recent advancements in DCM methodology, we were able to address some more specific questions about this wide-spread network and the changes it undergoes after consolidation of a motor memory. We found general pruning of the cortico-striatal-cerebellar network after consolidation of a motor sequence. Importantly, connectivity between bilateral putamen to cerebellum was found to be modulated by learning in the pre-sleep session whereas slow learning in the post-sleep session showed sequence-specific modulation of a connection from left cerebellum to right putamen. These results provide a deeper understanding of the brain networks involved in motor memory formation and automatization and might provide a basis for future explorations of striatal-cerebellar networks in the context of learning and memory.

Chapter 4

Reduced α-γ_{low} phase amplitude coupling over right parietal cortex underlies implicit visuomotor sequence learning [3]

4.1. Introduction

Visuomotor sequence learning is essential for daily behavior such as when typing visually presented text or playing an instrument by reading scores. Extensive fMRI work has revealed a wide-spread network including motor and premotor cortex, parietal regions as well as the basal ganglia and cerebellum which are engaged in different stages of motor learning (reviewed in Dayan and Cohen, 2011; meta-analysis by Hardwick et al., 2013). Less is known, however, about the temporal dynamics of neural activity in this network during motor memory formation. Electrophysiological studies in humans and animals point to a critical role of oscillatory activity and cross-frequency interactions for both motor control and memory functions (Axmacher et al., 2010; Canolty et al., 2006; Dürschmid et al., 2014; Friese et al., 2012; Tort et al., 2009; Tort et al., 2008; Tzvi et al., under review). Here, we linked these two lines of research by investigating the cortical oscillatory dynamics during motor memory formation in humans. Specifically, we studied the role of theta and alpha oscillations and phase-amplitude coupling between lower frequencies (theta, alpha) and gamma activity for visuomotor sequence learning using EEG in a large group of participants.

4.1.1 Implicit visuomotor sequence learning in the serial reaction time task

We used the serial reaction time task (Nissen and Bullemer, 1987) - an extensively applied method for studying implicit visuomotor sequence learning. Embedded within this task are two

[3] The author contributed to the analysis of the data and writing of the manuscript.

learning components: implicit learning of a hidden regularity in the stimulus- and response-sequence and explicit learning of visuomotor associations between a cue and a specific response (Robertson, 2007). Both of these learning components affect behavioral performance and may be driven by different neural mechanisms (Schwarb and Schumacher, 2009). A recent meta-analysis investigating 24 movement-controlled imaging studies employing the SRTT found a network of bilateral dorsal premotor cortex, left thalamus and right cerebellum which were activated during visuomotor sequence learning (Hardwick et al., 2013). Due to the direct link between cue and response in this task, different learning strategies may be implemented: learning the stimulus sequence or learning the sequence of responses. Results from a recent study implementing a SRTT variant in which these components could be distinguished showed that whereas the motor learning component activated the cortico-striato-cerebellar network, perceptual learning involved only bilateral hippocampus (Rose et al., 2011).

4.1.2 Learning, memory and neural oscillations

Extensive evidence exists for the importance of neural oscillations in learning and memory, starting with the characteristic theta rhythm of place cells in the hippocampus (Buzsaki, 2002). For example, both theta and gamma power were found to be increased for later remembered pictorial items during encoding and for recognized items during retrieval in human participants (Osipova et al., 2006). In a visual recognition memory task, increased gamma-band synchronization was evident in the hippocampus of macaque monkeys during successful encoding (Jutras et al., 2009). In local field potentials (LFP) recorded from the medial temporal lobe in monkeys, both beta and gamma power were differentially modulated by familiar vs. new stimuli in an associative learning study (Hargreaves et al., 2012).

Although oscillatory activity is prevalent in the motor system with its characteristic beta and alpha (or mu) rhythms (Pfurtscheller and Lopes da Silva, 1999), little is known about the role of oscillatory activity for visuomotor sequence learning. In a high-density EEG study of visuo-motor adaptation, increased gamma (>30 Hz) power over right parietal areas was found during the initial learning stage (Perfetti et al., 2011). In another study, while rhesus monkeys learned a series of visually guided hand movements (Lee, 2003), coherent gamma activity was observed between neurons recorded in supplementary motor area (SMA) around stimulus onset. Together, this line of evidence suggests that oscillations may play an important role in motor sequence learning.

4.1.3 Phase amplitude coupling in learning and memory

Whereas above-mentioned work focused on amplitude changes in particular frequency bands, interactions between frequency bands, so-called cross-frequency coupling, have been suggested to be similarly relevant for various cognitive processes including learning and memory (Canolty and Knight, 2010; Fell and Axmacher, 2011). Phase amplitude coupling (PAC) is one form of cross-frequency coupling in which presumably local neural activity expressed as high-frequency amplitude is gated by the timing (phase representation) of a wide-spread slow oscillation. PAC over different brain structures has been shown to underlie cognitive processes such as associative learning (Tort et al., 2009), attention (Szczepanski et al., 2014), and decision making (Tort et al., 2008), and was evident in simple visual tasks (Voytek et al., 2010) and altered in movement disorders (de Hemptinne et al., 2013). Specifically, theta-gamma PAC has been previously shown to underlie working memory and long-term memory processes (Lisman and Jensen, 2013). Recent studies in patients with electrodes implanted in the hippocampus found specific coupling between the phase of slow oscillations in the delta (<4 Hz) and theta (4-8 Hz) frequency

bands and gamma amplitude during successful encoding (Axmacher et al., 2010; Lega et al., 2014). An MEG study investigating effects of context-dependent episodic memory corroborated theses results in the hippocampus as well as provided evidence for theta-gamma and beta-gamma PAC over parietal areas during successful memory retrieval (Staudigl and Hanslmayr, 2013). Finally, Friese and colleages found increased theta phase to gamma amplitude coupling between frontal and parietal areas for items to be encoded which were represented by posterior gamma activity (Friese et al., 2012). This line of evidence has led researchers to hypothesize that PAC reflects memory encoding and retrieval processes (Hanslmayr and Staudigl, 2014).

In the context of motor learning, PAC has previously been investigated using intracranial recordings. In one such study, different sensori-motor tasks were used to investigate learning-related theta-high-gamma PAC over motor cortical areas. Increased theta-gamma PAC was observed over time for early learning, whereas late learning showed consistent theta-gamma PAC decrease (Dürschmid et al., 2014). Several studies in animals and humans examined PAC related to simple motor behavior. A study in rats showed distinct patterns of theta-gamma PAC over both sensorimotor cortex and striatum during motor behavior whereas during rest, gamma amplitude was coupled preferentially to the delta (<5 Hz) phase (von Nicolai et al., 2014). In humans, beta-gamma PAC was evident over sensorimotor cortex during fixation and abolished when patients initiated movement (Miller et al., 2012). Alpha-gamma PAC on the other hand was strongest when patients were waiting to execute a movement and was abolished when the movement was initiated (Yanagisawa et al., 2012). Similarly, increased alpha-gamma PAC over sensorimotor cortex was observed during response inhibition compared to movement in a Go/Nogo task (Tzvi et al., under review). This line of evidence suggests that PAC mechanisms underlie both motor and possibly memory functions required for visuomotor sequence learning.

In the present study, we investigated oscillatory activity and PAC over cortical regions known to be involved in motor sequence learning, namely premotor, motor and parietal cortex. As increased theta-gamma PAC has been observed in both short and long-term memory tasks, we hypothesized that learning-related cortical areas will exhibit increased theta-gamma PAC during learning. Alpha-gamma PAC on the other hand has been shown to decrease in motor areas during motor movement vs. rest. We therefore expected reduced alpha-gamma PAC during learning.

4.2. Materials and Methods

4.2.1 Subjects

In total, 109 participants (mean age: 22 years, range 18-31; 54 male) participated in the study after giving informed consent. The data was collected as part of a bigger project studying the effects of sleep on hemisphere-specific effects on motor sequence learning. Because of that, half of the participants performed the task with their right side (stimuli on the right and responding hand right; RS: N=54) and half with their left side (LS: N=55). ERP results with respect to gaining explicit knowledge of the motor sequence were recently published by Verleger and colleagues (2015). For the present analyses, we did not have any specific hypotheses with respect to hemisphere differences but nevertheless tested for possible hemisphere effects (see below for details). All subjects were right handed, had normal or corrected to normal vision with no color deficiency. The study was approved by the Ethics Committee of the University of Lübeck and was performed in accordance with the Declaration of Helsinki.

We excluded 6 participants due to explicit knowledge of the sequence (see section 4.2.4 for details). For the EEG data analysis, additional 30 participants were excluded due to artifacts in the analyzed electrodes and due to lack of sufficient trials in one of the experimental conditions

for the purpose of phase-amplitude coupling analysis (see section 0). This resulted in a total sample of 73 participants (37 women) for the analyses presented here.

4.2.2 Experimental paradigm

Participants performed a modified version of the standard serial reaction time task (SRTT) as shown in Fig. 4.1A. Visual stimuli were presented on a 17" Monitor (Samsung SyncMaster 757 DFX, 100 Hz, 1024 x 768 Pixel). Index to little fingers of the responding hand rested at the four active keys of a custom-made keyboard which contained sets of four keys for each hand. The four keys to be used with one hand were placed about 3 cm from each other in arc-shaped ergonomic arrangement. The keyboard was placed on an adjustable board in front of the participant. Half of the participants performed with their left hand (n = 37 of the analyzed sample; LS group) and half performed with their right hand (n = 36; RS group). In each trial, a colored circle (blue or red or yellow or green) was presented on one side of the screen, always left of fixation for the LS group and always right for the RS group. The stimulus side thus corresponded to the side of the response hand for each participant. Responses had to be made by pressing the correspondingly colored key on the keyboard as quickly as possible: Blue with the index finger, red with the middle finger, yellow with the ring finger, and green with the little finger.

In each trial (for the trial timing see Fig. 4.1B), first a fixation cross was presented for 400 ms. Next, the colored visual cue appeared for 200 ms. Its diameter was 1° and its center was located 4.5° laterally from the center of the white screen at horizontal midline. A dark-grey circle of same size was presented at the other side of the screen symmetrically to the color circle, in order to facilitate fixation at the center by having sudden onsets at either side. When a correct response was given, there was renewed presentation of the fixation cross for 200 ms and a thickening of

the cross (from 0.7 mm to 2.8 mm line width) for 200 ms, signaling a correct response, and the next trial began. Unbeknownst to the subjects, a hidden, second order predictive (Curran, 1997) 12-element sequence of stimuli and, therefore, button presses was introduced in parts of the experiment (Fig. 4.1C). These parts are referred to as sequence trials. In the other parts, there was no particular order of buttons to be pressed (hence, no order of colors). These parts are referred to as random trials.

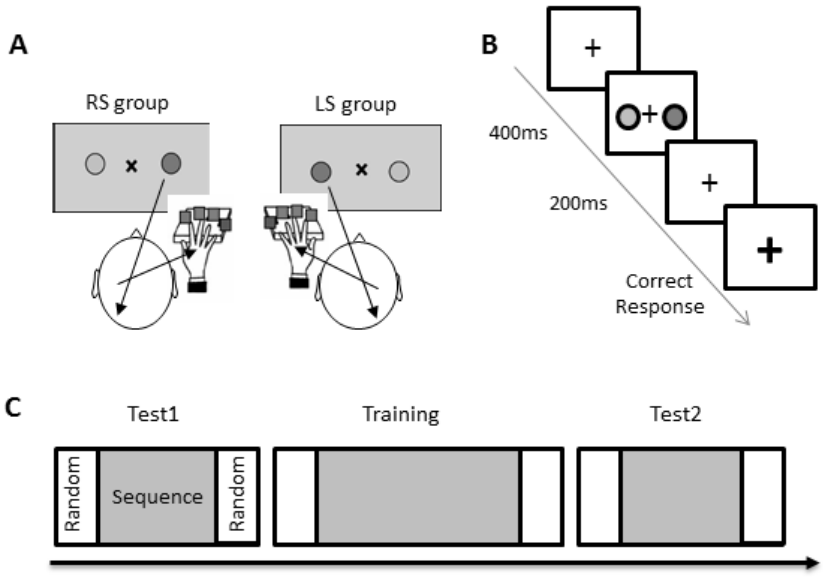

Figure 4.1. The serial reaction time task. **A** In the right side (RS) group, visual stimuli are presented to the right of a fixation cross. Subjects are requested to perform with the right hand. In the left side (LS) group, visual stimuli are presented to the left of a fixation cross. Subjects are requested to perform with the left hand. **B** Single trial timeline. Upon presentation of the visual stimuli, subjects were requested to respond with a corresponding button press. Feedback was given for correct responses. **C** Experimental design. Each of the three task sessions contained blocks of sequence trials sandwiched by blocks of random trials.

4.2.3 Procedure

The task was divided into three sessions (Cohen et al., 2005): "Test1", "Training" and "Test2", each containing a block of sequence trials "sandwiched" between two blocks of random trials (Fig. 4.1D). There were self-terminated breaks in between the three sessions. In each of the task

sessions (both “Test” and “Training”), random blocks contained 100 random trials divided into 50 trials preceding the sequence block and 50 trials following the sequence block. Sequence blocks in the “Test” sessions contained 180 trials corresponding to 15 repetitions of the 12-element sequence. The sequence block in the “Training” session contained 300 trials corresponding to 25 repetitions of the 12-element sequence. In total 960 stimuli were presented to the subjects.

4.2.4 Behavioral analysis

Reaction times

Reaction times (RTs) were computed in each session for each condition. For the random condition, we averaged the RTs across trials from both the sequence-preceding random block and the sequence-following random block. We excluded trials in which the subjects made an initial error as well as trials in which RTs were either longer than 3000 ms or deviated by more than 2.7 standard deviations (SD) from their average response time (corresponding to $p<0.01$). In order to assess implicit learning, we compared the average RTs in each of the conditions (SEQ, RND) and each of the three sessions using a 2 x 3 mixed effects ANOVA with the between-subject factor Group (LS vs. RS).

Error-rates

Trials were counted as correct when the correct key was pressed as the first response 150-3000 ms after stimulus onset. All other trials were counted as errors. Some subjects made premature responses, i.e. responded before the stimulus appeared. These responses were not taken into account for the analyses of error rates. Error rates were submitted to the same ANOVA as response times.

Assessment of explicit awareness

To have a homogeneous sample, the few participants who demonstrated full explicit knowledge about the sequence were excluded from analysis. Explicit knowledge was assessed after a second SRTT session that took place 12 hours after the SRTT session reported here. Participants were asked to write on paper any regular sequence they had noted. We excluded those participants who remembered 10-12 elements.

4.2.5 Electrophysiological recordings

Eye-tracker

Fixation was controlled by means of an infra-red remote eye tracker (Eyegaze Analysis System, Interactive Minds, Dresden, Germany) placed below the computer screen. When the eye-tracker noted at the onset of any trial that participants deviated from fixation by more than 1.4°, a large red exclamation mark was presented at screen center for 2 s, attracting gaze back to the center. Then the trial was restarted.

EEG recordings

EEG was recorded with Ag/AgCl electrodes (Easycap, www.easycap.de) from 26 scalp sites, including 4 midline positions (Fz, FCz, Cz, Pz) and 11 pairs of symmetric left and right sites (F7, F8; F3, F4; FC3, FC4; T7, T8; C3, C4; CP5, CP6, CP1, CP2; P7, P8; P3, P4; PO7, PO8; O1, O2). Additional electrodes were placed at the nose-tip for off-line reference and at Fpz as connection to ground. On-line reference was Fz. For artifact control, electrooculogram (EOG) was recorded, both vertically (vEOG) from above vs. below the right eye, and horizontally (hEOG) from positions next to the left and right tails of the eyes. Data were amplified from DC to 250 Hz by a BrainAmp MR plus and stored at 500 Hz per channel.

4.2.6 EEG data analysis

Pre-processing

Pre-processing and all subsequent analyses were performed using in-house Matlab (The Mathworks®, Natick, MA) scripts and the EEGLAB toolbox (Delorme and Makeig, 2004). Data were re-referenced to the nose electrode and segmented into epochs of -1 s to 4 s with regard to stimulus onset. This procedure was done in order to avoid high-frequency edge artifacts when performing artifact rejection. A high-pass filter (F_{cutoff}=0.5 Hz) was applied to the signals to remove slow drifts as well as a 200^{th} order notch filter (F_{cutoff} = 48-52 Hz) for removing power line noise. Based on an independent component analysis (ICA), we visually identified components related to eye blink artifacts and removed them (Delorme and Makeig, 2004). Additional artifacts were removed using a simple threshold (-70 µV, +70 µV) on the filtered data. As trial duration was shorter than 5 s, we additionally rejected overlapping epochs. In a substantial number of subjects, F7, F8, T7, T8, P7, P8, PO7, PO8, O1 and O2 electrodes were contaminated with noise (mostly from muscular activity). As these electrode locations were not relevant for our analysis, they were excluded resulting in N=16 total electrodes analyzed (Fz, FCz, Cz, Pz, F3, F4, FC3, FC4, C3, C4, CP5, CP6, CP1, CP2, P3, P4).

In order to increase the spatial resolution in our EEG data, we performed a current density transformation using the current source density toolbox for Matlab (Kayser and Tenke, 2006a, b). This method effectively reduces the effects of volume conduction by estimating a spatial Laplace transformation which provides topographical selectivity. Please note that after the transform, the units of the data were rescaled to $\mu V/cm^2$.

Spectral power analysis

In order to evaluate general changes in spectral power for the different task conditions, we first extracted the frequency bands of interest, i.e., θ (4-8 Hz), α (8-13 Hz) and γ_{low} (30-48 Hz), using a band pass filter with sharp-edge finite impulse response (FIR) filters (500^{th} order). Phase and amplitude representations were obtained using the Hilbert transform. Power estimates were calculated as the square of the amplitude, averaged within the 5 s time-window. For each of the experimental sessions (Test1, Training, Test2) and for each condition (Sequence, Random), we averaged the power of each frequency band across all corresponding epochs. In each electrode we performed a 2x2x3 mixed effects ANOVA accounting for spectral changes due to practice (the three sessions) and to learning (Sequence and Random) with the between-subject factor Group (LS vs. RS). We did not have any specific hypothesis regarding the effects of performance side on the learning-related effects on power. Differences were considered significant if $p<0.05$, FDR corrected for the number of electrodes.

Analysis of phase-amplitude coupling

Phase amplitude coupling (PAC) analysis was performed for all electrodes using the modulation index (MI; Tort et al., 2010) and in-house MATLAB scripts. In each of the 5 s epochs, α and θ oscillations were binned by their phase (6 bins, $\Delta\varphi = \frac{\pi}{3}$) and the amplitude envelope of γ_{low} was averaged within each phase bin. Each bin was then averaged across the number of oscillations identified in the 5 s epoch and across all epochs for each condition (Sequence, Random) and each session (Test1, Training, Test2). Subsequently, the averaged values were normalized across all bins resulting in a "phase-amplitude plot".

The divergence of the resulting phase-amplitude plot from a uniform distribution was calculated using the Kullback-Leibler distance and the Shannon entropy as follows:

$$MI = \frac{\log(N) + \sum_{j=1}^{N} P(j)\log[P(j)]}{\log(N)}$$

P(j) is the amplitude for a given bin j; N is the number of bins (in our case N=6) and log(N) represents the entropy of a uniform distribution.

In order to evaluate the influence of the number of epochs on the MI, we performed an analysis in which MI was calculated in real data (electrode Cz in one subject; 113 epochs) for different numbers of epochs (5 to 50 in steps of 5). This analysis was repeated 100 times for each number of epochs after shuffling the epoch order. We then calculated the mean MI across the 100 permutations for each epoch number. We found that the mean MI reaches a plateau when the number of epochs exceeds 20 and therefore used this threshold for our analysis: We excluded subjects who had less than 20 epochs for a given condition or session. As we did not observe any effects of the group factor (RS vs. LS) on performance and power (see results section), we did not consider the group factor for the PAC analyses. Log transformed MIs in each condition and session were thus statistically analyzed using the 2x3 random-effects ANOVA to identify learning related PAC changes.

High MI values across individual subjects and conditions reflect non-random distributions of amplitude values across phase bins. However, different subjects could still show coupling of γ amplitude to different phases of the α/θ oscillation. In order to only consider PACs that were consistent across subjects, we calculated the mean phase-amplitude plot across subjects for each condition and each session. Using a two-sample t-test we evaluated the difference between the bin with lowest amplitude value and the bin with the highest amplitude value. We considered

significant within-electrode PAC differences with $p<0.05$, FDR corrected for the number of electrodes for the main effect of condition and $p<0.05$, FDR corrected for the number of electrodes for the comparison between the bins.

Analysis of transition blocks

In the standard analysis of SRTT, learning-related effects are assessed by comparing the sequence condition to the random condition. Since the participants are unaware of the changes in task conditions, it is plausible that when sequence trials stop and random trials begin, participants still attempt to implement the sequence, even though the sequence material is no longer present. This should result in more performance errors and slower RTs in this transition phase. We performed an additional analysis of these "transition" effects to study whether the differences we observed between sequence blocks and random blocks exist as well between transition and random blocks. As a first step, in each session we computed the RTs and accuracy for the random sub-block which followed the sequence block separately from the random sub-block preceding the next sequence block. The sub-block directly following the sequence trials will be referred to as "transition" block, whereas the sub-block preceding the sequence trials will be referred to as "random" block. As this analysis dramatically reduces the amount of trials in the random condition, we had to exclude many of the participants who did not have enough trials in a given session (criteria for exclusion outlined in section 0). For this analysis, we pooled over LS and RS performers, resulting in a total of 26 participants after exclusion. Next we performed behavioral as well as PAC analyses with the conditions of interest using a 2 x 2 rmANOVA with factors block (random and transition) and session (1 to 2, 2 to 3).

4.3. Results

4.3.1 Behavioral data

We performed mixed effects ANOVA on reaction times (RTs) with condition and session as within-subject factors and side of stimuli and responses as between-subject factor to investigate the effects of learning. We found no significant main effects or interactions with the group factor (all $p>0.4$) suggesting that learning effects were not dependent on performing the task left or right. Participants performed the sequence blocks significantly faster than the random blocks ($F_{1,71}=70.9$, $p<0.001$) and showed a general speeding across sessions ($F_{2,142}=60.0$, $p<0.001$). The interaction between condition and session was not significant ($F_{2,142}=1.6$, $p=0.2$). In Figure 4.2A, we plot the normalized reaction times across all participants.

The error-rate was generally low (8.0% ±5.6%). Participants made significantly more errors in the random blocks compared to the sequence blocks ($F_{1,72}=9.0$, $p=0.004$) with no significant differences between sessions ($F_{2,144}=1.9$, $p=0.16$) and no condition x session interaction ($F_{2,144}=1.0$, $p=0.36$). Figure 4.2B presents the error rates across all participants.

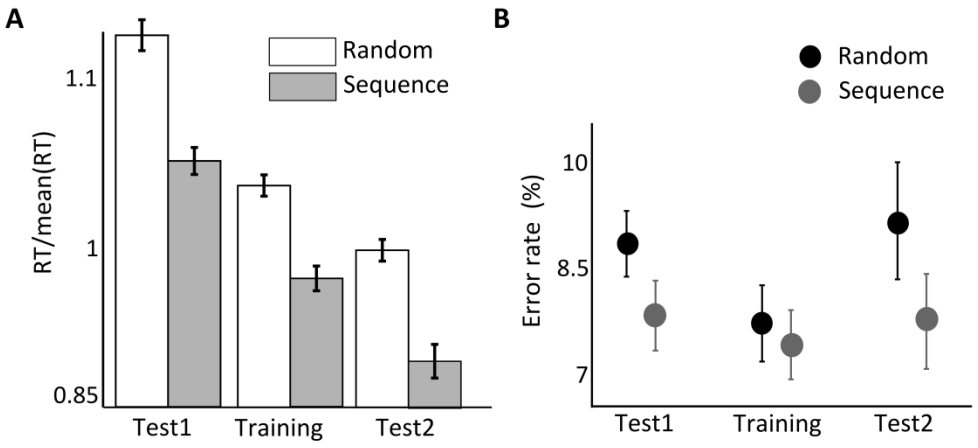

Figure 4.4. Behavioral analysis. **A** Normalized reaction times in random and sequence blocks across sessions. **B** Error-rates in random and sequence blocks across sessions.

4.3.2 Learning related α-, θ- and γlow -power changes

We investigated the effects of learning-related power changes in θ, α and γ_{low} frequency bands in each electrode. We performed a mixed effects ANOVA with condition and session as within-subject factors and side of performance as between-subject factor in each electrode for each of the frequency bands. We found condition x session x performance side interactions in theta power over CP5 ($p = 0.04$), and in alpha power over Fz ($p = 0.04$), but these interactions did not survive correction for multiple comparisons. Otherwise, there was no evidence for the effect of performance side on learning-related power changes in any of the frequency bands.

Across conditions, α power was strongest over parieto-occipital areas. Condition x session interaction effects in α power were wide-spread (see Figure 4.3A). As can be observed in Figure 4.3A (bottom row), α-power was increased in sequence relative to random blocks during Test1, but was decreased relative to random blocks during Test2. As can be observed from the maps in Figure 4.3A, the effects yielded significance at most electrodes but were strongest over parieto-occipital areas. Based on previous studies of motor sequence learning showing alpha power decrease over sensorimotor areas (Andres et al., 1999; Houweling et al., 2008; Hummel et al., 2003; Pollok et al., 2014; Zhuang et al., 1998), we further investigated the effects of learning on alpha power in electrodes: C3, Cz and C4 (data not shown). During Test1, alpha power increased significantly in sequence blocks compared to random blocks over Cz ($t_{1,72}=2.9$, $p=0.005$). In accordance with previous reports, in Test2, alpha power significantly decreased in sequence blocks compared to random blocks over C4 ($t_{1,72}=2.4$, $p=0.018$). No significant differences were observed over C3.

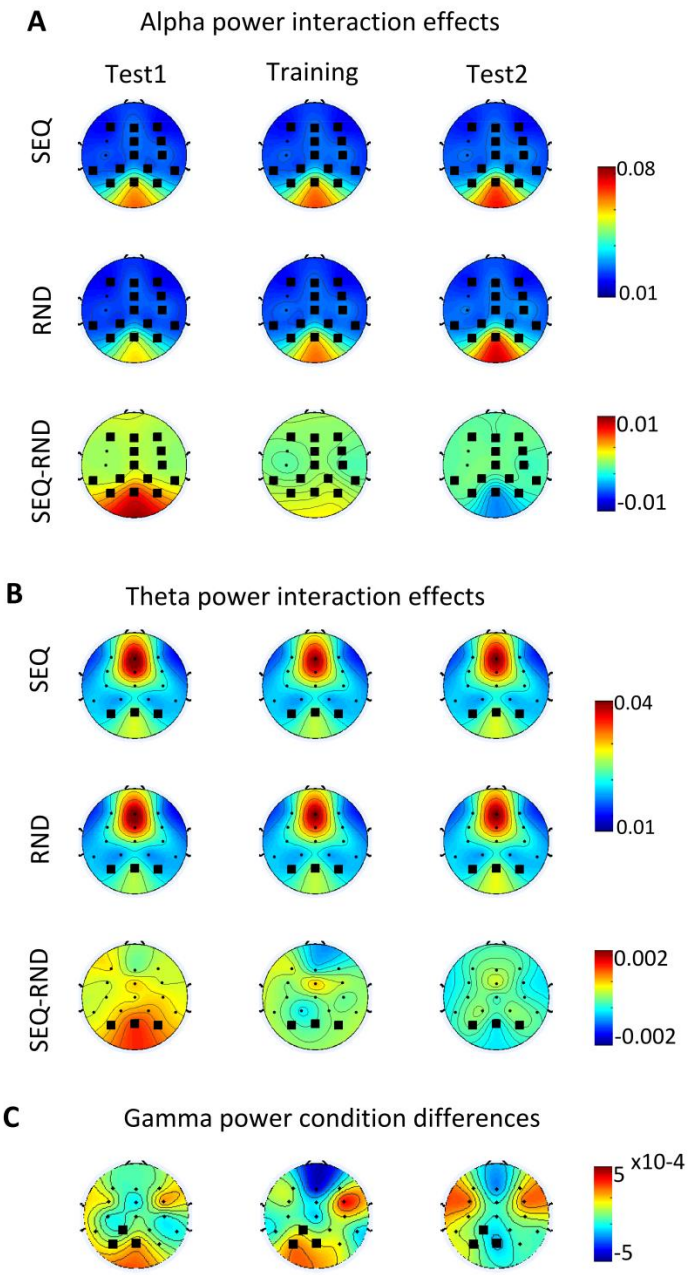

Figure 4.3. Power effects in alpha, theta and gamma band. Black dots are electrodes which were included in the analysis. Electrodes marked with a black square showed interaction effects ($p<0.05$, FDR corrected) in plots A and B and significant condition differences in plot C. Units for all plots are $(\mu V/cm^2)^2$. **A** In both sequence (SEQ) and random (RND) alpha power is increased over posterior parietal areas compared with other regions. Learning (SEQ-RND) is associated with alpha power increase in the first session over parietal areas and alpha power decrease in the later learning stage. **B** Theta power increase over frontal areas is observed for both SEQ and RND. Learning-related increase is evident in the first session over parietal areas. **C** Learning-related low-gamma power changes.

Across conditions, θ power was strongest over frontocentral sites. Significant θ power interaction effects (condition x session) were found over parietal areas (see Figure 4.3B). In these electrodes, θ power was increased for sequence vs. random in Test1. No main effects of condition were found for θ band. For γ_{low} power no such interaction was evident, but a significant increase during sequence compared to random trials was evident over left centro-parietal areas (Figure 4.3C).

4.3.3 Phase amplitude coupling

We assessed α-γ_{low} and θ-γ_{low} phase amplitude coupling using the modulation index (MI; Tort et al., 2010) and tested for PAC differences in task conditions and across sessions using a 2x3 ANOVA on log transformed MI values. In addition, we evaluated the consistency of the α/θ phase which γ_{low} amplitude is coupled to by using a paired t-test (see methods section for detailed description). Using both measures, we considered differences significant with a threshold of $p<0.05$, FDR corrected for the number of electrodes.

α-γ_{low} PAC was smaller in SEQ than in RND in several frontocentral and centroparietal electrodes: CP2 ($F_{1,72}=17.8$; $p<0.001$), FC3 ($F_{1,72}=7.4$; $p=0.008$), FC4 ($F_{1,72}=13.1$; $p<0.001$), and P4 ($F_{1,72}=8.4$; $p=0.005$) (see topographical plot in Figure 4.4A; electrodes marked with a square). The averaged MI at these electrodes presented in Figure 4.4A (bar plots) is showing the generally reduced coupling values in sequence trials. Although this difference over frontal electrodes seemed to be more pronounced for the "training" session, condition x block interaction was not significant (for FC3 and FC4: $p>0.1$). Importantly, the distribution of γ_{low} amplitude values across α phase bins averaged across all participants (Figure 4.4B) demonstrates a consistent relationship between low frequency phase and high frequency amplitude. In both sequence and random trials, γ_{low} amplitude was strongest at the trough of the α cycle.

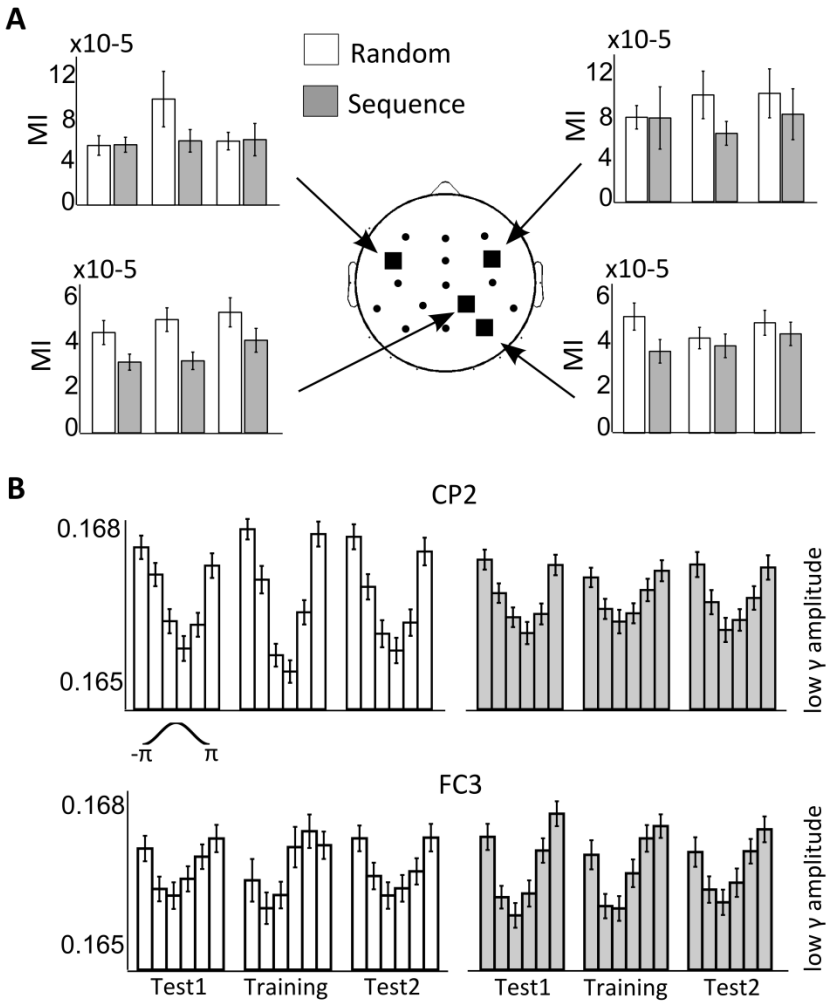

Figure 4.4. Alpha-low gamma phase amplitude coupling results. **A** The topographical plot shows the electrodes that had significant condition differences in alpha-low gamma PAC. The bar plots show the average MI (modulation index) across the task (error bars are SEMs across subjects) for the electrodes marked with a black arrow. **B** phase-amplitude plots for alpha-low gamma coupling in electrodes CP2 and FC3. The curve represents the alpha oscillation to which the low gamma amplitude is coupled to.

We found no signifcant difference in θ-γ_{low} PAC between conditions or sessions as well as no interaction effects. In addition, we tested for correlation of α-γ_{low} and θ-γ_{low} PAC with reaction times and with error-rates, however no signifcant correlation was found.

4.3.4 Analysis of transition blocks

Transition blocks (i.e., random blocks directly following sequence blocks) were compared to the following random blocks using a 2x2 ANOVA with factors: block (transition, random) and session (1 to 2, 2 to 3). This analysis was done in a subsample of 26 participants (16 RS and 10 LS) who had enough artefact-free trials in the transition phase.

The RT analysis revealed a significant main effect of block ($F_{1,25}$=12.1, p=0.002) but no significant interaction ($F_{1,25}$=0.0) reflecting slower RTs in the transition phase compared to the following random phase (Figure 4.5A). In addition, error-rates (6.4% ±4.3%; Figure 4.5B) were marginally larger in transition than in random blocks ($F_{1,25}$=3.3, p=0.08). Together, these results indicate that a behavioral transition took place in which subjects might have still attempted to implement the sequence, although sequence material was not present.

The same ANOVA was conducted on α-γ_{low} and θ-γ_{low} PAC values from random and transition blocks in each session, separately for each electrode. α-γ_{low} PAC was reduced in the transition phase compared to the following random phase, reflected by a main effect of Block at electrode CP2 ($F_{1,25}$=5.6; p=0.03; see Figure 4.5C). Although the difference in the second transition was nominally smaller, the interaction of block and session was not significant ($F_{1,25}$=2.4; p=0.14). Significant α-γ_{low} PAC interaction effects were, however, observed at electrodes FC3 ($F_{1,25}$=11.2; p=0.003) and C3 ($F_{1,25}$=4.3; p=0.048) (see topographical plot in Figure 4.5C; electrodes marked with a circle). In FC3, α-γ_{low} was reduced in the transition phase in Test1 relative to the following random phase in Training (t_{25}=2.81, p=0.01) but not when comparing the transition block in Training to random block in Test2 (t_{25}=-0.27, p=0.79) (Figure 4.5C, upper bar plot). In C3 (data not shown), no significant differences were observed between the transition and the random phases (p>0.2 for all post-hoc t-tests). We tested for a relationship of the phase-coupling

effects at CP2, FC3 and C3 with the behavioral transition effect by correlating the MI differences with the error rate difference, but the correlations were not significant.

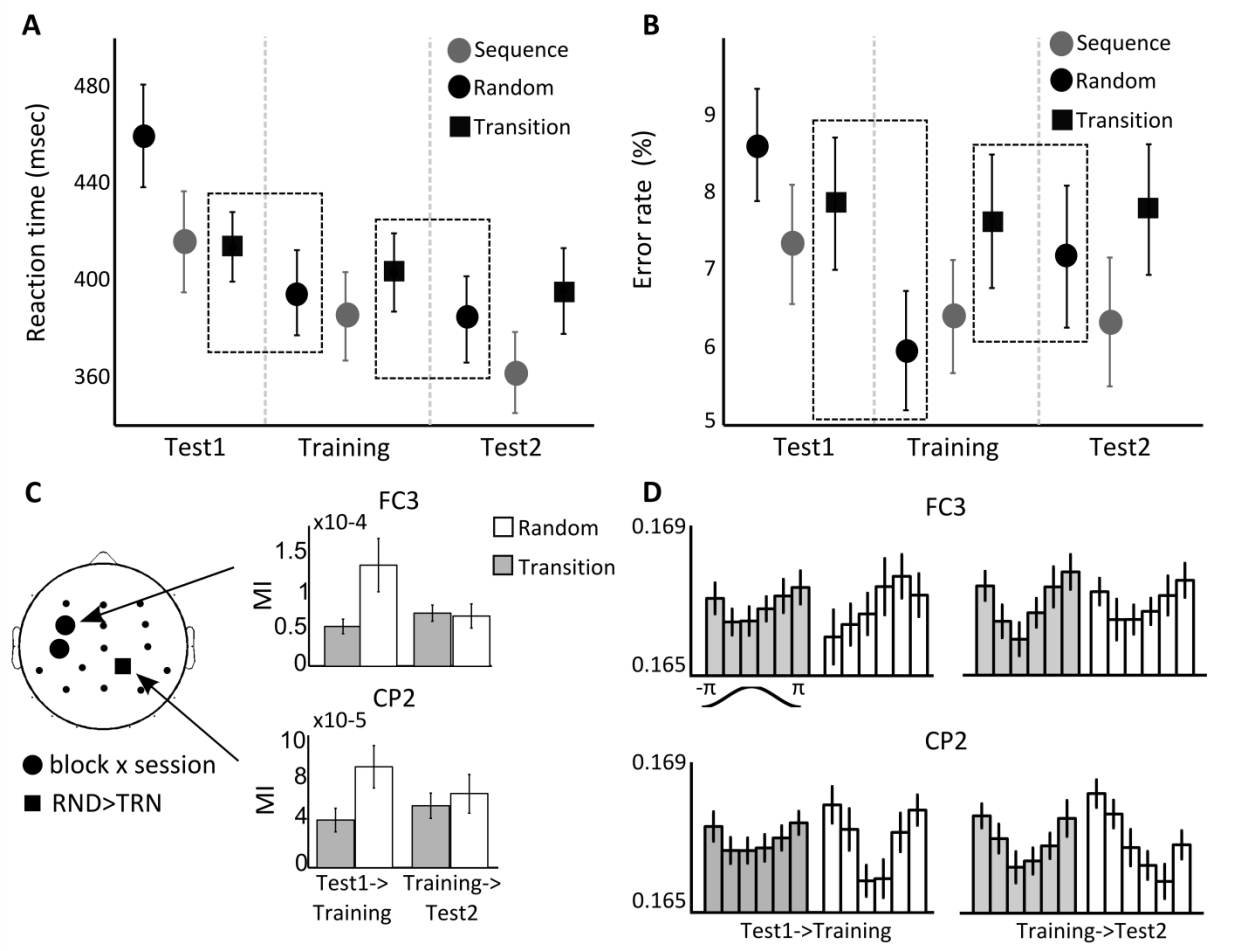

Figure 4.5. Transition analysis results. A Reaction times for the different conditions across sessions. B Percentage error rate for the different conditions across sessions. C Topographical plot shows the electrodes that showed significant condition differences in alpha-low gamma PAC (black square) or interaction effects (black circle). D phase-amplitude plots for alpha-low gamma coupling in each of the electrodes marked with a black arrow. The black curve represents the alpha oscillation to which the low gamma amplitude is coupled to.

4.4. Discussion

We investigated oscillatory markers of implicit visuomotor sequence learning in EEG-data of a large sample of subjects who performed the serial reaction time task (Nissen and Bullemer, 1987). We found a significant learning-related alpha-power increase early on in the task as well as a significant learning-related alpha-power decrease in a later session of the task. Moreover, alpha/low-gamma PAC was decreased in sequence blocks over right parietal cortex and over bilateral frontal cortex. Further analyses of the transition phase from sequence to random blocks, in which subjects still implicitly tried to implement the learned motor sequence leading to increased error rates, revealed the same effect: Transition relative to random blocks showed reduced alpha/low-gamma PAC over right parietal cortex and left frontal cortex. Together, these results suggest that implicitly learning and implementing a learned motor sequence leads to a reduction of alpha/low-gamma PAC in frontal and parietal cortex.

4.4.1 Behavioral effects of implicit visuomotor sequence learning

Analysis of reaction times revealed a significant difference between sequence and random blocks, indicating learning of the sequence. There was also a general reduction in reaction times with session which points to practice effects of the motor task itself. We found no significant condition x block interactions, suggesting that participants had adapted to the sequence regularity during the first block already and did not further gain with time. Error rates were low and were significantly higher for random blocks compared to sequence blocks. These results suggest that subjects were implicitly trying to implement the sequence during the random phase. In particular, we analyzed behavioral differences between regular random blocks and random blocks directly following sequence blocks (so called “transition” blocks) for which we hypothesized that

subjects were still attempting to implement the sequence. Indeed, subjects were slower and tended to commit more errors in the transition compared to the random block.

4.4.2 Alpha power changes as learning progresses

We found a learning-related alpha power increase over posterior parietal areas in the first learning session. In the later session, on the other hand, this effect was reversed and alpha power decreased over this region during sequence blocks. This condition difference was widely distributed with a maximum over occipito-parietal areas. Alpha power modulations over occipito-parietal regions have been previously linked to visuospatial attention mechanisms (Foxe et al., 1998; Worden et al., 2000). It is therefore probable that alpha power effects observed in this study are related to different attentional demands required for the sequence relative to the random material. Increased occipital alpha power is usually considered to be a sign of relative deactivation or inhibition of visual areas. For instance, Jensen and Mazaheri (Jensen and Mazaheri, 2010) suggested that increased alpha power over occipito-parietal areas during the delay period in WM tasks represents alpha-gated inhibition of task-irrelevant regions. In the context of our study, a relative alpha power increase in sequence compared to random blocks might reflect higher attentional demands required for the random trials in the first learning session, when S-R attentional demands are highest. Later on, when S-R associations have been established this effect decreases. This however does not explain the reversed pattern towards the end of the task in which alpha decreased over occipito-parietal areas. Others reported decreased alpha power over right occipito-parietal areas while learning a visual sequence (Moisello et al., 2013), which might be related to the later effects we observed here. This remains speculative, however, but could be addressed with a purely motor SRTT variant which does not entail a visual sequence (Tzvi et al., 2014).

In accordance with previous findings (Andres et al., 1999; Houweling et al., 2008; Hummel et al., 2003; Pollok et al., 2014; Zhuang et al., 1998), we found alpha-power decrease over right sensorimotor cortex associated with motor sequence learning in the late-learning stage. In addition, alpha-power increased during the early learning phase over Cz. Together with imaging studies showing learning-related increases over sensorimotor areas, these results indicate that oscillations at alpha frequency band play an important role in mediating learning over sensorimotor areas.

4.4.3 Theta and gamma-power effects during learning

In the theta band, we found an early learning-related power increase in electrodes over parietal areas which vanished in later learning sessions. Gamma power effects were evident over left centro-parietal areas. In a visuo-motor learning task, Perfetti and colleagues (2011) found an early gamma power increase over right centro-parietal electrodes during both planning and execution of the motor movements. At the same time, increased gamma phase coherence was evident between right and left centro-parietal electrodes. The authors suggest that these effects reflect attentional mechanisms in the learning task which promote information integration over parietal areas underlying formation of an internal model. Increased gamma power during motor sequence learning was also shown for the internal globus pallidus in dystonia patients prior to motor movement (Herrojo Ruiz et al., 2014). Together this line of evidence suggests that gamma plays an important role in forming an internal representation of a complex movement over parietal areas, possibly in interaction with the basal ganglia.

It has to be kept in mind though that our analysis approach in contrast to previous work focused on sustained power differences in contrast to transient stimulus- or response-related effects. It

might be thus that analyses of stimulus-related transient effects on theta, alpha or gamma power might have revealed a different picture.

4.4.4 Reduced alpha/low-gamma PAC in motor learning

We found a decrease in alpha/low-gamma PAC during learning over right parietal cortex and over bilateral fronto-central areas. PAC analysis further revealed that throughout the task, the trough of the alpha oscillation was driving the increase in low-gamma amplitude. This finding is conistent with previous reports of PAC between alpha and gamma (Tzvi et al., under review; Voytek et al., 2010; Yanagisawa et al., 2012) as well as between theta and gamma (Canolty et al., 2006; Dürschmid et al., 2014; Tort et al., 2008; van der Meij et al., 2012) and beta and gamma (de Hemptinne et al., 2013). In addition, we compared alpha/low-gamma PAC in regular random blocks to random blocks directly following sequence blocks (so called "transition" blocks) for which we hypothesized that participants were still attempting to implement the sequence. We found a significant alpha/low-gamma PAC decrease at the same right centro-parietal electrode during transition blocks compared to random blocks and over left frontal cortex during the first transition compared to the next random block.

Localizing EEG effects is generally difficult, but based on neuroimaging studies on motor sequence learning (for meta analysis see Hardwick et al., 2013) it seems likely that the right parietal PAC effect reflects processes arising from right superior parietal lobule (SPL) whereas the contralateral fronto-central effect might arise from dorsal premotor cortex (dPMC). In an fMRI study using the SRTT, increased activity over SPL was observed when comparing random vs. regular sequences (Gheysen et al., 2010). In addition, a recent meta-analysis of motor skill learning tasks over short (hours) and long (days) time scales showed that activity over bilateral SPL decreases with time when a skill is learned in short time scale (Lohse et al., 2014). Other

SRTT studies have shown learning-related involvement of right SPL when the task was performed either with the left or with the right hand (Aznarez-Sanado et al., 2013; Grafton et al., 2002). Anatomical studies in monkeys have shown that visual inputs are translated to motor output through specific projections from SPL to premotor areas (Johnson et al., 1996; Johnson et al., 1993; Wise et al., 1997). Thus, SPL might serve to integrate the visual input from occipital cortex to form an internal representation of the task (Caminiti et al., 1996; Desmurget et al., 1999). This information will then be forwarded to dPMC to create the appropriate motor response. As visuomotor sequence learning advances during the task, participants learn the sequence and therefore depend less on the integration of visual information to select the specific motor response. In our study, this might have happened already quite early in the task as participants were already faster in the first sequence block. Thus, the observed alpha/low-gamma PAC decrease over frontal and parietal areas during the regular sequence might represent a decrease in perceptually guided response selection.

An alternative explanation for these alpha/low-gamma PAC effects is that increased alpha/gamma PAC might reflect a “default mode”. Neural processing demands over the frontal-parietal network required for learning might thus be achieved by disengaging gamma activity from the phasic alpha. This suggestion is in-line with the "desynchronization hypothesis“ recently suggested by Hanslmayr and colleagues (2012). They hypothesize that information encoding into memory systems benefits from oscillatory desynchronization as it increases the entropy, i.e., the richness of the information. Although the authors refer to desynchronization as the decrease of low-frequency oscillatory power, the same principle might be applicable for phase-amplitude coupling mechanisms. Supporting this hypothesis, Osipova and colleagues (2008) found that during eyes-closed resting state, alpha/low-gamma PAC is evident over

occipito-parietal regions. This "default mode“ alpha/gamma PAC might not be limited to the parietal cortex only. Roux and colleagues (2013) showed that gamma amplitude over posterior parietal cortex was coupled to alpha phase of thalamic sources during closed-eyes resting state. And finally, in an ECoG study alpha/high-gamma PAC was evident over sensorimotor areas when patients were waiting to execute a movement (Yanagisawa et al., 2012). Together, this line of evidence suggests that alpha-gamma PAC may serve as a “default mode” and is reduced during cognitive processes or learning.

In sum, we offer two alternative explanations for the learning-related alpha/gamma PAC effects in this study. The one assumes that these effects stem from communication between SPL and dPMC for the successful implementation of the sequence. When learning progresses and is less dependent on visual information, the integration between SPL and dPMC is reduced and thus alpha/low-gamma PAC is reduced. Future studies could shed more light on this process by investigating alpha/gamma PAC in more complex motor learning tasks in which visuomotor integration is not as simple as in the SRTT (e.g. Houweling et al., 2008). The alternative explanation we provide is that increased alpha/gamma PAC effects reflect the “default mode” which is reduced during sequence learning. However, the control condition with higher alpha/gamma PAC was in our case the random block which was in fact more difficult as suggested by slower RTs and higher error rates. We therefore suggest that this alternative explanation could be addressed in future studies implementing the SRTT with an additional simple sequence condition (Steele and Penhune, 2010). Based on the second explanation, we hypothesize that alpha/gamma PAC would increase in the simple sequence condition compared to the novel sequence condition.

4.4.5 Conclusions

In a large group of participants, we showed that implicit visuomotor sequence learning results in specific changes in alpha power over posterior parietal area and a reduction of alpha/low-gamma PAC over right parietal and bilateral frontal cortex. This lateralization was independent of side of stimulation and responding. We suggest that reduced alpha/low-gamma PAC in frontal and parietal regions reflects a shift away from visually guided motor selection towards implementation of the learned motor sequence. The latter might rely on striatal-cerebellar-cortical interactions (Tzvi et al., 2014; Tzvi et al., 2015) not observable with EEG. The results presented in this work provide important insights into oscillatory mechanisms guiding implicit motor sequence learning and give further evidence for the importance of cross-frequency coupling in cognitive tasks.

Chapter 5

General Discussion

In the introduction, I gave a detailed description of the recent literature on the neural correlates of motor learning and memory and specifically motor sequence learning. This included studies in patients with movement disorders, stimulation studies using tDCS and TMS, imaging studies and electrophysiological studies in primates and rodents. This cross-methodological literature review suggested that several cortical and subcortical regions are involved in the acquisition and maintenance of motor memory representations following implicit MSL. In addition, I provided a methodological review and comparison between common approaches to assess causality in neurophysiological data as this is a common source of debates in the neuroscientific community (Daunizeau et al., 2011; Friston et al., 2013; Lohmann et al., 2012; Lohmann et al., 2013). In this thesis, I performed three studies which investigated neural networks underlying implicit MSL using both fMRI and EEG. The two fMRI studies attempted to delineate the cortico-striatal-cerebellar network using DCM during early learning (Studies 1 and 2) and after consolidation (Study 2). The focus of the EEG study (Study 3) was on specific interactions between neural oscillations, so-called PAC, as a measure for brain network interactions during early learning. In the next paragraphs I will shortly summarize the results of these three studies and discuss the behavioral aspects as well as the underlying neural correlates of implicit learning.

5.1. Implicit learning in the serial reaction time task

Across all studies outlined in this thesis, we employed the SRTT using a 12-element hidden sequence. The differences between the studies in terms of design and learning outcome are summarized in Table 5.1. In Study 2 we used the standard SRTT and in Studies 1 and 3 we used

a modified version of the SRTT which included colored stimuli. While in all studies learning of the hidden sequence was evident reflected in significant differences in reactions times (RT) between conditions (Sequence vs. Random), only in Study 2 did the RT show an interaction effect between condition and block indicating that sequence performance improved with time. In Study 1, our interpretation was that subjects did not reach the learning asymptote and therefore RT gains across time were not evident. In Study 3 however, it was more likely that subjects had already reached the behavioral asymptote in the first learning block and therefore additional gains were not observed later in the task. There are several reasons why we think implicit learning of the sequence in Study 1 was more difficult than implicit learning of the sequence in Study 3. First, in Study 1 we used a design (Rose et al., 2011) that dissociates the stimulus-response (S-R) association in each trial which enabled us to specifically target the motor component of implicit MSL. In Study 3 on the other hand, participants first learned specific S-R associations and therefore learning entailed probably both perceptual and motor components. Previous studies investigating the importance of S-R rules and response selection showed that these are critical for sequence learning (Schwarb and Schumacher, 2012). Therefore, sequence learning in Study 3 was probably easier than sequence learning in Study 1, where S-R rules were continuously changed. Second, in Study 1 the hidden sequence was structured such that no higher order prediction could be made (Reed and Johnson, 1994). This means that the target position on a given trial could not be predicted from the target position of the previous trial. For Study 3 no such control on the hidden sequence was performed and might be one reason why subjects learned the sequence faster compared to study 1. Finally, in Study 3 we implemented a design with slow alterations between sequence and random blocks such that the sequence was repeating many times uninterrupted by random material. This continuous exposure to the hidden

sequence could assist in faster forming of sequence representation in long-term memory. In Study 1 on the other hand, sequence and random blocks were altered more rapidly. This could be another reason for the fast learning effects observed in Study 3 compared to slow learning effects in Study 1.

Table 5.1: Comparison between study designs

	Response	**Stimuli**	**Implicit learning**	**Explicit learners**	**Second-order Associations**	**SEQ/RND Alterations**
Study 1	Two hands	Colored	No condition x	0	NO	Fast
	6 fingers	No S-R	Block interaction			SEQ: 3 rep
Study 2	Left hand	No Color	Condition x Block	10/31	NO	Fast
	4 fingers	S-R	interaction			SEQ: 4 rep
Study 3	One hand	Color	No condition x	6/109	YES	Slow
	4 fingers	S-R	Block interaction			SEQ: 25 rep

In terms of gaining explicit knowledge of the sequence, we found that in Study 2 explicit knowledge was gained by 10 out of 31 participants, whereas in Study 1, none of the participants gained explicit knowledge and in Study 3 only 6 out of 109 subjects gained explicit knowledge. This discrepancy might be mainly due to the different methods used for assessing explicit knowledge, all of which are legitimate and common in experiments employing the SRTT (Robertson, 2007).

5.2. Summary of the results: fMRI

We used dynamic causal modelling to investigate causal interactions within the motor cortical-striatal-cerebellar network in the two fMRI studies described in this thesis. In the first study, we

used three regions of interest in each hemisphere: M1, putamen and cerebellum. We found that learning negatively modulated the connections from M1 to contralateral cerebellum. We showed that this effect was specific for implicit learning of the hidden sequence but not for explicit learning of the motor task. In the second study, we sought to expand on these results and investigated causal interactions within a broader network, with additional regions of interest in premotor cortex and supplementary motor area. This approach posed the methodological challenge of computing and estimating causal interactions between 10 regions of interest. For this purpose, we used an advanced approach which is referred to as post-hoc DCM (Friston and Penny, 2011; Rosa et al., 2012). In terms of the driving input to the model, we found that in Study 1 input was to bilateral cerebellum whereas in Study 2, input was to the left cerebellum. As subjects performed the task with both hands in Study 1 and with the left hand in Study 2, this suggests that the performing hand directly effects the signal propagation from ipsilateral cerebellum to cortical and subcortical areas during performance of a motor task.

Similarly to Study 1, we found a negative modulation from left M1 to right cerebellum in Study 2, however less consistent. If M1 stores the representation of movements during sequence learning (Karni et al., 1995; Matsuzaka et al., 2007) and cerebellum continuously adjust an internal model of the sequence (Ito, 2008; Ramnani, 2006), then the connection from M1 to cerebellum might drive the formation of an internal model in the cerebellum. When learning continues, it is probable that this connection is diminished as it is no longer needed. As discussed in Chapter 3, the inconsistent modulation across subjects may arise from different strategies for implementing sequence learning in Study 2. If the negative modulation of the connection from M1 to cerebellum represents the motor component of learning, it is probable that in Study 2, in

which either or both motor and perceptual sequence learning could underlie performance improvement, this connection would not be consistent.

In Study 2, we also found a negative modulation of connections from bilateral putamen to cerebellum. Theses connections from putamen to cerebellum were not directly investigated in Study 1 as the main focus was on comparing cortico-striatal vs. cortico-cerebellar connections. Importantly, in Study 2, we could also investigate the network changes following consolidation. We found that a connection from left cerebellum to right putamen was negatively modulated specifically for the sequence condition, after learning was already established. Only recently have direct anatomical connections between striatum and cerebellum been discovered (Bostan and Strick, 2010), paving the road to research on striatal-cerebellar connectivity in the context of cognitive tasks. Connections between the cerebellum and basal ganglia were investigated as well in an fMRI study investigating learning of a finger-tapping task over 4 weeks of training (Ma et al., 2010). In accordance with our results, the authors reported that after learning was established, a negative modulation of the connection from cerebellum to putamen was observed. In addition, they reported a positive modulation of the connection from cerebellum to putamen before training started. If putamen (as part of a bigger striatal network) creates associations between subgroups of movements (Graybiel, 1998, 2008) and cerebellum continuously adjusts an internal model of the sequence (Ito, 2008; Ramnani, 2006), then the connection from cerebellum to putamen may underlie the initial grouping of movements into a sequence representation. When the sequence is already consolidated, this connection is diminished.

Clearly both interpretations proposed here for the roles which M1, putamen and cerebellum play in motor learning are only speculative. Future studies employing effective connectivity measures

are needed to provide additional evidence for the suggested role of causal interactions in the cortico-striato-cerebellar network in learning and cognition.

5.3. Summary of the results: EEG

The results from Study 3 showed involvement of theta, alpha and gamma oscillations in implicit MSL. We observed a wide-spread alpha power increase during early learning, which decreased when the sequence was already established. This effect was strongest over occipito-parietal areas and may reflect different attentional demands in the task. Most importantly, we found a consistent decrease in alpha/gamma phase amplitude coupling over right parietal cortex and bilateral fronto-central areas, possibly originating from right superior parietal lobule (SPL) and dorsal premotor cortex (dPMC) respectively. We offered two interpretations for these results. First, alpha/gamma PAC over right SPL and dPMC might reflect the integration between these regions for the purpose of creating the appropriate stimulus-response association in the task. Therefore when alpha-gamma PAC is reduced during learning, this integration is no longer needed and resources are focused on learning and implementing the hidden sequence. The alternative explanation relies on a recent hypothesis suggested by Hanslmayr and colleagues (2012) which states that information encoding into memory relies on oscillatory desynchronization. Thus, alpha/gamma PAC over learning-related brain regions might reflect a "default mode" which decreases during learning. However, as alpha/gamma PAC in the control condition in this study was higher than sequence it is hard to draw such a conclusion making the first interpretation more likely.

5.4. Implications for models of motor learning

As outlined in the introduction, the model of motor learning by Doyon and colleagues (Doyon and Benali, 2005) and by Hikosaka and colleagues (Hikosaka et al., 2002) suggests that striatum, cerebellum, and motor cortical regions mediate the fast learning stage. Questions regarding the nature of those interactions remained however unanswered. Study 1 showed that the fast stage of motor sequence learning is mediated by a cortico-cerebellar loop and more specifically by a negative causal interaction from M1 to cerebellum bilaterally. These results were supported by a similar finding in Study 2. Moreover, Study 2 provides evidence for striatal-cerebellar network involvement in the slow learning stage. This finding, which is in line with the Hikosaka model, contradicts the Doyon model which suggested the involvement of striatum and not cerebellum in the slow stage of motor sequence learning. Study 3 expands on both models and offers a plausible mechanism for cortical interactions underlying the fast learning stage. Phase amplitude coupling, which was previously shown to be involved in learning and memory, was modulated over parietal and premotor regions, structures which were suggested by both models of motor sequence learning.

5.5. Outlook

How do the results of the fMRI and EEG studies fit together? In all studies, we found a reduction in connectivity or estimates of connectivity (PAC) as learning progresses. Both fMRI studies showed reduction in causal connections between M1, cerebellum and putamen whereas in the EEG study, reduced alpha/gamma PAC was evident over parietal and fronto-central areas. It is not possible to specifically localize the sources of EEG oscillations but interactions within cortico-striato-cerebellar network could possibly leave traces on oscillatory activity measured on the surface of the brain. A possible way to investigate whether the cerebellum affects cortical

oscillations as suggested here would be to measure alpha/gamma PAC using EEG while participants perform in the serial reaction time task before and after applying tDCS to the cerebellum. We expect that anodal stimulation to the cerebellum which has previously been shown to improve motor adaptation (Galea et al., 2011) and implicit motor sequence learning (Ferrucci et al., 2013) would elicit reduced alpha/gamma PAC compared to sham stimulation reflecting increased learning. In addition, while we restricted our dynamic causal models to include only M1 and premotor areas for the cortical regions of interest, imaging studies support our finding from the EEG study that parietal areas are as well implicated in motor learning (Hardwick et al., 2013). Future studies could target the interactions between parietal cortex and cortical motor areas as well as striatum and cerebellum in order to understand the role of parietal cortex in implicit MSL.

References

Albert, N.B., Robertson, E.M., Mehta, P., Miall, R.C., 2009. Resting state networks and memory consolidation. Commun Integr Biol 2, 530-532.

Albouy, G., Sterpenich, V., Balteau, E., Vandewalle, G., Desseilles, M., Dang-Vu, T., Darsaud, A., Ruby, P., Luppi, P.H., Degueldre, C., Peigneux, P., Luxen, A., Maquet, P., 2008. Both the hippocampus and striatum are involved in consolidation of motor sequence memory. Neuron 58, 261-272.

Albouy, G., Sterpenich, V., Vandewalle, G., Darsaud, A., Gais, S., Rauchs, G., Desseilles, M., Boly, M., Dang-Vu, T., Balteau, E., Degueldre, C., Phillips, C., Luxen, A., Maquet, P., 2013. Interaction between hippocampal and striatal systems predicts subsequent consolidation of motor sequence memory. PLoS One 8, e59490.

Albus, J.S., 1971. A theory of cerebellar function. Mathematical Biosciences 10, 25-61.

Alexander, G.E., Crutcher, M.D., DeLong, M.R., 1990. Basal ganglia-thalamocortical circuits: parallel substrates for motor, oculomotor, "prefrontal" and "limbic" functions. Prog Brain Res 85, 119-146.

Alexander, G.E., DeLong, M.R., Strick, P.L., 1986. Parallel organization of functionally segregated circuits linking basal ganglia and cortex. Annu Rev Neurosci 9, 357-381.

Andres, F.G., Mima, T., Schulman, A.E., Dichgans, J., Hallett, M., Gerloff, C., 1999. Functional coupling of human cortical sensorimotor areas during bimanual skill acquisition. Brain 122 (Pt 5), 855-870.

Aru, J., Priesemann, V., Wibral, M., Lana, L., Pipa, G., Singer, W., Vicente, R., 2015. Untangling cross-frequency coupling in neuroscience. Curr Opin Neurobiol 31, 51-61.

Axmacher, N., Henseler, M.M., Jensen, O., Weinreich, I., Elger, C.E., Fell, J., 2010. Cross-frequency coupling supports multi-item working memory in the human hippocampus. Proc Natl Acad Sci U S A 107, 3228-3233.

Aznarez-Sanado, M., Fernandez-Seara, M.A., Loayza, F.R., Pastor, M.A., 2013. Functional asymmetries in early learning during right, left, and bimanual performance in right-handed subjects. J Magn Reson Imaging 37, 619-631.

Baddeley, A., 1992. Working memory. Science 255, 556-559.

Badgaiyan, R.D., Fischman, A.J., Alpert, N.M., 2007. Striatal dopamine release in sequential learning. Neuroimage 38, 549-556.

Bapi, R.S., Miyapuram, K.P., Graydon, F.X., Doya, K., 2006. fMRI investigation of cortical and subcortical networks in the learning of abstract and effector-specific representations of motor sequences. Neuroimage 32, 714-727.

Bennett, I.J., Madden, D.J., Vaidya, C.J., Howard, J.H., Jr., Howard, D.V., 2011. White matter integrity correlates of implicit sequence learning in healthy aging. Neurobiol Aging 32, 2317 e2311-2312.

Bernard, J.A., Seidler, R.D., 2013. Cerebellar contributions to visuomotor adaptation and motor sequence learning: an ALE meta-analysis. Front Hum Neurosci 7, 27.

Bo, J., Peltier, S.J., Noll, D.C., Seidler, R.D., 2011. Symbolic representations in motor sequence learning. Neuroimage 54, 417-426.

Bostan, A.C., Dum, R.P., Strick, P.L., 2010. The basal ganglia communicate with the cerebellum. Proc Natl Acad Sci U S A 107, 8452-8456.

Bostan, A.C., Dum, R.P., Strick, P.L., 2013. Cerebellar networks with the cerebral cortex and basal ganglia. Trends Cogn Sci 17, 241-254.

Bostan, A.C., Strick, P.L., 2010. The cerebellum and basal ganglia are interconnected. Neuropsychol Rev 20, 261-270.

Buckner, R.L., 2013. The cerebellum and cognitive function: 25 years of insight from anatomy and neuroimaging. Neuron 80, 807-815.

Buckner, R.L., Krienen, F.M., Castellanos, A., Diaz, J.C., Yeo, B.T., 2011. The organization of the human cerebellum estimated by intrinsic functional connectivity. J Neurophysiol 106, 2322-2345.
Buxton, R.B., Wong, E.C., Frank, L.R., 1998. Dynamics of blood flow and oxygenation changes during brain activation: the balloon model. Magn Reson Med 39, 855-864.
Buzsaki, G., 2002. Theta oscillations in the hippocampus. Neuron 33, 325-340.
Buzsaki, G., 2005. Theta rhythm of navigation: link between path integration and landmark navigation, episodic and semantic memory. Hippocampus 15, 827-840.
Caminiti, R., Ferraina, S., Johnson, P.B., 1996. The sources of visual information to the primate frontal lobe: a novel role for the superior parietal lobule. Cereb Cortex 6, 319-328.
Canolty, R.T., Edwards, E., Dalal, S.S., Soltani, M., Nagarajan, S.S., Kirsch, H.E., Berger, M.S., Barbaro, N.M., Knight, R.T., 2006. High gamma power is phase-locked to theta oscillations in human neocortex. Science 313, 1626-1628.
Canolty, R.T., Knight, R.T., 2010. The functional role of cross-frequency coupling. Trends Cogn Sci 14, 506-515.
Carbon, M., Argyelan, M., Ghilardi, M.F., Mattis, P., Dhawan, V., Bressman, S., Eidelberg, D., 2011. Impaired sequence learning in dystonia mutation carriers: a genotypic effect. Brain 134, 1416-1427.
Cardenas-Morales, L., Volz, L.J., Michely, J., Rehme, A.K., Pool, E.M., Nettekoven, C., Eickhoff, S.B., Fink, G.R., Grefkes, C., 2013. Network Connectivity and Individual Responses to Brain Stimulation in the Human Motor System. Cereb Cortex.
Cieslik, E.C., Zilles, K., Grefkes, C., Eickhoff, S.B., 2011. Dynamic interactions in the fronto-parietal network during a manual stimulus-response compatibility task. Neuroimage 58, 860-869.
Cohen, D.A., Pascual-Leone, A., Press, D.Z., Robertson, E.M., 2005. Off-line learning of motor skill memory: a double dissociation of goal and movement. Proc Natl Acad Sci U S A 102, 18237-18241.
Cohen, M.X., Elger, C.E., Fell, J., 2009. Oscillatory activity and phase-amplitude coupling in the human medial frontal cortex during decision making. J Cogn Neurosci 21, 390-402.
Coynel, D., Marrelec, G., Perlbarg, V., Pelegrini-Issac, M., Van de Moortele, P.F., Ugurbil, K., Doyon, J., Benali, H., Lehericy, S., 2010. Dynamics of motor-related functional integration during motor sequence learning. Neuroimage 49, 759-766.
Crespo-Garcia, M., Pinal, D., Cantero, J.L., Diaz, F., Zurron, M., Atienza, M., 2013. Working memory processes are mediated by local and long-range synchronization of alpha oscillations. J Cogn Neurosci 25, 1343-1357.
Curran, T., 1997. Higher-order associative learning in amnesia: evidence from the serial reaction time task. J Cogn Neurosci 9, 522-533.
Daunizeau, J., David, O., Stephan, K.E., 2011. Dynamic causal modelling: a critical review of the biophysical and statistical foundations. Neuroimage 58, 312-322.
David, O., Guillemain, I., Saillet, S., Reyt, S., Deransart, C., Segebarth, C., Depaulis, A., 2008. Identifying neural drivers with functional MRI: an electrophysiological validation. PLoS Biol 6, 2683-2697.
David, O., Kiebel, S.J., Harrison, L.M., Mattout, J., Kilner, J.M., Friston, K.J., 2006. Dynamic causal modeling of evoked responses in EEG and MEG. Neuroimage 30, 1255-1272.
Dayan, E., Cohen, L.G., 2011. Neuroplasticity subserving motor skill learning. Neuron 72, 443-454.
de Hemptinne, C., Ryapolova-Webb, E.S., Air, E.L., Garcia, P.A., Miller, K.J., Ojemann, J.G., Ostrem, J.L., Galifianakis, N.B., Starr, P.A., 2013. Exaggerated phase-amplitude coupling in the primary motor cortex in Parkinson disease. Proc Natl Acad Sci U S A 110, 4780-4785.
de Hemptinne, C., Swann, N.C., Ostrem, J.L., Ryapolova-Webb, E.S., San Luciano, M., Galifianakis, N.B., Starr, P.A., 2015. Therapeutic deep brain stimulation reduces cortical phase-amplitude coupling in Parkinson's disease. Nat Neurosci 18, 779-786.

Debas, K., Carrier, J., Barakat, M., Marrelec, G., Bellec, P., Hadj Tahar, A., Karni, A., Ungerleider, L.G., Benali, H., Doyon, J., 2014. Off-line consolidation of motor sequence learning results in greater integration within a cortico-striatal functional network. Neuroimage 99, 50-58.
Debas, K., Carrier, J., Orban, P., Barakat, M., Lungu, O., Vandewalle, G., Hadj Tahar, A., Bellec, P., Karni, A., Ungerleider, L.G., Benali, H., Doyon, J., 2010. Brain plasticity related to the consolidation of motor sequence learning and motor adaptation. Proc Natl Acad Sci U S A 107, 17839-17844.
Delorme, A., Makeig, S., 2004. EEGLAB: an open source toolbox for analysis of single-trial EEG dynamics including independent component analysis. J Neurosci Methods 134, 9-21.
Deshpande, G., Sathian, K., Hu, X., 2010. Effect of hemodynamic variability on Granger causality analysis of fMRI. Neuroimage 52, 884-896.
Desmurget, M., Epstein, C.M., Turner, R.S., Prablanc, C., Alexander, G.E., Grafton, S.T., 1999. Role of the posterior parietal cortex in updating reaching movements to a visual target. Nat Neurosci 2, 563-567.
Destrebecqz, A., Cleeremans, A., 2001. Can sequence learning be implicit? New evidence with the process dissociation procedure. Psychon Bull Rev 8, 343-350.
Destrebecqz, A., Peigneux, P., Laureys, S., Degueldre, C., Del Fiore, G., Aerts, J., Luxen, A., Van Der Linden, M., Cleeremans, A., Maquet, P., 2005. The neural correlates of implicit and explicit sequence learning: Interacting networks revealed by the process dissociation procedure. Learn Mem 12, 480-490.
Diekelmann, S., Born, J., 2010. The memory function of sleep. Nat Rev Neurosci 11, 114-126.
Ding, M., Bressler, S.L., Yang, W., Liang, H., 2000. Short-window spectral analysis of cortical event-related potentials by adaptive multivariate autoregressive modeling: data preprocessing, model validation, and variability assessment. Biol Cybern 83, 35-45.
Dirnberger, G., Novak, J., Nasel, C., 2013. Perceptual sequence learning is more severely impaired than motor sequence learning in patients with chronic cerebellar stroke. J Cogn Neurosci 25, 2207-2215.
Doyon, J., Bellec, P., Amsel, R., Penhune, V., Monchi, O., Carrier, J., Lehericy, S., Benali, H., 2009. Contributions of the basal ganglia and functionally related brain structures to motor learning. Behav Brain Res 199, 61-75.
Doyon, J., Benali, H., 2005. Reorganization and plasticity in the adult brain during learning of motor skills. Curr Opin Neurobiol 15, 161-167.
Doyon, J., Gaudreau, D., Laforce, R., Jr., Castonguay, M., Bedard, P.J., Bedard, F., Bouchard, J.P., 1997. Role of the striatum, cerebellum, and frontal lobes in the learning of a visuomotor sequence. Brain Cogn 34, 218-245.
Doyon, J., Owen, A.M., Petrides, M., Sziklas, V., Evans, A.C., 1996. Functional anatomy of visuomotor skill learning in human subjects examined with positron emission tomography. Eur J Neurosci 8, 637-648.
Doyon, J., Penhune, V., Ungerleider, L.G., 2003. Distinct contribution of the cortico-striatal and cortico-cerebellar systems to motor skill learning. Neuropsychologia 41, 252-262.
Doyon, J., Song, A.W., Karni, A., Lalonde, F., Adams, M.M., Ungerleider, L.G., 2002. Experience-dependent changes in cerebellar contributions to motor sequence learning. Proc Natl Acad Sci U S A 99, 1017-1022.
Dudai, Y., 2004. The neurobiology of consolidations, or, how stable is the engram? Annu Rev Psychol 55, 51-86.
Dürschmid, S., Quandt, F., Krämer, U.M., Hinrichs, H., Heinze, H.J., Schulz, R., Pannek, H., Chang, E.F., Knight, R.T., 2014. Oscillatory dynamics track motor performance improvement in human cortex. PLoS One 9, e89576.
Eickhoff, S.B., Dafotakis, M., Grefkes, C., Shah, N.J., Zilles, K., Piza-Katzer, H., 2008. Central adaptation following heterotopic hand replantation probed by fMRI and effective connectivity analysis. Exp Neurol 212, 132-144.
Evarts, E.V., 1968. Relation of pyramidal tract activity to force exerted during voluntary movement. J Neurophysiol 31, 14-27.

Fell, J., Axmacher, N., 2011. The role of phase synchronization in memory processes. Nat Rev Neurosci 12, 105-118.
Ferrucci, R., Brunoni, A.R., Parazzini, M., Vergari, M., Rossi, E., Fumagalli, M., Mameli, F., Rosa, M., Giannicola, G., Zago, S., Priori, A., 2013. Modulating human procedural learning by cerebellar transcranial direct current stimulation. Cerebellum 12, 485-492.
Fischer, S., Hallschmid, M., Elsner, A.L., Born, J., 2002. Sleep forms memory for finger skills. Proc Natl Acad Sci U S A 99, 11987-11991.
Fischer, S., Nitschke, M.F., Melchert, U.H., Erdmann, C., Born, J., 2005. Motor memory consolidation in sleep shapes more effective neuronal representations. J Neurosci 25, 11248-11255.
Fletcher, P.C., Zafiris, O., Frith, C.D., Honey, R.A., Corlett, P.R., Zilles, K., Fink, G.R., 2005. On the benefits of not trying: brain activity and connectivity reflecting the interactions of explicit and implicit sequence learning. Cereb Cortex 15, 1002-1015.
Floyer-Lea, A., Matthews, P.M., 2005. Distinguishable brain activation networks for short- and long-term motor skill learning. J Neurophysiol 94, 512-518.
Foxe, J.J., Simpson, G.V., Ahlfors, S.P., 1998. Parieto-occipital similar to 10 Hz activity reflects anticipatory state of visual attention mechanisms. Neuroreport 9, 3929-3933.
Fries, P., 2005. A mechanism for cognitive dynamics: neuronal communication through neuronal coherence. Trends Cogn Sci 9, 474-480.
Friese, U., Koster, M., Hassler, U., Martens, U., Trujillo-Barreto, N., Gruber, T., 2012. Successful memory encoding is associated with increased cross-frequency coupling between frontal theta and posterior gamma oscillations in human scalp-recorded EEG. Neuroimage 66C, 642-647.
Friston, K., Daunizeau, J., Stephan, K.E., 2013. Model selection and gobbledygook: response to Lohmann et al. Neuroimage 75, 275-278; discussion 279-281.
Friston, K., Mattout, J., Trujillo-Barreto, N., Ashburner, J., Penny, W., 2007. Variational free energy and the Laplace approximation. Neuroimage 34, 220-234.
Friston, K., Penny, W., 2011. Post hoc Bayesian model selection. Neuroimage 56, 2089-2099.
Friston, K.J., Buechel, C., Fink, G.R., Morris, J., Rolls, E., Dolan, R.J., 1997. Psychophysiological and modulatory interactions in neuroimaging. Neuroimage 6, 218-229.
Friston, K.J., Harrison, L., Penny, W., 2003. Dynamic causal modelling. Neuroimage 19, 1273-1302.
Galea, J.M., Vazquez, A., Pasricha, N., de Xivry, J.J., Celnik, P., 2011. Dissociating the roles of the cerebellum and motor cortex during adaptive learning: the motor cortex retains what the cerebellum learns. Cereb Cortex 21, 1761-1770.
Gao, Q., Tao, Z., Zhang, M., Chen, H., 2014. Differential contribution of bilateral supplementary motor area to the effective connectivity networks induced by task conditions using dynamic causal modeling. Brain Connect 4, 256-264.
Georgopoulos, A.P., Caminiti, R., Kalaska, J.F., Massey, J.T., 1983. Spatial coding of movement: a hypothesis concerning the coding of movement direction by motor cortical populations. Exp Brain Res Suppl 7, 336.
Gheysen, F., Van Opstal, F., Roggeman, C., Van Waelvelde, H., Fias, W., 2010. Hippocampal contribution to early and later stages of implicit motor sequence learning. Exp Brain Res 202, 795-807.
Gitelman, D.R., Penny, W.D., Ashburner, J., Friston, K.J., 2003. Modeling regional and psychophysiologic interactions in fMRI: the importance of hemodynamic deconvolution. Neuroimage 19, 200-207.
Gomez-Beldarrain, M., Garcia-Monco, J.C., Rubio, B., Pascual-Leone, A., 1998. Effect of focal cerebellar lesions on procedural learning in the serial reaction time task. Exp Brain Res 120, 25-30.
Grafton, S.T., Hazeltine, E., Ivry, R., 1995. Functional mapping of sequence learning in normal humans. J Cogn Neurosci 7, 497-510.
Grafton, S.T., Hazeltine, E., Ivry, R.B., 2002. Motor sequence learning with the nondominant left hand. A PET functional imaging study. Exp Brain Res 146, 369-378.

Granger, C.W.J., 1969. Investigating Causal Relations by Econometric Models and Cross-Spectral Methods. Econometrica 37, 414-&.
Graybiel, A.M., 1998. The basal ganglia and chunking of action repertoires. Neurobiol Learn Mem 70, 119-136.
Graybiel, A.M., 2008. Habits, rituals, and the evaluative brain. Annu Rev Neurosci 31, 359-387.
Grefkes, C., Eickhoff, S.B., Nowak, D.A., Dafotakis, M., Fink, G.R., 2008a. Dynamic intra- and interhemispheric interactions during unilateral and bilateral hand movements assessed with fMRI and DCM. Neuroimage 41, 1382-1394.
Grefkes, C., Nowak, D.A., Eickhoff, S.B., Dafotakis, M., Kust, J., Karbe, H., Fink, G.R., 2008b. Cortical connectivity after subcortical stroke assessed with functional magnetic resonance imaging. Ann Neurol 63, 236-246.
Grefkes, C., Nowak, D.A., Wang, L.E., Dafotakis, M., Eickhoff, S.B., Fink, G.R., 2010. Modulating cortical connectivity in stroke patients by rTMS assessed with fMRI and dynamic causal modeling. Neuroimage 50, 233-242.
Gruber, T., Keil, A., Muller, M.M., 2001. Modulation of induced gamma band responses and phase synchrony in a paired associate learning task in the human EEG. Neurosci Lett 316, 29-32.
Hanslmayr, S., Staudigl, T., 2014. How brain oscillations form memories--a processing based perspective on oscillatory subsequent memory effects. Neuroimage 85 Pt 2, 648-655.
Hanslmayr, S., Staudigl, T., Fellner, M.C., 2012. Oscillatory power decreases and long-term memory: the information via desynchronization hypothesis. Front Hum Neurosci 6, 74.
Hardwick, R.M., Rottschy, C., Miall, R.C., Eickhoff, S.B., 2013. A quantitative meta-analysis and review of motor learning in the human brain. Neuroimage 67, 283-297.
Hargreaves, E.L., Mattfeld, A.T., Stark, C.E., Suzuki, W.A., 2012. Conserved fMRI and LFP signals during new associative learning in the human and macaque monkey medial temporal lobe. Neuron 74, 743-752.
Hazeltine, E., Grafton, S.T., Ivry, R., 1997. Attention and stimulus characteristics determine the locus of motor-sequence encoding. A PET study. Brain 120 (Pt 1), 123-140.
Herrojo Ruiz, M., Brucke, C., Nikulin, V.V., Schneider, G.H., Kuhn, A.A., 2014. Beta-band amplitude oscillations in the human internal globus pallidus support the encoding of sequence boundaries during initial sensorimotor sequence learning. Neuroimage 85 Pt 2, 779-793.
Hikosaka, O., Nakamura, K., Sakai, K., Nakahara, H., 2002. Central mechanisms of motor skill learning. Curr Opin Neurobiol 12, 217-222.
Hillebrandt, H., Dumontheil, I., Blakemore, S.J., Roiser, J.P., 2013. Dynamic causal modelling of effective connectivity during perspective taking in a communicative task. Neuroimage 76, 116-124.
Hoddes, E., Dement, W.C., Zarcone, V., 1972. The development and use of the Stanford Sleepiness Scale (SSS). Psychophysiology 9, 150.
Hoffman, D.S., Strick, P.L., 1995. Effects of a primary motor cortex lesion on step-tracking movements of the wrist. J Neurophysiol 73, 891-895.
Honda, M., Deiber, M.P., Ibanez, V., Pascual-Leone, A., Zhuang, P., Hallett, M., 1998. Dynamic cortical involvement in implicit and explicit motor sequence learning. A PET study. Brain 121 (Pt 11), 2159-2173.
Hoshi, E., Tremblay, L., Feger, J., Carras, P.L., Strick, P.L., 2005. The cerebellum communicates with the basal ganglia. Nat Neurosci 8, 1491-1493.
Houweling, S., Daffertshofer, A., van Dijk, B.W., Beek, P.J., 2008. Neural changes induced by learning a challenging perceptual-motor task. Neuroimage 41, 1395-1407.
Hummel, F., Kirsammer, R., Gerloff, C., 2003. Ipsilateral cortical activation during finger sequences of increasing complexity: representation of movement difficulty or memory load? Clin Neurophysiol 114, 605-613.

Ito, M., 1982. Cerebellar control of the vestibulo-ocular reflex--around the flocculus hypothesis. Annu Rev Neurosci 5, 275-296.
Ito, M., 2008. Control of mental activities by internal models in the cerebellum. Nat Rev Neurosci 9, 304-313.
Jackson, G.M., Jackson, S.R., Harrison, J., Henderson, L., Kennard, C., 1995. Serial reaction time learning and Parkinson's disease: evidence for a procedural learning deficit. Neuropsychologia 33, 577-593.
Janke, W., Debus, G., 1978. Die Eigenschaftswörterliste (EWL). Hogrefe, Göttingen.
Jenkins, I.H., Brooks, D.J., Nixon, P.D., Frackowiak, R.S., Passingham, R.E., 1994. Motor sequence learning: a study with positron emission tomography. J Neurosci 14, 3775-3790.
Jensen, O., Mazaheri, A., 2010. Shaping functional architecture by oscillatory alpha activity: gating by inhibition. Front Hum Neurosci 4, 186.
Jin, X., Costa, R.M., 2010. Start/stop signals emerge in nigrostriatal circuits during sequence learning. Nature 466, 457-462.
Jin, X., Tecuapetla, F., Costa, R.M., 2014. Basal ganglia subcircuits distinctively encode the parsing and concatenation of action sequences. Nat Neurosci.
Johnson, P.B., Ferraina, S., Bianchi, L., Caminiti, R., 1996. Cortical networks for visual reaching: physiological and anatomical organization of frontal and parietal lobe arm regions. Cereb Cortex 6, 102-119.
Johnson, P.B., Ferraina, S., Caminiti, R., 1993. Cortical networks for visual reaching. Exp Brain Res 97, 361-365.
Jueptner, M., Frith, C.D., Brooks, D.J., Frackowiak, R.S., Passingham, R.E., 1997. Anatomy of motor learning. II. Subcortical structures and learning by trial and error. J Neurophysiol 77, 1325-1337.
Jutras, M.J., Fries, P., Buffalo, E.A., 2009. Gamma-band synchronization in the macaque hippocampus and memory formation. J Neurosci 29, 12521-12531.
Kalaska, J.F., Cohen, D.A., Hyde, M.L., Prud'homme, M., 1989. A comparison of movement direction-related versus load direction-related activity in primate motor cortex, using a two-dimensional reaching task. J Neurosci 9, 2080-2102.
Kandel, E.R., Schwartz, J.H., Jessell, T.M., Siegelbaum, S.A., Hudspeth, A.J. (Eds.), 2013. Principles of Neural Science, 5th ed. McGraw-Hill, New York.
Kang, E.K., Paik, N.J., 2011. Effect of a tDCS electrode montage on implicit motor sequence learning in healthy subjects. Exp Transl Stroke Med 3, 4.
Karabanov, A., Cervenka, S., de Manzano, O., Forssberg, H., Farde, L., Ullen, F., 2010. Dopamine D2 receptor density in the limbic striatum is related to implicit but not explicit movement sequence learning. Proc Natl Acad Sci U S A 107, 7574-7579.
Karni, A., Meyer, G., Jezzard, P., Adams, M.M., Turner, R., Ungerleider, L.G., 1995. Functional MRI evidence for adult motor cortex plasticity during motor skill learning. Nature 377, 155-158.
Karni, A., Meyer, G., Rey-Hipolito, C., Jezzard, P., Adams, M.M., Turner, R., Ungerleider, L.G., 1998. The acquisition of skilled motor performance: fast and slow experience-driven changes in primary motor cortex. Proc Natl Acad Sci U S A 95, 861-868.
Kass, R.E., Raftery, A.E., 1995. Bayes Factors. Journal of the American Statistical Association 90, 773-795.
Kayser, J., Tenke, C.E., 2006a. Principal components analysis of Laplacian waveforms as a generic method for identifying ERP generator patterns: I. Evaluation with auditory oddball tasks. Clin Neurophysiol 117, 348-368.
Kayser, J., Tenke, C.E., 2006b. Principal components analysis of Laplacian waveforms as a generic method for identifying ERP generator patterns: II. Adequacy of low-density estimates. Clin Neurophysiol 117, 369-380.

Kim, S., Stephenson, M.C., Morris, P.G., Jackson, S.R., 2014. tDCS-induced alterations in GABA concentration within primary motor cortex predict motor learning and motor memory: a 7 T magnetic resonance spectroscopy study. Neuroimage 99, 237-243.
Kirov, R., Kolev, V., Verleger, R., Yordanova, J., 2015. Labile sleep promotes awareness of abstract knowledge in a serial reaction time task. Front Psychol 6, 1354.
Klimesch, W., 1999. EEG alpha and theta oscillations reflect cognitive and memory performance: a review and analysis. Brain Res Brain Res Rev 29, 169-195.
Knopman, D., Nissen, M.J., 1991. Procedural learning is impaired in Huntington's disease: evidence from the serial reaction time task. Neuropsychologia 29, 245-254.
Korman, M., Doyon, J., Doljansky, J., Carrier, J., Dagan, Y., Karni, A., 2007. Daytime sleep condenses the time course of motor memory consolidation. Nat Neurosci 10, 1206-1213.
Kwak, Y., Muller, M.L., Bohnen, N.I., Dayalu, P., Seidler, R.D., 2010. Effect of dopaminergic medications on the time course of explicit motor sequence learning in Parkinson's disease. J Neurophysiol 103, 942-949.
Kwak, Y., Muller, M.L., Bohnen, N.I., Dayalu, P., Seidler, R.D., 2012. l-DOPA changes ventral striatum recruitment during motor sequence learning in Parkinson's disease. Behav Brain Res 230, 116-124.
Lachaux, J.P., Rodriguez, E., Martinerie, J., Varela, F.J., 1999. Measuring phase synchrony in brain signals. Hum Brain Mapp 8, 194-208.
Laforce, R., Jr., Doyon, J., 2001. Distinct contribution of the striatum and cerebellum to motor learning. Brain Cogn 45, 189-211.
Lee, D., 2003. Coherent oscillations in neuronal activity of the supplementary motor area during a visuomotor task. J Neurosci 23, 6798-6809.
Lee, J., Jeong, J., 2013. Correlation of risk-taking propensity with cross-frequency phase-amplitude coupling in the resting EEG. Clin Neurophysiol 124, 2172-2180.
Lega, B., Burke, J., Jacobs, J., Kahana, M.J., 2014. Slow-Theta-to-Gamma Phase-Amplitude Coupling in Human Hippocampus Supports the Formation of New Episodic Memories. Cereb Cortex.
Lehericy, S., Benali, H., Van de Moortele, P.F., Pelegrini-Issac, M., Waechter, T., Ugurbil, K., Doyon, J., 2005. Distinct basal ganglia territories are engaged in early and advanced motor sequence learning. Proc Natl Acad Sci U S A 102, 12566-12571.
Li, B., Daunizeau, J., Stephan, K.E., Penny, W., Hu, D., Friston, K., 2011. Generalised filtering and stochastic DCM for fMRI. Neuroimage 58, 442-457.
Li, S., Bai, W., Liu, T., Yi, H., Tian, X., 2012. Increases of theta-low gamma coupling in rat medial prefrontal cortex during working memory task. Brain Res Bull 89, 115-123.
Lisman, J.E., Jensen, O., 2013. The theta-gamma neural code. Neuron 77, 1002-1016.
Lohmann, G., Erfurth, K., Muller, K., Turner, R., 2012. Critical comments on dynamic causal modelling. Neuroimage 59, 2322-2329.
Lohmann, G., Muller, K., Turner, R., 2013. Response to commentaries on our paper: Critical comments on dynamic causal modelling. Neuroimage 75, 279-281.
Lohse, K.R., Wadden, K., Boyd, L.A., Hodges, N.J., 2014. Motor skill acquisition across short and long time scales: a meta-analysis of neuroimaging data. Neuropsychologia 59, 130-141.
Ma, L.S., Wang, B.Q., Narayana, S., Hazeltine, E., Chen, X.Y., Robin, D.A., Fox, P.T., Xiong, J.H., 2010. Changes in regional activity are accompanied with changes in inter-regional connectivity during 4 weeks motor learning. Brain Research 1318, 64-76.
Malekmohammadi, M., Elias, W.J., Pouratian, N., 2015. Human thalamus regulates cortical activity via spatially specific and structurally constrained phase-amplitude coupling. Cereb Cortex 25, 1618-1628.
Marr, D., 1969. A theory of cerebellar cortex. J Physiol 202, 437-470.

Matsumoto, N., Hanakawa, T., Maki, S., Graybiel, A.M., Kimura, M., 1999. Role of [corrected] nigrostriatal dopamine system in learning to perform sequential motor tasks in a predictive manner. J Neurophysiol 82, 978-998.
Matsuzaka, Y., Picard, N., Strick, P.L., 2007. Skill representation in the primary motor cortex after long-term practice. J Neurophysiol 97, 1819-1832.
McGaugh, J.L., 2000. Memory--a century of consolidation. Science 287, 248-251.
Meier, B., Cock, J., 2014. Offline consolidation in implicit sequence learning. Cortex 57, 156-166.
Middleton, F.A., Strick, P.L., 1994. Anatomical evidence for cerebellar and basal ganglia involvement in higher cognitive function. Science 266, 458-461.
Miller, K.J., Hermes, D., Honey, C.J., Hebb, A.O., Ramsey, N.F., Knight, R.T., Ojemann, J.G., Fetz, E.E., 2012. Human motor cortical activity is selectively phase-entrained on underlying rhythms. PLoS Comput Biol 8, e1002655.
Miyachi, S., Hikosaka, O., Lu, X., 2002. Differential activation of monkey striatal neurons in the early and late stages of procedural learning. Exp Brain Res 146, 122-126.
Miyachi, S., Hikosaka, O., Miyashita, K., Karadi, Z., Rand, M.K., 1997. Differential roles of monkey striatum in learning of sequential hand movement. Exp Brain Res 115, 1-5.
Moisello, C., Meziane, H.B., Kelly, S., Perfetti, B., Kvint, S., Voutsinas, N., Blanco, D., Quartarone, A., Tononi, G., Ghilardi, M.F., 2013. Neural activations during visual sequence learning leave a trace in post-training spontaneous EEG. PLoS One 8, e65882.
Molinari, M., Leggio, M.G., Solida, A., Ciorra, R., Misciagna, S., Silveri, M.C., Petrosini, L., 1997. Cerebellum and procedural learning: evidence from focal cerebellar lesions. Brain 120 (Pt 10), 1753-1762.
Moran, D.W., Schwartz, A.B., 1999. Motor cortical activity during drawing movements: population representation during spiral tracing. J Neurophysiol 82, 2693-2704.
Moran, R.J., Campo, P., Maestu, F., Reilly, R.B., Dolan, R.J., Strange, B.A., 2010. Peak frequency in the theta and alpha bands correlates with human working memory capacity. Front Hum Neurosci 4, 200.
Mormann, F., Fell, J., Axmacher, N., Weber, B., Lehnertz, K., Elger, C.E., Fernandez, G., 2005. Phase/amplitude reset and theta-gamma interaction in the human medial temporal lobe during a continuous word recognition memory task. Hippocampus 15, 890-900.
Muellbacher, W., Ziemann, U., Wissel, J., Dang, N., Kofler, M., Facchini, S., Boroojerdi, B., Poewe, W., Hallett, M., 2002. Early consolidation in human primary motor cortex. Nature 415, 640-644.
Muslimovic, D., Post, B., Speelman, J.D., Schmand, B., 2007. Motor procedural learning in Parkinson's disease. Brain 130, 2887-2897.
Nemeth, D., Janacsek, K., Londe, Z., Ullman, M.T., Howard, D.V., Howard, J.H., 2010. Sleep has no critical role in implicit motor sequence learning in young and old adults. Experimental Brain Research 201, 351-358.
Nissen, M.J., Bullemer, P., 1987. Attentional Requirements of Learning - Evidence from Performance-Measures. Cognitive Psychology 19, 1-32.
Nitsche, M.A., Schauenburg, A., Lang, N., Liebetanz, D., Exner, C., Paulus, W., Tergau, F., 2003. Facilitation of implicit motor learning by weak transcranial direct current stimulation of the primary motor cortex in the human. J Cogn Neurosci 15, 619-626.
Nudo, R.J., Milliken, G.W., 1996. Reorganization of movement representations in primary motor cortex following focal ischemic infarcts in adult squirrel monkeys. J Neurophysiol 75, 2144-2149.
O'Reilly, J.X., Woolrich, M.W., Behrens, T.E., Smith, S.M., Johansen-Berg, H., 2012. Tools of the trade: psychophysiological interactions and functional connectivity. Soc Cogn Affect Neurosci 7, 604-609.
Ohyama, T., Nores, W.L., Murphy, M., Mauk, M.D., 2003. What the cerebellum computes. Trends in Neurosciences 26, 222-227.

Oldfield, R.C., 1971. The assessment and analysis of handedness: the Edinburgh inventory. Neuropsychologia 9, 97-113.
Orban, P., Peigneux, P., Lungu, O., Albouy, G., Breton, E., Laberenne, F., Benali, H., Maquet, P., Doyon, J., 2010. The multifaceted nature of the relationship between performance and brain activity in motor sequence learning. Neuroimage 49, 694-702.
Osipova, D., Hermes, D., Jensen, O., 2008. Gamma power is phase-locked to posterior alpha activity. PLoS One 3, e3990.
Osipova, D., Takashima, A., Oostenveld, R., Fernandez, G., Maris, E., Jensen, O., 2006. Theta and gamma oscillations predict encoding and retrieval of declarative memory. J Neurosci 26, 7523-7531.
Palva, J.M., Monto, S., Kulashekhar, S., Palva, S., 2010. Neuronal synchrony reveals working memory networks and predicts individual memory capacity. Proc Natl Acad Sci U S A 107, 7580-7585.
Pascual-Leone, A., Grafman, J., Clark, K., Stewart, M., Massaquoi, S., Lou, J.S., Hallett, M., 1993. Procedural learning in Parkinson's disease and cerebellar degeneration. Ann Neurol 34, 594-602.
Pascual-Leone, A., Nguyet, D., Cohen, L.G., Brasil-Neto, J.P., Cammarota, A., Hallett, M., 1995. Modulation of muscle responses evoked by transcranial magnetic stimulation during the acquisition of new fine motor skills. J Neurophysiol 74, 1037-1045.
Pavlides, C., Miyashita, E., Asanuma, H., 1993. Projection from the Sensory to the Motor Cortex Is Important in Learning Motor-Skills in the Monkey. Journal of Neurophysiology 70, 733-741.
Penhune, V.B., Steele, C.J., 2012. Parallel contributions of cerebellar, striatal and M1 mechanisms to motor sequence learning. Behav Brain Res 226, 579-591.
Penny, W.D., Duzel, E., Miller, K.J., Ojemann, J.G., 2008. Testing for nested oscillation. J Neurosci Methods 174, 50-61.
Penny, W.D., Stephan, K.E., Daunizeau, J., Rosa, M.J., Friston, K.J., Schofield, T.M., Leff, A.P., 2010. Comparing families of dynamic causal models. Plos Computational Biology 6, e1000709.
Perfetti, B., Moisello, C., Landsness, E.C., Kvint, S., Lanzafame, S., Onofrj, M., Di Rocco, A., Tononi, G., Ghilardi, M.F., 2011. Modulation of gamma and theta spectral amplitude and phase synchronization is associated with the development of visuo-motor learning. J Neurosci 31, 14810-14819.
Pfurtscheller, G., Lopes da Silva, F.H., 1999. Event-related EEG/MEG synchronization and desynchronization: basic principles. Clin Neurophysiol 110, 1842-1857.
Pollok, B., Latz, D., Krause, V., Butz, M., Schnitzler, A., 2014. Changes of motor-cortical oscillations associated with motor learning. Neuroscience 275, 47-53.
Pool, E.M., Rehme, A.K., Fink, G.R., Eickhoff, S.B., Grefkes, C., 2013. Network dynamics engaged in the modulation of motor behavior in healthy subjects. Neuroimage 82, 68-76.
Porter, R., 1985. The corticomotoneuronal component of the pyramidal tract: corticomotoneuronal connections and functions in primates. Brain Research 357, 1-26.
Press, D.Z., Casement, M.D., Pascual-Leone, A., Robertson, E.M., 2005. The time course of off-line motor sequence learning. Brain Res Cogn Brain Res 25, 375-378.
Raghavachari, S., Kahana, M.J., Rizzuto, D.S., Caplan, J.B., Kirschen, M.P., Bourgeois, B., Madsen, J.R., Lisman, J.E., 2001. Gating of human theta oscillations by a working memory task. J Neurosci 21, 3175-3183.
Ramnani, N., 2006. The primate cortico-cerebellar system: anatomy and function. Nat Rev Neurosci 7, 511-522.
Rauch, S.L., Savage, C.R., Brown, H.D., Curran, T., Alpert, N.M., Kendrick, A., Fischman, A.J., Kosslyn, S.M., 1995. A PET investigation of implicit and explicit sequence learning. Human Brain Mapping 3, 271-286.
Rauch, S.L., Whalen, P.J., Savage, C.R., Curran, T., Kendrick, A., Brown, H.D., Bush, G., Breiter, H.C., Rosen, B.R., 1997. Striatal recruitment during an implicit sequence learning task as measured by functional magnetic resonance imaging. Hum Brain Mapp 5, 124-132.

Reber, A.S., 1967. Implicit Learning of Artificial Grammars. Journal of Verbal Learning and Verbal Behavior 6, 855-&.
Reed, J., Johnson, P., 1994. Assessing Implicit Learning with Indirect Tests - Determining What Is Learned About Sequence Structure. Journal of Experimental Psychology-Learning Memory and Cognition 20, 585-594.
Rehme, A.K., Eickhoff, S.B., Wang, L.E., Fink, G.R., Grefkes, C., 2011. Dynamic causal modeling of cortical activity from the acute to the chronic stage after stroke. Neuroimage 55, 1147-1158.
Reis, J., Schambra, H.M., Cohen, L.G., Buch, E.R., Fritsch, B., Zarahn, E., Celnik, P.A., Krakauer, J.W., 2009. Noninvasive cortical stimulation enhances motor skill acquisition over multiple days through an effect on consolidation. Proc Natl Acad Sci U S A 106, 1590-1595.
Rigoux, L., Stephan, K.E., Friston, K.J., Daunizeau, J., 2014. Bayesian model selection for group studies - revisited. Neuroimage 84, 971-985.
Robertson, E.M., 2007. The serial reaction time task: implicit motor skill learning? J Neurosci 27, 10073-10075.
Robertson, E.M., Pascual-Leone, A., Miall, R.C., 2004a. Current concepts in procedural consolidation. Nat Rev Neurosci 5, 576-582.
Robertson, E.M., Pascual-Leone, A., Press, D.Z., 2004b. Awareness modifies the skill-learning benefits of sleep. Curr Biol 14, 208-212.
Robertson, E.M., Press, D.Z., Pascual-Leone, A., 2005. Off-line learning and the primary motor cortex. J Neurosci 25, 6372-6378.
Rosa, M.J., Friston, K., Penny, W., 2012. Post-hoc selection of dynamic causal models. J Neurosci Methods 208, 66-78.
Rose, M., Haider, H., Salari, N., Buchel, C., 2011. Functional dissociation of hippocampal mechanism during implicit learning based on the domain of associations. J Neurosci 31, 13739-13745.
Rose, M., Haider, H., Weiller, C., Buchel, C., 2002. The role of medial temporal lobe structures in implicit learning: an event-related FMRI study. Neuron 36, 1221-1231.
Roux, F., Uhlhaas, P.J., 2014. Working memory and neural oscillations: alpha-gamma versus theta-gamma codes for distinct WM information? Trends Cogn Sci 18, 16-25.
Roux, F., Wibral, M., Singer, W., Aru, J., Uhlhaas, P.J., 2013. The phase of thalamic alpha activity modulates cortical gamma-band activity: evidence from resting-state MEG recordings. J Neurosci 33, 17827-17835.
Sakamoto, T., Arissian, K., Asanuma, H., 1989. Functional role of the sensory cortex in learning motor skills in cats. Brain Res 503, 258-264.
Sami, S., Miall, R.C., 2013. Graph network analysis of immediate motor-learning induced changes in resting state BOLD. Front Hum Neurosci 7, 166.
Sami, S., Robertson, E.M., Miall, R.C., 2014. The time course of task-specific memory consolidation effects in resting state networks. J Neurosci 34, 3982-3992.
Sarnthein, J., Petsche, H., Rappelsberger, P., Shaw, G.L., von Stein, A., 1998. Synchronization between prefrontal and posterior association cortex during human working memory. Proc Natl Acad Sci U S A 95, 7092-7096.
Sato, N., Yamaguchi, Y., 2007. Theta synchronization networks emerge during human object-place memory encoding. Neuroreport 18, 419-424.
Sauseng, P., Klimesch, W., Doppelmayr, M., Hanslmayr, S., Schabus, M., Gruber, W.R., 2004. Theta coupling in the human electroencephalogram during a working memory task. Neurosci Lett 354, 123-126.
Sauseng, P., Klimesch, W., Heise, K.F., Gruber, W.R., Holz, E., Karim, A.A., Glennon, M., Gerloff, C., Birbaumer, N., Hummel, F.C., 2009. Brain oscillatory substrates of visual short-term memory capacity. Curr Biol 19, 1846-1852.

Schack, B., Klimesch, W., Sauseng, P., 2005. Phase synchronization between theta and upper alpha oscillations in a working memory task. Int J Psychophysiol 57, 105-114.
Schambra, H.M., Abe, M., Luckenbaugh, D.A., Reis, J., Krakauer, J.W., Cohen, L.G., 2011. Probing for hemispheric specialization for motor skill learning: a transcranial direct current stimulation study. J Neurophysiol 106, 652-661.
Schendan, H.E., Searl, M.M., Melrose, R.J., Stern, C.E., 2003. An FMRI study of the role of the medial temporal lobe in implicit and explicit sequence learning. Neuron 37, 1013-1025.
Schmahmann, J.D., Pandya, D.N., 1997. The cerebrocerebellar system. Int Rev Neurobiol 41, 31-60.
Schmahmann, J.D., Sherman, J.C., 1998. The cerebellar cognitive affective syndrome. Brain 121 (Pt 4), 561-579.
Scholz, J., Klein, M.C., Behrens, T.E., Johansen-Berg, H., 2009. Training induces changes in white-matter architecture. Nat Neurosci 12, 1370-1371.
Schulz, R., Wessel, M.J., Zimerman, M., Timmermann, J.E., Gerloff, C., Hummel, F.C., 2014. White Matter Integrity of Specific Dentato-Thalamo-Cortical Pathways is Associated with Learning Gains in Precise Movement Timing. Cereb Cortex.
Schwarb, H., Schumacher, E.H., 2009. Neural evidence of a role for spatial response selection in the learning of spatial sequences. Brain Research 1247, 114-125.
Schwarb, H., Schumacher, E.H., 2012. Generalized lessons about sequence learning from the study of the serial reaction time task. Advances in Cognitive Psychology 8, 165-178.
Sederberg, P.B., Schulze-Bonhage, A., Madsen, J.R., Bromfield, E.B., McCarthy, D.C., Brandt, A., Tully, M.S., Kahana, M.J., 2007. Hippocampal and neocortical gamma oscillations predict memory formation in humans. Cereb Cortex 17, 1190-1196.
Seghier, M.L., Zeidman, P., Neufeld, N.H., Leff, A.P., Price, C.J., 2010. Identifying abnormal connectivity in patients using dynamic causal modeling of FMRI responses. Front Syst Neurosci 4.
Sehm, B., Kipping, J., Schafer, A., Villringer, A., Ragert, P., 2013. A Comparison between Uni- and Bilateral tDCS Effects on Functional Connectivity of the Human Motor Cortex. Front Hum Neurosci 7, 183.
Seidler, R.D., Purushotham, A., Kim, S.G., Ugurbil, K., Willingham, D., Ashe, J., 2002. Cerebellum activation associated with performance change but not motor learning. Science 296, 2043-2046.
Seidler, R.D., Purushotham, A., Kim, S.G., Ugurbil, K., Willingham, D., Ashe, J., 2005. Neural correlates of encoding and expression in implicit sequence learning. Exp Brain Res 165, 114-124.
Seidler, R.D., Tuite, P., Ashe, J., 2007. Selective impairments in implicit learning in Parkinson's disease. Brain Research 1137, 104-110.
Seitz, R.J., Roland, E., Bohm, C., Greitz, T., Stone-Elander, S., 1990. Motor learning in man: a positron emission tomographic study. Neuroreport 1, 57-60.
Serrien, D.J., Pogosyan, A.H., Brown, P., 2004. Influence of working memory on patterns of motor related cortico-cortical coupling. Exp Brain Res 155, 204-210.
Seth, A.K., Chorley, P., Barnett, L.C., 2013. Granger causality analysis of fMRI BOLD signals is invariant to hemodynamic convolution but not downsampling. Neuroimage 65, 540-555.
Shimamoto, S.A., Ryapolova-Webb, E.S., Ostrem, J.L., Galifianakis, N.B., Miller, K.J., Starr, P.A., 2013. Subthalamic nucleus neurons are synchronized to primary motor cortex local field potentials in Parkinson's disease. J Neurosci 33, 7220-7233.
Shin, J.C., Ivry, R.B., 2003. Spatial and temporal sequence learning in patients with Parkinson's disease or cerebellar lesions. J Cogn Neurosci 15, 1232-1243.
Siegel, M., Warden, M.R., Miller, E.K., 2009. Phase-dependent neuronal coding of objects in short-term memory. Proc Natl Acad Sci U S A 106, 21341-21346.

Sisti, H.M., Geurts, M., Gooijers, J., Heitger, M.H., Caeyenberghs, K., Beets, I.A., Serbruyns, L., Leemans, A., Swinnen, S.P., 2012. Microstructural organization of corpus callosum projections to prefrontal cortex predicts bimanual motor learning. Learn Mem 19, 351-357.
Smith, J., Siegert, R.J., McDowall, J., Abernethy, D., 2001. Preserved implicit learning on both the serial reaction time task and artificial grammar in patients with Parkinson's disease. Brain Cogn 45, 378-391.
Song, S., Howard, J.H., Jr., Howard, D.V., 2007. Sleep does not benefit probabilistic motor sequence learning. J Neurosci 27, 12475-12483.
Spencer, R.M., Ivry, R.B., 2009. Sequence learning is preserved in individuals with cerebellar degeneration when the movements are directly cued. J Cogn Neurosci 21, 1302-1310.
Squire, L.R., Zola-Morgan, S., 1991. The medial temporal lobe memory system. Science 253, 1380-1386.
Staudigl, T., Hanslmayr, S., 2013. Theta oscillations at encoding mediate the context-dependent nature of human episodic memory. Curr Biol 23, 1101-1106.
Steele, C.J., Penhune, V.B., 2010. Specific increases within global decreases: a functional magnetic resonance imaging investigation of five days of motor sequence learning. J Neurosci 30, 8332-8341.
Steele, C.J., Scholz, J., Douaud, G., Johansen-Berg, H., Penhune, V.B., 2012. Structural correlates of skilled performance on a motor sequence task. Front Hum Neurosci 6, 289.
Stein, J.F., Glickstein, M., 1992. Role of the cerebellum in visual guidance of movement. Physiol Rev 72, 967-1017.
Stephan, K.E., Penny, W.D., Daunizeau, J., Moran, R.J., Friston, K.J., 2009. Bayesian model selection for group studies. Neuroimage 46, 1004-1017.
Stephan, K.E., Penny, W.D., Moran, R.J., den Ouden, H.E., Daunizeau, J., Friston, K.J., 2010. Ten simple rules for dynamic causal modeling. Neuroimage 49, 3099-3109.
Stephan, K.E., Weiskopf, N., Drysdale, P.M., Robinson, P.A., Friston, K.J., 2007. Comparing hemodynamic models with DCM. Neuroimage 38, 387-401.
Stephan, M.A., Meier, B., Zaugg, S.W., Kaelin-Lang, A., 2011. Motor sequence learning performance in Parkinson's disease patients depends on the stage of disease. Brain Cogn 75, 135-140.
Stickgold, R., Hobson, J.A., Fosse, R., Fosse, M., 2001. Sleep, learning, and dreams: off-line memory reprocessing. Science 294, 1052-1057.
Summerfield, C., Mangels, J.A., 2005. Coherent theta-band EEG activity predicts item-context binding during encoding. Neuroimage 24, 692-703.
Sun, F.T., Miller, L.M., Rao, A.A., D'Esposito, M., 2007. Functional connectivity of cortical networks involved in bimanual motor sequence learning. Cereb Cortex 17, 1227-1234.
Szczepanski, S.M., Crone, N.E., Kuperman, R.A., Auguste, K.I., Parvizi, J., Knight, R.T., 2014. Dynamic changes in phase-amplitude coupling facilitate spatial attention control in fronto-parietal cortex. PLoS Biol 12, e1001936.
Tamas Kincses, Z., Johansen-Berg, H., Tomassini, V., Bosnell, R., Matthews, P.M., Beckmann, C.F., 2008. Model-free characterization of brain functional networks for motor sequence learning using fMRI. Neuroimage 39, 1950-1958.
Tesche, C.D., Karhu, J., 2000. Theta oscillations index human hippocampal activation during a working memory task. Proc Natl Acad Sci U S A 97, 919-924.
Thorn, C.A., Atallah, H., Howe, M., Graybiel, A.M., 2010. Differential dynamics of activity changes in dorsolateral and dorsomedial striatal loops during learning. Neuron 66, 781-795.
Thorn, C.A., Graybiel, A.M., 2014. Differential entrainment and learning-related dynamics of spike and local field potential activity in the sensorimotor and associative striatum. J Neurosci 34, 2845-2859.
Toni, I., Krams, M., Turner, R., Passingham, R.E., 1998. The time course of changes during motor sequence learning: a whole-brain fMRI study. Neuroimage 8, 50-61.
Torriero, S., Oliveri, M., Koch, G., Caltagirone, C., Petrosini, L., 2004. Interference of left and right cerebellar rTMS with procedural learning. J Cogn Neurosci 16, 1605-1611.

Torriero, S., Oliveri, M., Koch, G., Lo Gerfo, E., Salerno, S., Ferlazzo, F., Caltagirone, C., Petrosini, L., 2011. Changes in cerebello-motor connectivity during procedural learning by actual execution and observation. J Cogn Neurosci 23, 338-348.
Tort, A.B., Komorowski, R., Eichenbaum, H., Kopell, N., 2010. Measuring phase-amplitude coupling between neuronal oscillations of different frequencies. J Neurophysiol 104, 1195-1210.
Tort, A.B., Komorowski, R.W., Manns, J.R., Kopell, N.J., Eichenbaum, H., 2009. Theta-gamma coupling increases during the learning of item-context associations. Proc Natl Acad Sci U S A 106, 20942-20947.
Tort, A.B., Kramer, M.A., Thorn, C., Gibson, D.J., Kubota, Y., Graybiel, A.M., Kopell, N.J., 2008. Dynamic cross-frequency couplings of local field potential oscillations in rat striatum and hippocampus during performance of a T-maze task. Proc Natl Acad Sci U S A 105, 20517-20522.
Tzvi, E., Munte, T.F., Kramer, U.M., 2014. Delineating the cortico-striatal-cerebellar network in implicit motor sequence learning. Neuroimage 94C, 222-230.
Tzvi, E., Stoldt, A., Witt, K., Kramer, U.M., 2015. Striatal-cerebellar networks mediate consolidation in a motor sequence learning task: An fMRI study using dynamic causal modelling. Neuroimage 122, 52-64.
Tzvi, E., Y., F., Crone, N.E., Chang, E.F., Parvizi, J., Knight, R.T., Kramer, U.M., under review. Cross-frequency coupling and inhibitory motor control in prefrontal and motor networks.
Vahdat, S., Darainy, M., Milner, T.E., Ostry, D.J., 2011. Functionally specific changes in resting-state sensorimotor networks after motor learning. J Neurosci 31, 16907-16915.
van der Meij, R., Kahana, M., Maris, E., 2012. Phase-Amplitude Coupling in Human Electrocorticography Is Spatially Distributed and Phase Diverse. Journal of Neuroscience 32, 111-123.
van Wingerden, M., van der Meij, R., Kalenscher, T., Maris, E., Pennartz, C.M., 2014. Phase-amplitude coupling in rat orbitofrontal cortex discriminates between correct and incorrect decisions during associative learning. J Neurosci 34, 493-505.
Varela, F., Lachaux, J.P., Rodriguez, E., Martinerie, J., 2001. The brainweb: phase synchronization and large-scale integration. Nat Rev Neurosci 2, 229-239.
Verleger, R., Seitz, A., Yordanova, J., Kolev, V., 2015. Is insight a godsend? Explicit knowledge in the serial response-time task has precursors in EEG potentials already at task onset. Neurobiol Learn Mem 125, 24-35.
von Nicolai, C., Engler, G., Sharott, A., Engel, A.K., Moll, C.K., Siegel, M., 2014. Corticostriatal coordination through coherent phase-amplitude coupling. J Neurosci 34, 5938-5948.
Voytek, B., Canolty, R.T., Shestyuk, A., Crone, N.E., Parvizi, J., Knight, R.T., 2010. Shifts in gamma phase-amplitude coupling frequency from theta to alpha over posterior cortex during visual tasks. Front Hum Neurosci 4, 191.
Wagner, U., Gais, S., Haider, H., Verleger, R., Born, J., 2004. Sleep inspires insight. Nature 427, 352-355.
Walker, M.P., Brakefield, T., Morgan, A., Hobson, J.A., Stickgold, R., 2002. Practice with sleep makes perfect: sleep-dependent motor skill learning. Neuron 35, 205-211.
Walker, M.P., Brakefield, T., Seidman, J., Morgan, A., Hobson, J.A., Stickgold, R., 2003. Sleep and the time course of motor skill learning. Learn Mem 10, 275-284.
Walker, M.P., Stickgold, R., Alsop, D., Gaab, N., Schlaug, G., 2005. Sleep-dependent motor memory plasticity in the human brain. Neuroscience 133, 911-917.
Ward, L.M., 2003. Synchronous neural oscillations and cognitive processes. Trends Cogn Sci 7, 553-559.
Weiss, S., Rappelsberger, P., 2000. Long-range EEG synchronization during word encoding correlates with successful memory performance. Brain Res Cogn Brain Res 9, 299-312.
Wilkinson, L., Teo, J.T., Obeso, I., Rothwell, J.C., Jahanshahi, M., 2010. The contribution of primary motor cortex is essential for probabilistic implicit sequence learning: evidence from theta burst magnetic stimulation. J Cogn Neurosci 22, 427-436.
Willingham, D.B., 1998. A neuropsychological theory of motor skill learning. Psychol Rev 105, 558-584.

Wise, S.P., Boussaoud, D., Johnson, P.B., Caminiti, R., 1997. Premotor and parietal cortex: corticocortical connectivity and combinatorial computations. Annu Rev Neurosci 20, 25-42.
Wolpert, D.M., Miall, R.C., Kawato, M., 1998. Internal models in the cerebellum. Trends Cogn Sci 2, 338-347.
Worden, M.S., Foxe, J.J., Wang, N., Simpson, G.V., 2000. Anticipatory biasing of visuospatial attention indexed by retinotopically specific alpha-band electroencephalography increases over occipital cortex. J Neurosci 20, RC63.
Wu, T., Chan, P., Hallett, M., 2008. Modifications of the interactions in the motor networks when a movement becomes automatic. J Physiol 586, 4295-4304.
Yanagisawa, T., Yamashita, O., Hirata, M., Kishima, H., Saitoh, Y., Goto, T., Yoshimine, T., Kamitani, Y., 2012. Regulation of motor representation by phase-amplitude coupling in the sensorimotor cortex. J Neurosci 32, 15467-15475.
Yin, H.H., Mulcare, S.P., Hilario, M.R., Clouse, E., Holloway, T., Davis, M.I., Hansson, A.C., Lovinger, D.M., Costa, R.M., 2009. Dynamic reorganization of striatal circuits during the acquisition and consolidation of a skill. Nat Neurosci 12, 333-341.
Zhuang, P., Dang, N., Waziri, A., Gerloff, C., Cohen, L.G., Hallett, M., 1998. Implicit and explicit learning in an auditory serial reaction time task. Acta Neurol Scand 97, 131-137.

Curriculum Vitae

Elinor Tzvi-Minker

Personal Information

Address	Seydlitzstraße 8 23564 Lübeck Germany
Born	October 14th, 1985 in Karmiel (Israel)
Nationality	Israeli

Education

6/2012 – 2/2016	**Doctoral Candidate** Department of Neurology, University of Lübeck Supervisor: Prof. Dr. rer. nat Ulrike M. Krämer
9/2010 - 5/2012	**Master of Science Biomedical Engineering** Cognitive neuroscience, Medical Imaging University of Lübeck & FH Lübeck Master Thesis: *Analysis of Phase Amplitude Coupling in Electrocorticography signals during a "Go-NoGo" Task* Supervisor: Prof. Dr. rer. nat Ulrike M. Krämer
10/2005 - 06/2009	**Bachelor of Science Biomedical Engineering** Medical Signal and Image processing Ben Gurion University, Beer-Sheva Bachelor Thesis: *Automatic atrial activity detection in surface ECG signal of rodents using a Matlab GUI* Supervisor: Dr. Yaniv Zigel

School Education

2000 - 2003	**Amit Karmiel High School** Concentration: Physics, Computer Science Awarded with excellence by the Ministry of Education, The state of Israel

Publications

Tzvi, E., Verleger, R., Münte, T. F., & Krämer, U. M. (under review). *Reduced alpha-gamma phase amplitude coupling over right parietal cortex underlies implicit visuomotor sequence learning.* Neuroimage

Fonken, Y. M., Rieger, J. W., **Tzvi, E.**, Crone, N. E., Chang, E., Parvizi, J., & Krämer, U. M. (2016). *Frontal and motor cortex contributions to response inhibition: evidence from electrocorticography.* Journal of neurophysiology: jn-00708.

Tzvi, E., Stoldt, A., Witt, K., & Krämer, U. M. (2015). *Striatal–cerebellar networks mediate consolidation in a motor sequence learning task: An fMRI study using dynamic causal modelling.* NeuroImage*,* 122*, 52-64.*

Tzvi, E., Münte, T. F., & Krämer, U. M. (2014). *Delineating the cortico-striatal-cerebellar network in implicit motor sequence learning.* Neuroimage, 94, 222-230.

Zigel, Y., Mor, M., **Tzvi, E.**, Tsviling, V., Gil, O., Katz, A., & Etzion, Y. (2011). *A surface ECG-based algorithm to determine the atrial refractoriness of rodents during electrophysiological study.* Cardiovascular Engineering and Technology, 2(4), 388-398.

Conferences

19/6/2014-21/6/2014
Lübeck, Germany

40. Tagung "Psychologie und Gehirn"
Poster contribution: *Motor memory consolidation alters effective connectivity in the cortico-striatal-cerebellar network*
Poster Prize Winner (DGPA)

8/6/2014-14/6/2014
Hamburg, Germany

20th Annual Meeting of the Organization of Human Brain Mapping
Poster contribution: *Effective connectivity in the cortico-cerebellar loop mediates implicit motor sequence learning: A DCM study*

16/6/2013-20/6/2013
Seattle, Washington, USA

19th Annual Meeting of the Organization of Human Brain Mapping
Poster contribution: *Theta-gamma phase amplitude coupling in prefrontal and motor cortex during response inhibition*

29/10/2012-31/10/2012
Berlin, Germany

Neural Computation: From Perception to Cognitive Function
Poster contribution: *Connectivity in prefrontal and motor cortex during response inhibition assessed by phase amplitude coupling*